CLASS VI PERMIT
PROJECT NARRATIVE

40 CFR §146.82(a)

Caliche Beaumont Sequestration Project
Beaumont, Jefferson County, Texas

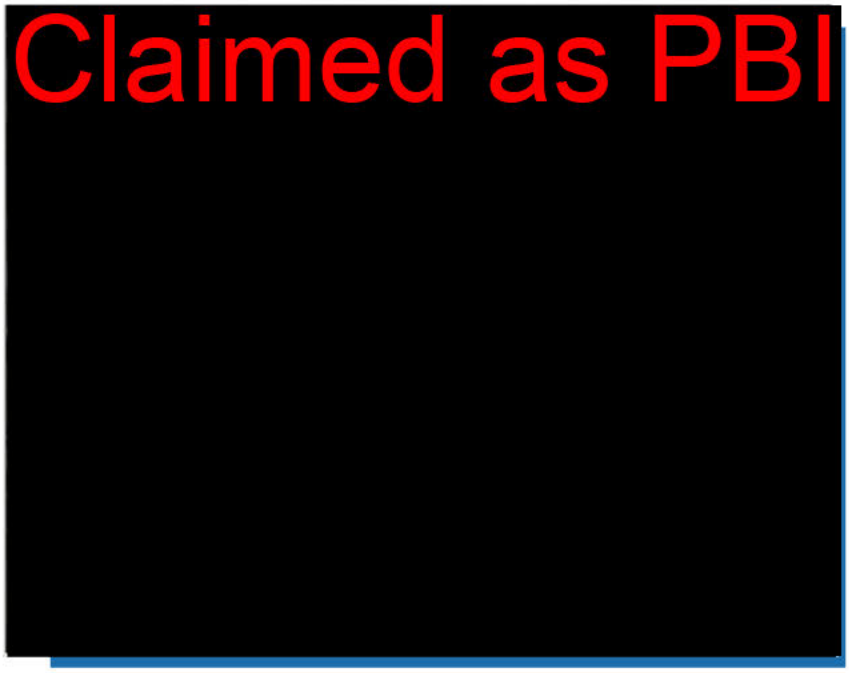

Issued: 23 April 2024

Prepared for: **CDP II CO2 SEQUESTRATION, LLC**
919 Milam St. Suite 2425
Houston, Texas 77002

Prepared by: **GSI ENVIRONMENTAL INC.**
2211 Norfolk, Suite 1000
Houston, Texas 77098
(713) 522 6300 | www.gsienv.com

CLASS VI PERMIT
PROJECT NARRATIVE
Caliche Beaumont Sequestration Project
Beaumont, Jefferson County, Texas

TABLE OF CONTENTS

CLASS VI PERMIT
PROJECT NARRATIVE
Caliche Beaumont Sequestration Project
Beaumont, Jefferson County, Texas

TABLE OF CONTENTS

CLASS VI PERMIT
PROJECT NARRATIVE
Caliche Beaumont Sequestration Project
Beaumont, Jefferson County, Texas

TABLE OF CONTENTS

EXHIBITS

CLASS VI PERMIT
PROJECT NARRATIVE
Caliche Beaumont Sequestration Project
Beaumont, Jefferson County, Texas

TABLE OF CONTENTS

CLASS VI PERMIT
PROJECT NARRATIVE
Caliche Beaumont Sequestration Project
Beaumont, Jefferson County, Texas

TABLE OF CONTENTS

TABLES

CLASS VI PERMIT
PROJECT NARRATIVE
Caliche Beaumont Sequestration Project
Beaumont, Jefferson County, Texas

TABLE OF CONTENTS

FIGURES

CLASS VI PERMIT
PROJECT NARRATIVE
Caliche Beaumont Sequestration Project
Beaumont, Jefferson County, Texas

TABLE OF CONTENTS

CLASS VI PERMIT
PROJECT NARRATIVE
Caliche Beaumont Sequestration Project
Beaumont, Jefferson County, Texas

TABLE OF CONTENTS

CLASS VI PERMIT
PROJECT NARRATIVE
Caliche Beaumont Sequestration Project
Beaumont, Jefferson County, Texas

TABLE OF CONTENTS

APPENDICES

CLASS VI PERMIT
PROJECT NARRATIVE
Caliche Beaumont Sequestration Project
Beaumont, Jefferson County, Texas

1.0 PROJECT OVERVIEW

1.1 Facility Information and Introduction

Facility/Project Name:	Caliche Beaumont Sequestration Project
Facility/Project Contact:	W. Graham Payne, Director of Energy Transition CDP II CO2 Sequestration, LLC ("Caliche") 919 Milam Street, Suite 2425 Houston TX, 77002 (832) 500-7590 / Claimed as PBI
Well Locations:	Beaumont, Jefferson County, Texas Injection Well Nos. 1, 2, and 3
SIC Code(s):	4923
Entity Type:	Private
Indian Lands:	No

Well ID	Latitude	Longitude
Injection Well 1	Claimed as PBI	
Injection Well 2	Claimed as PBI	
Injection Well 3	Claimed as PBI	

1.2 Project Goals and Stakeholders

Caliche is submitting this Underground Injection Control (UIC) Class VI injection well permit application for the sequestration of carbon dioxide (CO_2) in a deep underground geologic formation. Caliche's business projects focus primarily on underground storage of natural gas, industrial gases like hydrogen and helium, and carbon sequestration. The Golden Triangle Storage Facility (GTS Facility), Caliche's main operation facility, is located within the natural gas liquids (NGL) corridor next to several operational and proposed NGL export facilities in Beaumont, Jefferson County, Texas (see attached **Figure A.1.1**). The GTS Facility, located at the Spindletop salt dome in Beaumont, Texas, includes gas compression and extensive pipeline infrastructures for natural gas storage in two salt caverns, which currently comprise a working combined capacity of approximate 16 billion cubic feet (BCF). The GTS Facility is classified as a natural gas transmission industry according to the Standard Industry Classification (SIC) with SIC Code 4923 and is not located on Indian lands.

Caliche has three primary objectives for the Caliche Beaumont Sequestration Project:

1. To inject and sequester CO_2 from several direct emission sources in the vicinity of its GTS Facility, with the expectation that the primary locations of commercial clientele are in the cities of Port Arthur and Beaumont in Jefferson County, Texas;

2. To meet the rigorous requirements of applicable federal and state CCS regulations and guidelines; and
3. To participate in voluntary programs such as the California Air Resources Board (CARB) Low-Carbon Fuel Standard (LCFS) Carbon Credit and/or Federal Internal Revenue Service (IRS) 45Q Carbon Oxide Sequestration Credit programs.

According to emission data from the United States Environmental Protection Agency (USEPA) Facility Level Information on Greenhouse Gases Tool (FLIGHT) for Large Facilities, more than 25 million metric tons (MM Tons) of CO_2 were emitted in 2021 by facilities in Port Arthur and Beaumont, Texas (USEPA, 2022). The proximity of the Caliche Beaumont Sequestration Project to those facilities and its expertise in underground gas and liquid storage strategically positions Caliche to help reduce CO_2 emissions to the atmosphere and bridge the gaps for those facilities to reach net-zero emission targets and goals. The facilities targeted by Caliche primarily include power generation plants, petrochemical and chemical facilities, and NGL processing facilities.

1.3 Project CO_2 Injection Details

To meet project objectives, Caliche will inject and sequester CO_2 at up to three injection wells, all anticipated to be located within the "City of Beaumont Acreage" which is leased by Caliche from the City of Beaumont (see attached **Figure A.1.1**). This permit application includes information pertaining to all three injection wells and the entirety of the cumulative Area of Review (AoR). A completed Class VI Permit Application Completeness Checklist is provided in attached **Table A.1.1** and provides the location of information relevant to the "Required Items" within the permit application.

The injection wells will be installed and screened within the Upper Frio Formation injection zone, between Claimed as PBI As discussed in Section 2.2 of this *Module A*, the Upper Frio Formation injection zone, which is Claimed as PBI thick at the Caliche Beaumont Sequestration Project Site, is overlain by an Upper Confining System consisting of (in ascending order) 1) an approximately Claimed as PBI thick Upper Frio shale containment layer, 2) the Claimed as PBI hick low-permeability marine shale called the Anahuac Formation (Swanson et al., 2013, Abstract), and 3) a Claimed as PBI thick shale rich containment layer in the Lower Oakville Formation. In addition, overlying the Upper Confining System is a "Buffer Aquifer/ Aquiclude System" consisting of the Middle and Upper Oakville Buffer aquifer system of the Jasper aquifer and the Middle Oakville and Lagarto Buffer Aquiclude System.

As discussed in Section 2.2 of this *Module A*, the target injection zone within the Upper Frio Formation is comprised of a succession of sandstones and shales deposited in deltaic and marginal-marine environments (Swanson et al., 2013, PDF p. 14, Section 4). The Upper Frio sands that have been targeted for injection are named the Upper Frio "Green," "Yellow," and "Gold" Sands (i.e., the Upper Frio Sand injection zone). The Upper Frio Formation is underlain by the Upper Hackberry unit of the Middle Frio Formation, consisting of abnormally pressured shales and serving as the Lower Confining Zone, and the deeper Vicksburg Group, a regional confining unit between the Coastal Uplands aquifer system from the Coastal Lowlands aquifer system and is comprised primarily of marine clays and thin-bedded sands (Chowdhury and Turco, 2006, PDF p. 37, Oligocene Series).

Modeling suggests that the Caliche Beaumont Sequestration Project has the above- and below-geologic seals (i.e., confining zones) required to safely and effectively inject and contain Claimed as PBI using all three proposed injection wells for a

total of Claimed as PBI of CO_2 sequestered over the life of the project (see Sections 2.2 and of this *Module A*).

1.4 Project Timeline

Caliche expects to obtain all necessary construction and environmental permits for the construction of the infrastructure required to safely inject and sequester CO_2 by 2025. The construction activities are anticipated to require 18 months for completion, and injection activities are expected to commence by 2026. Claimed as PBI . Caliche will monitor the pressure front and CO_2 plume extent for at least 50 years or for the duration of the alternative timeframe approved by the USEPA pursuant to requirements of 40 CFR §146.93(c) and then up to 100 years post-injection operations, per the CARB LCFS protocol requirements.

1.5 List of Permits

For the operation of the Caliche Beaumont Sequestration Project described in Section 1.2 above, Caliche will obtain all required permits as necessary before the construction and injection of CO_2 into the Upper Frio Formation at the Caliche Beaumont Sequestration Project site. A list and summary of anticipated federal, state, and local regulatory and statutory authorities potentially relevant to the Caliche Beaumont Sequestration Project is provided in attached **Table A.1.2**.

For this Class VI permit application, an injection depth waiver and aquifer expansion are not required and therefore are not being requested for the Caliche Beaumont Sequestration Project.

1.6 List of Contacts for States, Tribes, and Territories

State Officials		
Title	**Name**	**Contact Information**
Texas State Governor	Mr. Greg Abbott	P.O. Box 12428 Austin, Texas 78711-2428 (512) 463-2000
Texas State House Representative (House District 22)	Mr. Christian Manuel Hays	P.O. Box 2910 Austin, TX 78768 (512) 463-0662
Texas State Senator (Senate District 3)	The Honorable Robert Nichols	P.O. Box 12068 Capitol Station Austin, TX 78711 (512) 463-0103

Local Officials		
Title	**Name**	**Contact Information**
Jefferson County Judge	Mr. Jeff Branick	1149 Pearl Street Beaumont, Texas 77701 (409) 835-8466 jbranick@co.jefferson.tx.us
Jefferson County Director of Public Health	Dr. Ezea Ede	1295 Pearl Street Beaumont, TX 77701 (409) 835-8530 Ezea.Ede@jeffcotx.us
Mayor of Beaumont	Mr. Roy West	801 Main Street P.O. Box 3827 Beaumont, TX 77704-3827 (409) 880-3770
Director of Public Health of Beaumont	Mr. Kenneth Coleman, Sr.	3040 College Street P.O. Box 3827 Beaumont, TX 77701 (409) 654-3603

2.0 SITE CHARACTERIZATION

The geologic suitability of a specific stratigraphic interval for the injection and confinement of CO_2 is determined primarily by the following criteria:

- Lateral extent, thickness, interconnected porosity, permeability, and geomechanical properties of the injection zone;
- Lateral extent, thickness, minimal porosity, impermeability, and geomechanical properties of the overlying confining zone;
- Hydrogeologic compatibility of the injected carbon dioxide with the rock formation material and in-situ brine solutions;
- Faulting or fracturing of the injection zone, overlying aquiclude, and confining zone; and
- Seismic risk.

These criteria can be evaluated based on the regional and local depositional and structural histories of the geologic strata.

In this section, regional subsurface geology at the Caliche Beaumont Sequestration Project Site, represented by the composite stratigraphic column in attached **Figure A.2.1**, is presented and discussed to demonstrate the potential of the strata underlying the project site to be used for the sequestration of carbon dioxide. The data used in this permit application has been obtained from multiple sources, which include regional and local data interpretations performed for the study of the AoR, published literature, well logs, core evaluations, and empirical data where available. A more detailed discussion of the local geology and structures is provided in Section 2.2.

An onsite well, Claimed as PBI [redacted] has been designated as the Type Log for the Caliche Beaumont Sequestration Project Site (see attached **Figure A.2.2**). The key regulatory intervals are reported in the below ground elevation. Geologic maps and cross-sections illustrating the regional geology, hydrogeology, and the geologic structure of the local area are provided and discussed in this narrative.

2.1 Regional Geology

The Caliche Beaumont Sequestration Project Site is located immediately south of Beaumont in Jefferson County, Texas. **Figure A.2.3** (attached) shows the location of the Caliche Beaumont Sequestration Project Site on the Geology Map of Texas. The Caliche Beaumont Sequestration Project Site is located along the Gulf of Mexico and is in the Coastal Prairies portion of the Gulf Coastal Plains physiographic province (UT-BEG, 1996).

During the Mesozoic Era, tensional deformation associated with crustal extension was the primary control on the development of the Gulf of Mexico. **Figure A.2.4** (attached) presents a series of cross-sections that illustrate the structural evolution of the Gulf of Mexico during this time. Extension of the pre-existing continental crust created a series of basement grabens and half grabens that filled with terrestrial red beds and volcanics early in the basin's development. Subsidence associated with crustal cooling and sediment loading continued to depress the basin, allowed the deposition of the thick sedimentary sequences, and formed a clearly defined shelf edge and slope that separates the abyssal plain from the coastal plain (Galloway, 2008).

As shown on **Figure A.2.5** (attached), the stratigraphic-structural framework of the Gulf of Mexico Basin can be subdivided into four provinces, which correspond to the major lithofacies provinces that persist from the Late Jurassic to the Holocene (Galloway, 2008).

- Central basin deep water abyssal plain.
- Eastern carbonate margins of the Florida and Yucatan platforms.
- Laramide-modified western compressional margin of Mexico.
- Northwestern progradational margin that extends from northeastern Mexico to Alabama.

The Caliche Beaumont Sequestration Project Site is located within the northwestern progradational margin structural province, which is an onshore broad coastal plain (attached **Figure A.2.5**). The rate of non-marine sediment influx has been greater than the rate of basin subsidence since the end of rifting during the Cretaceous and has resulted in a significant progradation of the continental shelf margin (attached **Figure A.2.6**).

The coastal zone of the northwestern progradational margin is characterized by extreme extension and subsidence, resulting in Mesozoic strata that are buried beneath a 10 to 15-km-thick sedimentary prism of Upper Cretaceous and Cenozoic deposits. Progradation of the shelf margin by hundreds of kilometers in seaward direction destabilized the Jurassic salt layer (Galloway, 2008), and listric, enechelon, and syndepositional growth fault systems, and diapir provinces formed as a result.

During the Cenozoic Era, the geometry of deposition in the Gulf of Mexico Basin was primarily controlled by the interaction of the following factors:

- Changes in the source locations and rates of sediment input, resulting in major shifts in the distribution of areas with maximum sedimentation;
- Changes in the relative position of the sea level, resulting in the development of series of large-scale depositional cycles;
- Diapiric intrusions of salt and mudrock material in response to sediment loading; and
- Flexures and growth faults caused by sediment loading and gravitational instability.

2.1.1 Regional Stratigraphy

A stratigraphic column of Gulf Coast Cenozoic depositional episodes is provided on attached **Figure A.2.7**. The regional formations and regulatory intervals that will be penetrated by the proposed injection well(s) are discussed below and are shown on the regional geologic cross-section on attached **Figure A.2.8**. The formations are discussed in ascending order beginning with the Frio Formation.

2.1.1.1 Frio Formation

The Frio Formation is of Oligocene age. As shown on attached **Figure A.2.9**, Frio deposition in the Beaumont area was present predominantly in the Buna strand-plain barrier system of southeast Texas. Sediments that were carried along strike from the Houston delta system and deposited approximately parallel to the present coastline distinguish the Frio depositional system (Galloway et al., 1982, p. 10).

In Jefferson County, the Frio section ranges from about 2,000 ft to more than 6,000 ft thick and can be divided into three units (lower, middle, and upper), which are discussed below (Ewing and Reed, 1984, p. 6). The upper Frio unit is the target zone for injection of CO_2 at the Caliche Beaumont Sequestration Project Site.

- **Lower Frio Unit:** The ***lower unit*** of the Frio is relatively thin and sandstone poor and is lithologically similar to the underlying Vicksburg, which in the Beaumont area consists primarily of shale with some discontinuous sandstone bodies (Ewing, 1986, p. 8; Coleman, 1990, pp. 96 and 99).
- **Middle Frio Unit:** The ***middle unit*** of the Frio contains abundant sandstones updip but only a few discontinuous sandstones downdip. This unit was extensively eroded at the sub-Hackberry unconformity, so that its original thickness is difficult to determine (Ewing and Reed, 1984, pp. 7-8).

  Shale and sandstone of the Hackberry Member form a seaward-thickening wedge in southeast Texas and southwest Louisiana that lies within the Frio marine succession and pinches out to the north. The lower portion of the Hackberry is typically a sand-rich unit that fills channels that were eroded up to several hundred feet into pre-Hackberry sediments. Previous studies have indicated that these sands were deposited in a submarine canyon-fan environment. A more uniformly distributed, seaward thickening wedge of shale overlies the lower Hackberry sands. This shale grades into upper Frio sediments of shallow-water origin (Ewing and Reed, 1984, pp. 2 and 4).

  Figure A.2.10 (attached) is an isopach map of the Lower Hackberry in the area near the Caliche Beaumont Sequestration Project Site. Several large channel axes along with minor channels surround isolated high areas on the pre-Hackberry unconformity (Ewing and Reed, p. 12)
- **Upper Frio Unit:** The ***upper unit*** of the Frio consists of sandstone in updip areas and alternating sandstone and shale downdip. The sandstones in the Upper Frio include upward-coarsening cycles that are continuous along strike. They are inferred to be barrier-bar or strandplain sand bodies, or both. The Upper Frio sand system prograded with time, capping the deep-water Hackberry shale (Ewing and Reed, 1984, p. 8).

  Electric logs of the upper Frio generally exhibit a blocky pattern with irregularly upward-coarsening sandy intervals, indicative of wave-reworked sands from recurrent delta-destructional phases. The dominant sandy facies of the Upper Frio are stacked aggregational shoreface and beach deposits. The massive sand units are often separated by finer grained clastics, which accumulated in marsh and other low-energy environments during periods of regression (Galloway et al., 1982, pp. 10-11).

2.1.1.2 Anahuac Formation

The Anahuac Formation is of early Miocene age and consists primarily of shallow marine calcareous shale (Ewing and Reed, 1984, p. 8). The Anahuac Formation is regional in extent, thickening from its onshore margin to nearly 2,000 ft in the Gulf of Mexico (Galloway et al., 1982). As discussed in Section 2.2, the Anahuac is about Claimed as PBI around the Caliche Beaumont Sequestration Project Site based on review of geophysical logs of oil and gas exploration and production wells. The dense, low permeability shale layers in the Anahuac Formation provide excellent confinement and sealing capabilities for oil and gas traps and would also provide isolation for injection of CO_2 into the underlying sandstones of the upper Frio unit.

A relatively thin limestone member is present within the Anahuac Formation, and this limestone formed reefs around several salt domes and salt uplifts in southeast Texas. Pinnacle reef accumulations more than 100 ft thick occur in the Port Arthur area at the Hildebrandt Bayou, Orange, and Port Neches fields (Ewing, 1986, pp. 67 and 70).

2.1.1.3 Fleming Group (Oakville and Lagarto Formations)

The Fleming Group is early to late Miocene in age and includes the Oakville and Lagarto Formations. The Fleming Group is bounded by regional marine shales in downdip areas and by the bases of massive fluvial sandstones updip.

The depth to the base of the Oakville Formation in northern Jefferson County is typically between approximately 5,000 and 7,000 ft bgs (Young et al., 2012, Figure 6-2). The depth to the base of the Lagarto Formation in northern Jefferson County is typically between approximately 4,500 ft and 6,500 ft bgs (Young et al., 2012, Figure 6-10).

In a 2012 study of the Gulf Coast Aquifer, the lower boundary of the Fleming Group (i.e., base of Oakville Formation) was delineated by correlating between the Anahuac Shale downdip and the base of the massive Oakville sandstone updip and in outcrop, and the upper boundary of the Fleming Group (i.e., top of Lagarto Formation) was delineated by connecting the Amphistegina B Shale downdip with the base of the massive Goliad sandstone updip (Young et al., 2012, p. 3-4).

The Oakville and Lagarto Formations together comprise a major fluvial-deltaic episode in which the Oakville forms the lower progradational part and the Lagarto forms the upper retro gradational part. In the onshore Texas coast, the Oakville is generally sand-rich, whereas the Lagarto is relatively more mud-rich. However, both formations contain thick sandstone in the far northeast part of the Texas coast (Young et al., 2012, p. 3-6). As discussed in Section 2.2, the low permeability shales interspersed with sandstones in the Miocene lower Lagarto Formation and upper Oakville Formation provide a secondary confining zone above the Anahuac Formation.

There is a major fluvial channel belt known as the Newtown fluvial system in the northeast corner of the Texas coastal plain, and the fluvial and shore-zone sandstones are generally well connected in this area. The Lagarto Formation is generally sandier than the Oakville Formation along the upper Texas coast (Young et al., 2012, pp. 3-6 and 3-8).

Injection of CO_2 into the Miocene sandstones of the Oakville Formation is not included in this permit application.

2.1.1.4 Goliad Formation

The Goliad Formation is primarily middle-to-late Miocene in age and only occurs in the onshore part of the Texas Coastal Plain, where it is defined by nonmarine depositional systems and facies. In the modern offshore area, middle-upper Miocene strata include fluvial, deltaic, and marine depositional systems. The depth to the base of the Goliad Formation in northern Jefferson County is typically between approximately 2,500 ft and 4,000 ft bgs (Young et al., 2012, p. 3-8 and Figure 6-14).

Goliad fluvial depositional systems include channel fill and interchannel fill facies. Fluvial channel fill facies are composed mainly of medium- to coarse-grained sand and gravel, whereas the interchannel facies include sandy crevasse splays and muddy floodplain and playa lake deposits.

The Goliad Formation in Texas includes three large fluvial systems, each of which contained multiple channel axes that formed the drainage network. Channels preferentially occupied the same locations on the coastal plain, resulting in vertical stacking of sand bodies. Due to an arid paleoclimate and lack of bank-stabilizing vegetation, the fluvial channels had poorly developed levees, channel migration was relatively unconstrained, and channel-fill deposits tended to coalesce laterally. Thus, Goliad channel-fill sand bodies form broad belts that are much thicker and wider than the river channels in which they were deposited. Goliad fluvial systems vary in

overall composition and sandstone development, and generally become sandier in the northeastern part of the Texas Gulf Coast (Young et al., 2012, p. 3-10).

2.1.1.5 Willis Formation

The Willis Formation is approximately Pliocene in age. Like the Goliad Formation, the Willis Formation consists predominantly of nonmarine fluvial depositional systems in the onshore part of the Texas coastal plain (Young et al., 2012, p. 3-12). This formation outcrops in Hardin County, which is the county to the north of Jefferson County (UT-BEG, 1992b). The depth to the base of the Willis Formation in northern Jefferson County is typically between approximately 1,250 ft and 1,750 ft bgs (Young et al., 2012, Figure 6-17).

The Willis Formation ranges in thickness from about 100 ft in outcrop to 500 ft near the coast and generally becomes thicker in the northeastern part of the Texas Gulf Coast. The Willis dips coastward at about 15 to 20 feet per mile. Individual Willis sands vary widely in thickness from about 20 ft to 200 ft and are separated by muds of similar thickness (Young et al., 2012, p. 3-12).

The percentage of sand in the Willis Formation in Jefferson County is typically in the range of 40 to 60% except in the northernmost portion of Jefferson County, where the percentage of sand is in the range of 60 to 80% (Young et al., 2012, Figure 3-8).

2.1.1.6 Lissie Formation

The Lissie Formation is approximately early Pleistocene in age. In the portion of the Gulf Coast located north of the Brazos River, it has been mapped at the surface as the Montgomery and Bentley Formations. In the subsurface, the Lissie is defined as the interval between the Willis and Beaumont Formations. The depth to the base of the Lissie Formation in northern Jefferson County is typically between 500 ft and 1,000 ft bgs (Young et al., 2012, p. 3-13 and Figure 6-18).

The Lissie consists primarily of nonmarine sediments in the onshore part of the Texas coastal plain. Lissie deposition was strongly influenced by glacial-interglacial cycles on the North American continent, and high-frequency sea level fluctuations during the Pleistocene resulted in shorter depositional episodes, thinner stratigraphic sequences, and greater erosional downcutting. The Lissie Formation ranges in thickness from about 100 ft at outcrop to greater than 700 ft at the coast. The Lissie dips coastward at about 5 ft to 20 ft per mile. In the area along the northeastern Texas coast, the Lissie is less sandy than the Willis. In Jefferson County, the percentage of sand in the Lissie is between 40% and 60% (Young et al., 2012, p. 3-13 and Figure 3-9).

2.1.1.7 Beaumont Formation

The Beaumont Formation is of late Pleistocene age and outcrops in Jefferson County, except where the coastal plain is cut by modern river valleys (**Figure A.2.6**). The Beaumont is comprised of clay-rich sediments transected by sandy fluvial and deltaic-distributary channels. The depth to the base of the Beaumont Formation in northern Jefferson County typically ranges from <100 ft to 400 ft bgs (Young et al., 2012, p. 3-14 and Figure 6-19).

North of the Brazos River, the Beaumont Formation ranges in thickness from a thin veneer in updip areas to about 500 ft near the modern coast, and it thickens to the northeast. Individual sands range from 20 ft to 50 ft thick, staking locally to reach 150 ft in some locations. Interbedded muddy intervals are generally of similar thickness to the sands. Within the fluvial channel belts, the Beaumont Formation is 50% to 65% sand. The channel belts are separated by sand-poor floodplain, delta-plain, and bay-lagoon systems (Young et al., 2012, p. 3-14).

2.1.1.8 Holocene Deposits

Holocene sediments that have been deposited during the past 18,000 years along the Texas Gulf Coast consist mainly of isolated river valley fills that merge coastward with bays, lagoons, and barrier islands. The base of the Holocene is an erosional surface that formed during the sea-level lowstand at the end of the Pleistocene (Young et al., 2012, pp. 3-14 and 3-15).

River valleys were deeply incised into the pre-existing Beaumont coastal plain and filled slowly with bay-estuary muds as sea levels rose. Subsequently, fluvial-deltaic systems prograded seaward filling the updip part of the valleys with sandy alluvial deposits, but only the Rio Grande, Brazos River, and Colorado River have filled their valleys to the coast. The other Texas coastal river valleys are still partly occupied by bays and lagoons (Young et al., 2012, pp. 3-15).

2.1.2 Regional Structural Geology

Miocene and Oligocene age sediments deposited along the northern margin of the Gulf Coast Tertiary Basin were characterized by rapid subsidence in areas of high sediment loading. Major progradational wedges are typically characterized by an updip section of interbedded continental and marginal marine sediments that are underlain by a thick marine section composed of undercompacted slope and basin claystone. The instability caused by the direct rapid loading of water saturated, unconsolidated sediments resulted in the development of large scale down-to-basin faulting and intraformational deformation (Galloway et al., 1982a).

Three major structural styles (Rio Grande Embayment, San Marcos Arch, and Houston Embayment) have been defined along the Texas Gulf Coast, based on the depositional province and the type of diapiric activity involved in the deformational process. The Caliche Beaumont site is in the broadly defined province called the Houston Embayment of Southeast Texas (**Figures A.2.11 and A.2.12**). This structural province is characterized by salt diapirism with its associated faulting and characteristically large salt withdrawal sub-basins (Bebout et al., 1978).

2.1.2.1 Regional Faulting

The Gulf Coast Basin is comprised of predominantly two types of faulting: listric normal growth faulting and faulting associated with shale or salt piercement structures (diapirism). Growth faults form contemporaneously with sedimentation so that their throw increases with depth, and strata on the downthrown side are thicker than the correlative strata on the upthrown side of the fault (**Figure A.2.13**). The faults form in clastic sequences that build out into unconfined depositional sites that have prograded to the edge of the continental margin, resulting in contemporaneous failure of the prograding sediments (Jackson and Galloway, 1984). The buoyant rise of shale or salt through brittle geologic sections produces diapirs and ridges.

Subsurface strata in southeast Texas are disrupted by salt domes and a regional system of listric growth faults which roughly parallel the coast. Growth faults begin as normal faults but continue to displace along the downthrown, hanging side of the fault due to the increasing weight of additional sediments on the downthrown side of the fault. The major fault systems are thought to have formed by either differential compaction of sediments during regressive phases of deposition or from gravity sliding where the rate of basin subsidence exceeded the rate of deposition (Bruce, 1973).

A major system of normal faults is well developed parallel to the coastline in southeast Texas. These normal faults are arranged in a sequential, stair-step fashion, with displacements normally down towards the coast (often referred to as “down to the coast” faulting). These are deep-seated

faults that extend upward to within an average of 7,000 feet of the land surface, with some local extension into shallower strata. Displacement along these faults typically ranges from an often undetectable fifty feet or less to over 1,000 feet, increasing with depth. These faults have developed in response to tension and separation, due to subsidence of the Gulf Coast depositional basin under the increasing weight of new sediment deposition.

Figure A.2.14 shows the major fault zones and shallow salt domes in the onshore part of the Texas coastal zone. The major regional fault zones shown on **Figure A.2.14** include the Wilcox, Yegua, Frio, and Fleming fault zones.

In 1981 the Bureau of Economic Geology at The University of Texas at Austin (UT-BEG) published a set of structural cross-sections of Tertiary formations for the entire Texas Gulf Coast region (Dodge and Posey, 1981). **Figure A.2.15** shows the locations of all cross-sections that were prepared for that project and highlights the locations of three cross-sections located close to the Caliche Site. **Figures A.2.16 and A.2.17** are north-south cross-sections and show correlation of formations from the base of the Wilcox to the top of the Frio. **Figure A.2.18** is oriented approximately west to east and is located relatively close to the coast. It shows the correlations of the top and base of the Frio. These cross-sections also show major faults and salt domes.

A 2012 report prepared for the Texas Water Development Board (TWDB) included structure maps, isopach maps, and cross sections showing the Miocene, Pliocene, and Pleistocene formations along the northern portion of the Texas Gulf Coast. **Figures A.2.19 and A.2.20** are cross-sections that include Jefferson County and show correlation of the Oakville, Lagarto, Goliad, Willis, Lissie, and Beaumont Formations (Young et al., 2012, Chapter 6).

2.1.2.2 Salt Domes

Salt domes along the Upper Texas Gulf Coast are diapiric, with the salt originating at depths often greater than 30,000 ft bgs, from the Jurassic age Louann Salt. The density difference between the less dense salt beds and the denser, overlying sediments, coupled with the overburden pressures on the salt beds, has “squeezed” salt upward in a plastic state, forming numerous diapirs. Deformation and piercement of the overlying sediments have created doming of overlying strata, i.e., salt domes.

The salt domes typically pierce upward a considerable distance above the Louann Salt with some dome tops very near the current land surface. In the immediate vicinity of the salt domes, the subsurface strata dip radially away from the dome. It is typical, due to the stresses resulting from the piercement of the sediments, for strain to be manifested as a series of radially oriented faults, displacing the sediment layers over and adjacent to the dome.

As shown on **Figure A.1.1**, the Spindletop Salt Dome is located approximately 10,000 ft (1.9 miles) east of the eastern boundary of the Caliche Beaumont Sequestration Project Site. As shown on the schematic cross-section of Spindletop on **Figure A.2.21**, the dip of the beds around the salt dome varies, with dips being steeper near the dome and becoming less steep further away from the dome.

2.1.2.3 Key Findings from a Regional Study Near the Caliche Site

In 1984, UT-BEG issued a report on depositional systems and structural controls of Hackberry sandstone reservoirs in the Beaumont-Port Arthur area (Ewing and Reed, 1984). As discussed above, the Hackberry sandstones are in the middle unit of the Frio. Additional findings regarding the structural style of growth faults in the Beaumont-Port Arthur area were discussed in a

subsequent report (Ewing, 1986, pp. 57-75). **Figures A.2.22 and A.2.23** are regional structure maps for the Beaumont-Port Arthur area that were modified from maps in the second publication (Ewing, 1986, pp. 69 and 71).

Figure A.2.22 is an isopach map for the interval between the top of the Anahuac and the base of the upper Frio unit (i.e., top of the Hackberry Shale). The published figure has been modified to highlight significant growth faults that influenced upper Frio and Anahuac deposition and to indicate the locations of the Caliche Beaumont Sequestration Project Site, Spindletop, and five other salt domes in the area. The map also shows a north-south elongated high area, believed to be a salt-cored ridge, extending from Lovells Lake south to the La Belle Oilfield and extending northeastward past the present-day Spindletop salt dome. The author noted that more faults were present than were shown on the published figure (Ewing, 1986, p. 69)

A rapidly expanding section in the southern and southeastern part of the study area shown on **Figure A.2.22**, probably marks the upper Frio and Anahuac shelf margin. Growth faulting in the area is generally of low displacement except for abundant and long-lived growth faults at the shelf margin that may have moved substantially in some periods (Ewing, 1986, p. 67). One of the growth faults shown on **Figure A.2.22** extends into the southernmost portion of the Caliche Beaumont Sequestration Project Site.

Figure A.2.23 is a structure map of the top of the Frio. The author reported that this map best showed the post-Anahuac phase of structural development in the area and indicates that uplift of the Orange and Port Neches salt domes continued, as did uplift of the Big Hill, McFaddin Ranch, and Fannett salt domes. Continued activity on regional growth faults in the area created the rollover anticlines that localize many important oilfields in the area, including the Amelia, West Beaumont, Lovells Lake, and La Belle Oilfields, which are labeled on **Figure A.2.23** (Ewing, 1986, p. 67).

Figure A.2.23 highlights the radial faulting associated with salt structures in the area near the Caliche Site. One of the radial faults extends from the Spindletop salt dome to the Fannett salt dome to the southwest, and it passes through the southernmost portion of the Caliche Beaumont Sequestration Project Site. Another inferred radial fault extends west of Spindletop and may extend into the northernmost portion of the Caliche Beaumont Sequestration Project Site.

In most of the study area shown on **Figures A.2.22 and A.2.23**, the top of geopressure is near the base of the upper Frio sandstones; the Hackberry and deeper sandstones southeast of Spindletop salt dome are geopressured. In the northwestern part of the study area, the top of geopressure lies below the base of the Frio (Ewing, 1986, p. 61).

As noted previously, the sandstones in the upper unit of the Frio comprise the target zone for injection of CO_2 at the Caliche Beaumont Sequestration Project Site.

Further investigation of the faults at the Caliche Site was conducted during the characterization of local geology and will be discussed in the following section of this narrative.

2.2 Local Geology

The Caliche Beaumont Sequestration Project Site includes Claimed as PBI [redacted] (see *Module B – Area of Review and Corrective Action*) located Claimed as PBI [redacted] of the town of Beaumont, Jefferson County, Texas (see **Figure A.2.24**). The AoR includes approximately 3.9-square miles of leased acreage from the Claimed as PBI [redacted]). The AoR lies on the southwestern side of the Neches River, located Claimed as PBI [redacted]. The AoR includes the far western edge of the Spindletop salt dome

and merges with the southeasterly regional dip in the area. Topographically, the region is relatively flat with surface elevations no greater than 25 feet in the area of interest. The following sections detail the geology on a local scale, specific to the area within and around the AoR. Site-specific geology maps in the following discussion are attached to this *Module A*.

The Spindletop salt dome is nearly circular in shape and approximately one mile in diameter (Clark and Halbouty, 1952). The southwestern periphery of the salt dome is located Claimed as PBI [redacted] of the proposed Class VI injection wells. Wells situated along the periphery of the salt dome have established the top of the salt to a depth of approximately 3,000 ft bgs. The outer edge of the salt dome is known to dip very steeply since the 4,000-foot offset flank wells are not known to encounter any salt (PB-KBB, Inc., 1990).

2.2.1 Data Sets Used for Site Evaluation

Multiple sets of data are used to evaluate and characterize the geology for the Caliche Beaumont Sequestration Project Site. Various forms of input data are available (publicly, commercially, and internally) for generating the integrated subsurface description of the Caliche Beaumont Sequestration Project Site. An extent of 60 square miles is investigated to develop the local geology maps and cross-sections.

Base Maps and Well Locations

An initial basemap for the project was acquired from a third-party commercial service (P2 Energy Services Tobin basemap) and is used as the primary source (source 1) for oil and gas (legacy) surface and bottom hole well locations. This primary source was then compared and updated with additional well data from other commercial and public sources: the Texas Railroad Commission (RRC) (source 2), and IHS Markit (source 3). An additional final check was compared with historical maps provided by Geomap (Cambe Maps), which was used as a quality check for historical well locations. Locations were cross-checked with data provided from log headers and drilling records to resolve discrepancies.

2.2.1.1 Offset Well Logs

Well log data were acquired for wells within an approximately 60-square-mile area surrounding the proposed Caliche Beaumont Sequestration Project Site (see **Figure A.2.25**). Formation tops were correlated across the area of interest and used to develop structure maps, isopach maps, and cross-sections. Located in the northeast portion of the study area is the Spindletop oil and gas field. Initial oil production in the field was from the cap rock of the salt dome, at a depth of approximately 1,000 ft bgs or less (Eby and Halbouty, 1937). Subsequently, in 1925, oil was discovered on the flanks of the dome (Halbouty, 1967). More than 156 million barrels of oil had been produced when production slowed down in the 1990s, from cap rock, Miocene, Pliocene, and Oligocene-aged strata. All flank oil and gas production occurred close to the periphery of the salt dome from disturbed, truncated structural and stratigraphic traps. The AoR also includes active brine disposal wells associated with mined cavern operations within the Spindletop salt dome. Publicly available and purchased well logs utilized in this Section 2.2 – Local Geology are provided in **Appendices A.A and A.B**, respectively.

2.2.1.2 Seismic Data

Two-dimensional (2D) geophysical seismic data were used to confirm general structural attitudes in the project area. A total of six 2D seismic lines were acquired from commercial vendors who

own the rights to the data (business confidential). The available 2D seismic data that cross the project area are of sufficient quality to be utilized in a seismic interpretation (**Figure A.2.26**).

- Claimed as PBI [redacted]

The seismic lines were reviewed for quality assurance/quality control (QA/QC) and the data were deemed adequately processed to meet the primary objectives of the Caliche Beaumont Sequestration Project Site – to derive attitudes (strike and dip) of the stratal surfaces and to confirm placements of faults transected by the lines.

The 2D seismic data were loaded into Kingdom™ Seismic and Geological Software using the Texas South NAD27 projection. Because of the relative lack of near-surface velocity anomalies and only moderate subsurface dip rates, the seismic data were utilized to calibrate structural control and to identify deeper subsurface anomalies. Interpretations were made in two-way travel time.

2.2.2 Local Stratigraphy

The injection and confinement system present beneath the Caliche Beaumont Sequestration Project Site is composed of sediments of Miocene-Oligocene sands and shales. The local stratigraphy is established on a type-log (**Figure A.2.2**) and is used as a basis for correlation with the offset well data. Using this type-log, and nearby logs, which represent the shallower stratigraphy, including the lowermost underground source of drinking water (USDW), the following local stratigraphic formations are evaluated (in ascending order beginning with the Frio Formation):

- Catahoula Group (Frio and Anahuac)
- Fleming Group (Oakville and Lagarto)
- Goliad
- Willis
- Lissie and Beaumont

The proposed injection zone encompasses three distinct sand intervals within the Upper Frio Formation. The injection zone portion of the storage complex is confined by the overlying shales of the Upper Frio, Anahuac, and Lower Oakville Formations; however, the bottom of the Anahuac Formation is identified as the primary confining unit and therefore is the top horizon in the static and dynamic models. Injection is confined between Claimed as PBI [redacted] across the Caliche Beaumont Sequestration Project Site. The base of the injection zone coincides with the Upper Hackberry Unconformity, a channeled unconformity surface through the Middle and

Lower Frio Formation (Ewing, 1986). The Upper Hackberry shales below the Upper Frio sands are abnormally pressured, with a natural pressure gradient approaching 0.8 pounds per square inch per foot (psi/ft). Therefore, the Upper Hackberry shale provides a lower pressure boundary in the modeling.

Isopach maps referenced in Section 2.2 are attached to this *Module A* and discussed in ascending order beginning with the Frio Formation.

2.2.2.1 Catahoula Group

The Catahoula Group is generally the deepest deposits penetrated in the local area. The Catahoula Group is subdivided into two formations: the Frio Formation and the Anahuac Formation.

Upper Frio Formation – Injection Zone

The Frio Formation is a regressive sequence deposited under deltaic conditions near its base and shallow marine environments near its top.

Deposition of the pro-gradational Frio Formation marine wedge was initiated during a major global sea level fall and continued along the entire Texas Gulf Coast under the influence of a slowly rising sea (Galloway et al., 1982b). Upper Frio deposition in the Beaumont area was present predominantly in the Buna strand-plain barrier system of southeast Texas (Galloway et al., 1982b) (see **Exhibit A.2.1** below). Sediments carried along strike from the Houston delta system and deposited approximately parallel to the present coastline distinguish the Frio depositional system.

Electric logs of the interval generally exhibit a blocky pattern with irregularly upward-coarsening sandy intervals, indicative of wave-reworked sands from recurrent delta-destructional phases. The dominant sandy facies of the Upper Frio are stacked, aggradational shoreface, and beach deposits. The massive sand units are often separated by finer grained clastics, which accumulated in marsh and other low-energy environments during periods of regression.

Basinward shelf-slope equivalents of the Buna strand-plain deposits include the Texas portion of the Hackberry slope canyon-embayment system. Studies of equivalent strata in Louisiana have established a deep-water origin for the unit. Underlying the Upper Frio Sand shoreface and beach deposits are pro-delta shales (Galloway et al., 1982b).

As shown on **Figure A.2.24**, two structural cross-section transects (Northwest-Southeast (NW-SE; **Figure A.2.27**) and Southwest-Northeast (SW-NE; **Figure A.2.28**)) are indicated across the Caliche Beaumont Sequestration Project Site. As shown on **Figures A.2.27 and A.2.28**, the Upper Frio Formation exhibits good lateral continuity. As shown on **Figure A.2.2**, the Upper Frio Formation exhibits good reservoir characteristics, as seen in Claimed as PBI [redacted]. The Upper Frio injection zone contains three injection intervals (locally designated as the “Green,” “Yellow,” and “Gold” Sands on **Figure A.2.2**; the “Upper Frio Sand”). Net Sand isopach maps are prepared for the Green, Yellow, and Gold Sands in the Upper Frio (see **Figures A.2.29 to A.2.31**), which indicate that the injection intervals range in thickness from Claimed as PBI [redacted]. A low vertical permeability, approximately 50-foot-thick shale interval is present between both the Green and Yellow Sands and between the Yellow and Gold Sands, which provide for hydraulic isolation of each of the three Sands from each other and impede potential flow vertically along faults across various sand units. As shown on **Figure A.2.32**, the altitude of the base of the Upper Frio Sand injection zone across the AoR ranges between approximately Claimed as PBI [redacted].

Exhibit A.2.1. Frio Depositional Systems.

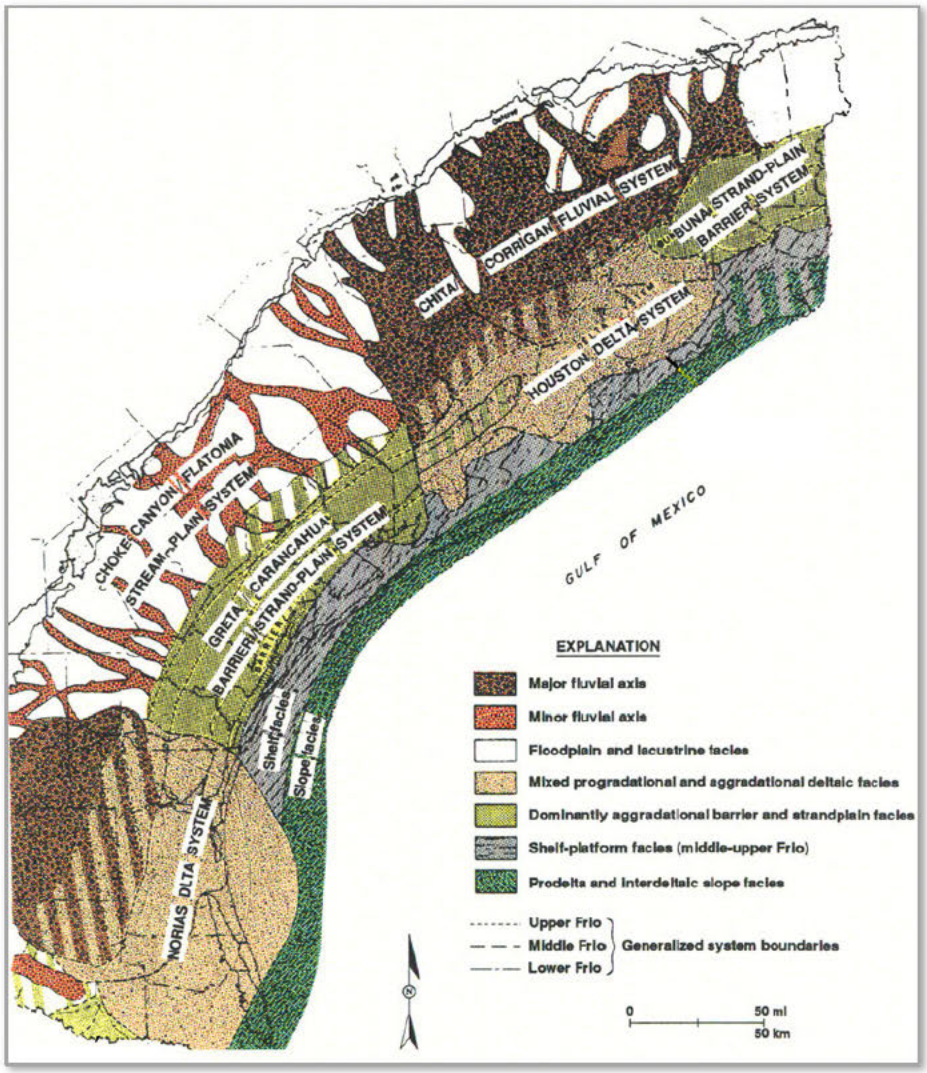

SOURCE: Galloway et al., 1982b, Figure 3-6.

Within the AoR, the Upper Frio Sand thickens to the northeast and thins toward the south (**Figure A.2.33**). Claimed as PBI [redacted] Upper Frio Sand in the combined injection intervals. The Upper Frio section consists of fine to medium-grained sandstones and gray to brown shale. As shown on **Figures A.2.27 and A.2.28**, the Upper Frio Formation also includes the laterally extensive shale-rich containment layer just above the Frio Green Sand and below the Frio "Orange" Sand. This confining layer of about [redacted] thickness provides for additional containment of the injected CO_2 into the Upper Frio Sand injection zone and also was observed at the Frio Brine Pilot Study Site (Hovorka et al., 2006).

Porosity of the Upper Frio Sand ranges from Claimed as PBI with an average of [redacted] based upon data gathered from Claimed as PBI [redacted] of the Spindletop salt dome and southeast of the AoR, and from Claimed as PBI [redacted] east of Spindletop salt dome and AoR.

Anahuac Formation – Confining Zone

Overlying the Upper Frio is the Anahuac Formation. The Anahuac shale is regionally known as an impermeable cap rock (Swanson et al., 2013; Hovorka et al., 2003). The Anahuac Formation is predominately a shale of marine origin containing a few tight limestone beds. The Anahuac Formation was deposited in an outer shelf and slope environment throughout the Texas coastal plain. Within the upper portion of the Anahuac Formation is a locally developed limestone member known informally as the Heterostegina ("Het") limestone. This limestone formed reefs around several salt domes and salt uplifts in southeast Texas and probably accumulated wherever uplifts raised the seafloor above the muddy bottom. In the project area, the tight micritic Het limestone forms an east-west band across the area lying between the updip margin of the Anahuac north of Spindletop salt dome and the downdip limit of environments favorable for carbonate deposition south of Hildebrandt Bayou Field. Claimed as PBI [redacted]

The Anahuac Formation thickens to the south-southeast and thins toward the northwest and has an average thickness of [redacted] feet in the AoR (**Figure A.2.34**). Claimed as PBI [redacted].

2.2.2.2 Fleming Group

The Fleming Group is comprised of the Oakville Formation (lower Miocene) and the Lagarto Formation (upper Miocene).

Oakville

The Oakville Formation forms the lowermost unit of the thick Miocene Fleming Group terrigenous clastic wedge that was deposited throughout the Texas Gulf Coast. Deposition of the Oakville Formation occurred in relatively shallow water across the broad, submerged shelf platform constructed during Frio deposition. The Oakville is covered by the transgressive Lagarto shale (see **Figure A.2.1** in Section 2.1 of this *Module A*). Oakville sedimentation along the Texas Gulf Coast occurred in two distinct fluvial-deltaic systems which were separated by a barrier-strandplain depositional system along the central Texas Gulf Coast (Galloway et al., 1986). In the Beaumont area, the Oakville Formation sands (lower Miocene) were deposited in a fluvial environment and are composed of channel, meander belt, and crevasse splay deposits. Sandstone of the Oakville Formation form the Jasper aquifer in Jefferson County. As shown on **Figures A.2.27 and A.2.28**, two distinct laterally consistent shale-rich containment layers of about Claimed as PBI thickness are present in the Lower and Middle Oakville Formation at top depths of Claimed as PBI [redacted], respectively.

The Oakville Formation thins on the flanks of Spindletop and Port Neches salt domes that were positive features during the early Miocene. The Oakville Sand interval extends from Claimed as PBI [redacted]

Lagarto

The Lagarto Formation (upper Miocene) was deposited in a deltaic environment. When progradation of the lower Miocene Oakville reached the Frio paleo-continental margin, the rate slowed as large-scale growth faulting created a narrow expansion zone. Long-term shoreline stability and retreat characterized Lagarto deposition with occasional temporary progradation. The Calcasieu delta system is a better developed reservoir in the Lagarto in Jefferson County. Progradation of the Upper Fleming depositional unit constructed a prominent seaward bulge in the continental margin. The delta system contains two primary facies assemblages:

(1) interbedded pro-delta mudstones and expanded sandy progradational successions along the distal margin, and
(2) stacked, delta-front, coastal-barrier and delta destructional shoreline sandstone of the main delta body complex.

As shown on **Figures A.2.27 and A.2.28**, the Middle Lagarto Formation also includes the laterally extensive shale-rich Burkeville confining system of about Claimed as PBI thickness present at a top depth of Claimed as PBI .

The wave-reworked delta margin facies extend up-dip into Jefferson County, where sandstone averages up to Claimed as PBI of the total Lagarto interval. As shown on **Figures A.2.27 and A.2.28**, the entirety of the Lagarto Formation is considered to be a secondary containment interval between the first transmissive zone of the Oakville Formation and the Lower Chicot USDW (see Section 2.2).

2.2.2.3 Goliad Formation (Late-Miocene to Early Pliocene)

Overlying the Fleming Group sediments are sediments of the Goliad Formation. The Goliad represents the last regionally significant influx of terrigenous clastic sediments into the western Gulf of Mexico Basin during the late Miocene to early Pliocene. The Goliad sedimentary sequence is similar in character to the underlying Upper Fleming unit, having been deposited in fluvial, deltaic, and marginal marine environments. The Goliad Formation consists of a sequence of interbedded sands and clays, representing a switch to a more terrestrial/fluvial origin than the underlying marine Miocene sediments. Sandstone of the Goliad Formation, along with the upper Lagarto, form the Evangeline aquifer in Jefferson County (Aronow and Wesselman, 1971). The section thickens in a dip direction and has a variable thickness along strike. In the project area, the unit reaches a thickness of Claimed as PBI and is composed of interbedded fluvial and deltaic sandstone with local minor conglomerates.

2.2.2.4 Pliocene, Pleistocene and Holocene

Lying conformably above the Goliad are the Pliocene and Pleistocene sediments of the Willis, Lissie, and Beaumont Formations which were deposited under the influence of the complex glacial and interglacial climatic and sea level changes of the Pleistocene (see **Figure A.2.1** in Section 2.1 of this *Module A*).

The Willis Formation was deposited in fluvial and deltaic environments and thickens in a dip direction as well as along strike toward the southwest. Overlying the Willis Formation is the Lissie Formation (see **Figure A.2.1** in Section 2.1 of this *Module A*). Throughout Southeast Texas, the Lissie Formation is subdivided into the Bentley and Montgomery Formations. Both the Lissie and overlying Beaumont Formations were deposited in fluvial environments and are composed of interbedded channel sandstone, crevasse splays, gravels, and flanking meander belt deposits in the Beaumont area.

The Beaumont Formation is generally less than 100 feet thick in the Beaumont area and is the oldest unit found in outcrop in Jefferson County (Aronow and Wesselman, 1971). The unit is commonly a fine-grained facies (clay) in surface exposures. Pleistocene sediments thicken along the Texas-Louisiana border and in a dip direction where there was significant deposition along growth faults during Pleistocene low sea level stands. The combined thickness of the Pliocene-Pleistocene formations is approximately 1,000 feet in the plant vicinity. The Pleistocene sediments grade conformably into the overlying Holocene depositional units.

With the retreat of the Pleistocene glaciers, sea level began a final irregular rise to its present level. As sea level rose, the lower reaches of the river valleys slowly filled with brackish to marine water and subsequently began filling with fluvial sediments. In the Beaumont area, Holocene sediments (see **Figure A.2.1** in Section 2.1 of this *Module A*) were deposited in river valley meander belts and are primarily composed of point-bar sandstone with interbedded finer grained overbank deposits (Fisher et al., 1973). The most extensive Holocene sedimentation occurred in coastal marsh, mud flat, and beach environments located along the southern coastal margin of Jefferson and Chambers Counties (Aronow and Wesselman, 1971). Together the Pliocene, Pleistocene, and Holocene strata comprise the Chicot aquifer (Aronow and Wesselman, 1971).

During recent times, sediment compaction, slow basin subsidence, and minor glacial fluctuations have resulted in relatively insignificant relative sea level changes (Fisher et al., 1973). The coastal zone in Southeast Texas has evolved to its present condition through the continuing processes of erosion, deposition, compaction, and subsidence. Alluvium deposition in Jefferson County is restricted to the geomorphic floodplain of the present Neches River system and to the entrenched valleys of the ancestral Neches River system, which had down-cut into the underlying Pleistocene deposits during sea level low stands. This alluvial fill has been found to be as thick as 120 feet at the mouth of the Neches River (Aronow and Wesselman, 1971). The alluvium at the Beaumont Works is composed of a basal coarse-grained sand to gravel, grading upward into finer sandstone, siltstone, and clay and is approximately 20 feet thick.

2.2.3 Local Structure

The Caliche Beaumont Sequestration Project Site is located on the eastern side of the Houston Embayment, within the western side of the Gulf Coast Salt Basin along the Upper Texas Gulf Coast (**Figure A.2.11**). This area is characterized by salt diapirism, faulting, and unfaulted salt withdrawal sub-basins (Bebout et al., 1978). The Oligocene through Holocene section thickens basinward (towards the coast), periodically interrupted by coast-parallel fault systems and salt diapirism, which often become increasingly complex as they extend upward through the section (Galloway et al., 1982a). Most of the Gulf Coast is underlain by Jurassic age Louann Salt in structurally controlled basins. Sedimentation on top of the Louann Salt has caused gravitational instability resulting in compaction, lateral flowage, and intrusions of the salt (salt domes). The main structural feature nearest the Caliche Beaumont Sequestration Project Site is the Spindletop salt dome. This structural feature influences the nature and structural orientation of the formations present below the Caliche Beaumont Sequestration Project Site as supported by regional cross sections (**Figures A.2.15 through A.2.18**).

Local structure maps are based on correlation of well log tops across the project and include:

- Top of Anahuac: Primary Confining Unit (see **Figure A.2.35).**
- Top of Frio Orange: Top of Upper Frio Formation (see **Figure A.2.36).**
- Top of Frio Green: Top of the Upper Frio Sand Injection Zone (see **Figure A.2.37**).
- Base of Frio Gold: Base of the Upper Frio Sand Injection Zone (see **Figure A.2.32).**

Additionally, 2D seismic data were evaluated for both structure and evaluation of the presence or absence of any faulting in the Caliche Beaumont Sequestration Project Site (**Appendix A.C**). Check Shot Velocity surveys were used to tie in the well logs with the seismic data. Seismic Line Claimed as PBI was used as the base line and is tied into the Claimed as PBI [redacted]. A bright seismic marker is located at the depth of the top of the Anahuac and Het limestone interval and reflects the velocity/density change within the micritic limestone.

Analysis of the seismic data confirms the presence of faults defined by analysis of the area oil and gas well logs in the project area (**Figure A.2.38**). A large down-to-the-southeast fault, designated as Fault "A", extends from the southwestern margin of Spindletop salt dome (as a domal radial fault-extending and influencing regional strata) and passes through the subsurface in a northeast to southwest trending direction, transecting the southernmost portions of the Caliche Beaumont Sequestration Project Site and terminating into Lovells Lake Field (where it is the master field fault). The fault has Claimed as PBI of displacement along its length at the top of the Upper Frio Formation (**Figure A.2.36**) and extends above the top of the Anahuac confining unit (**Figure A.2.38**). A small throw antithetic fault to Fault A is identifiable on several of the seismic lines. However, this antithetic fault does not appear to intersect any of the area oil and gas wells. This fault is depicted on the structure maps presented in this Section 2.2 – Local Geology.

A cross-section location and index map (**Figure A.2.24**), and two perpendicular structural-stratigraphic cross sections (**Figures A.2.27 and A.2.28**), are constructed to characterize the subsurface structure and stratigraphy across the project area. These sections show the lateral continuity of the Upper Frio Sand and the lithologic character of the upper confining system of the Upper Frio Sand injection zone across the area. Thick shales of the upper confining system (Upper Frio, Anahuac, and lowermost Oakville Formations) and the lower confining unit (Frio-Hackberry shale) are sufficiently impermeable, thick, and laterally extensive to protect all strata above and below the Upper Frio Sand injection zone from contamination by injected CO_2. The sections also show the presence of several shale-dominated intervals within the Miocene section that would provide secondary and tertiary containment to the Confining Zone. These are identified as:

- Mid-Oakville Containment Interval, and
- Lagarto Containment Interval (includes the Burkeville Confining System).

Additionally, there are several identifiable layers that can be characterized as the “Buffer Aquifer/ Aquiclude System” per Fed. Reg. v. 53, n. 143, p. 28133 (26 July 1988), defined as a *“…sequence of permeable and less permeable strata..”* per 40 CFR §146.62(d)(1). These intervals are identified as the Middle and Upper Oakville Buffer Aquifer System of the Jasper aquifer. These Buffer Aquifer intervals allow for bleed-off of pressure and are adequate reservoirs capable of containing any CO_2 or other fluids that breach the Upper Confining System; therefore, the Buffer Aquifer/Aquiclude System provides an additional safeguard of protection for the Caliche Beaumont Sequestration Project Site.

2.2.3.1 Faulting in the Area of Interest

Per 40 CFR §146.82(a)(3)(ii)], the structure and isopach maps and the seismic data of the Caliche Beaumont Sequestration Project Site indicate the presence of faults (see **Figure A.2.32**). Detailed analyses derived from subsurface structure mapping and cross-section lines of well logs penetrating the Oakville and Frio Formations in the Beaumont area indicate that the Caliche Beaumont Sequestration Project Site is located in a structural low or syncline. A discussion of the three identified local faults is provided below.

Fault A

As shown on **Figure A.2.32**, a large down-to-the-southeast fault, designated as Fault "A", extends from the southwestern margin of Spindletop salt dome (as a domal radial and growth fault – extending and influencing regional strata) and passes through the subsurface in a northeast to southwest trending direction, transecting the southernmost portions of the Caliche Beaumont

Sequestration Project Site and terminating into Lovells Lake Field (where it is the master field fault). The fault has Claimed as PBI of displacement along its length at the top of the Frio Formation and transects approximately [redacted] wells across the project area. These fault cuts are documented on the structure maps in this Section 2.2 – Local Geology. The Claimed as PBI [redacted] and the Claimed as PBI [redacted] are approximately normal to the fault trace with a fault cut in each wellbore. Based on the horizontal distance between the two wells and the subsea depth of fault cut in each well, an angle of approximately [redacted] from horizontal is calculated for the fault plane.

Fault A can be observed on all the evaluated 2D seismic lines, with the exception of Seismic Line No. WGI-EHB-2, which does not cross the fault. Offset is approximately Claimed as PBI at the top of the Anahuac horizon. At depth for the top of the Anahuac, this equates to a displacement of Claimed as PBI [redacted], based on check shot velocities.

A small throw antithetic fault is associated with Fault A. This antithetic fault is only apparent on the 2D seismic as the fault does not appear to intersect any of the wellbores in the area. On the 2D seismic data, the fault terminates into Fault A above the top of the Frio/Anahuac interval; however, the intersection of the antithetic fault into the fault plane of Fault A may be deeper the closer to the location of Spindletop salt dome. The antithetic fault is shown in "green" on the southeastern side of Fault A on the structure maps.

Fault B

A down-to-the-north fault, designated as Fault "B", extends from the western margin of Spindletop Dome (as a domal radial fault) and passes through the subsurface in an east to west trending direction, terminating into the northernmost portions of the City of Beaumont Acreage. The fault has Claimed as PBI [redacted] of offset near the dome but feathers out to lesser throw (Claimed as PBI [redacted] of displacement) to the west along its length. These fault cuts for Fault B are documented on the structure maps in this Section 2.2 – Local Geology. Claimed as PBI [redacted] are approximately normal to the fault trace with a fault cut in each wellbore. Based on the distance between the two wells and the subsea depth of fault cut in each well, an angle of approximately [redacted] from horizontal is calculated for the fault plane.

Fault B may be resolvable on 2D line Claimed as PBI [redacted] where a shallow discontinuity appears at about Claimed as PBI [redacted] vertical depth between shot points Claimed as PBI [redacted]. Offset is limited and the plane of the fault falls only within the Miocene section. It is possible that the fault moves out of the plane of the seismic line as the indicated fault cuts in the saltwater disposal wells and contouring at the Frio level indicates a deeper fault. Fault B is well defined based on fault cuts in the Claimed as PBI [redacted] Fault B does not intersect the AoR and therefore is not included for further consideration.

Fault C

A third domal radial fault, Fault "C", is shown on **Figure A.2.32** as well extending from the northern margin of Spindletop salt dome. This down-to-the-west fault trends South-North and does not intersect the Caliche Beaumont Sequestration Project Site and therefore is not included for further consideration.

2.2.3.2 Fault Transmissivity

The Oligocene Frio-Hackberry Formation is a highly productive, fluvio-deltaic, oil and gas bearing unit along the northern shore of the Gulf of Mexico (Swanson et al., 2013; see **Exhibit A.2.2**). Across the northern shore of the Gulf, there are structural and stratigraphic traps that include

numerous domal radial and, most notably, normal growth faults that intersect both Miocene and Oligocene formations (Swanson et al., 2013). Several lines-of-evidence (LOEs) demonstrate that these Gulf Coast faults exhibit minimal to no transmissivity, including:

1. Shales beneath the Caliche Beaumont Sequestration Project Site are ductile at the depths of interest.
2. Juxtaposition of ductile shale beds or sand-to-shale beds across a fault forms a vertical barrier to fluid flow.
3. Zones of deformed clay/shale can become greatly attenuated and trapped along fault planes.
4. Fault slippage generally "self-heals" over time.
5. Numerous oil and gas accumulations are trapped by the Gulf Coast faults and are targeted for oil and gas production.
6. Miocene formation pressure gradients exceed Oligocene formation pressure gradients.

As further discussed below, local faults below the Caliche Beaumont Sequestration Project Site bound the Upper Frio Sand injection zone laterally and prevent vertical preferential flow via the fault plane.

Exhibit A.2.2. Hydrocarbon Plays Along the Gulf Coast.

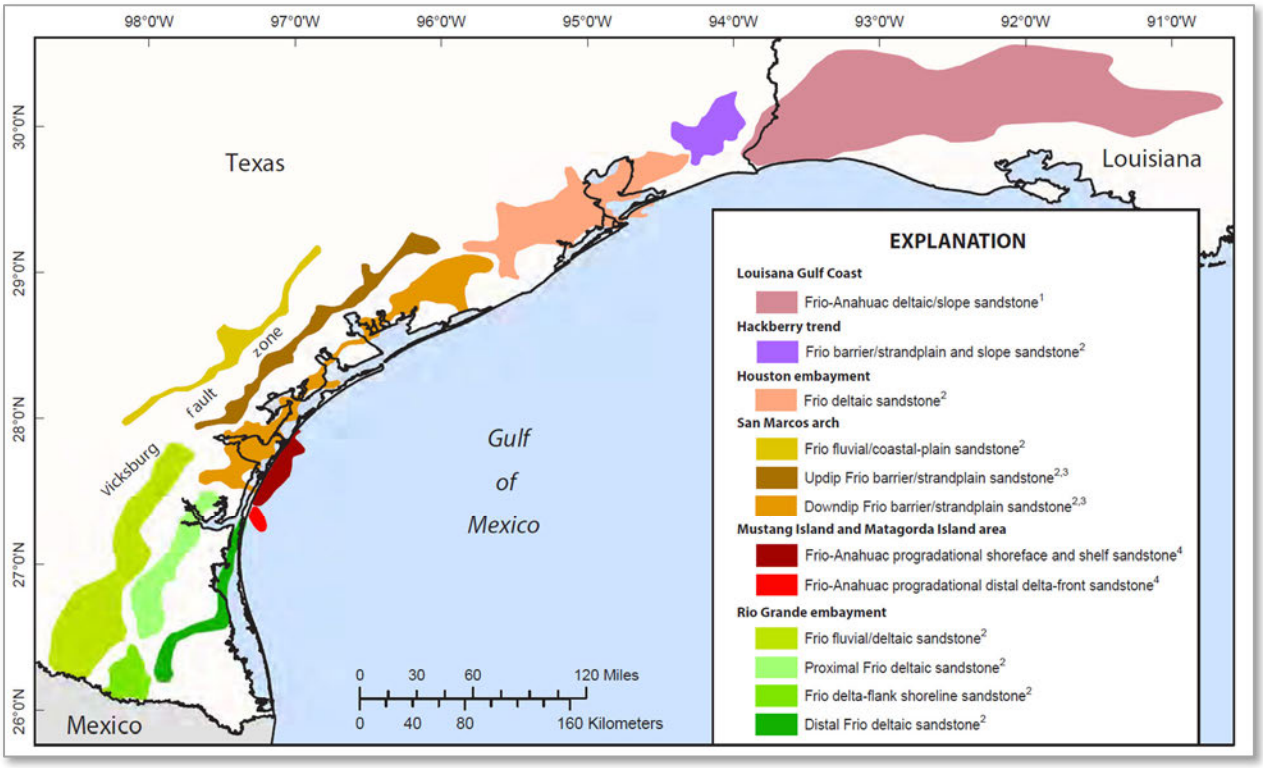

SOURCE: Modified from Swanson et al., 2013.

Vertical Fault Transmissivity

The potential for fault-plane clay smear material to provide a vertical avenue for fluid movement through shale-to-shale juxtaposed lithologies is minimal beneath the Caliche Beaumont

Sequestration Project Site. The vertical sealing nature of shale-to-shale juxtaposed lithologies can be seen in the numerous Gulf Coast oil and gas fields that have fault traps where both the top and the lateral seals are provided by shale beds. These hydrocarbon accumulations would not have occurred if the nearby faults were vertically transmissive above the productive intervals.

Site-specific evidence of vertical sealing is provided by shallower Miocene and deeper Vicksburg and Yegua oil and gas accumulations near the Caliche Beaumont Sequestration Project Site. Clark and Halbouty (1952) determined that faulting strongly controls oil accumulation at the Spindletop salt done. Some fault blocks are very prolific, whereas adjacent blocks are dry (i.e., "wet"), containing no hydrocarbons. At Spindletop, where faults directly control the position of oil, there are great differences in drilling depths, formations, and oil production present between offset wells. Wells located close together, but on opposite sides of a fault, prove the effect of fault block separation and sealing. These faults separate the oils into individual compartments and prevent movement of fluids from one fault block to another.

Halbouty (1990), in a special study for DuPont (Lucite International, 2008), demonstrated that Miocene oil production is fault-sealed at the Spindletop salt dome. Claimed as PBI [redacted] (see **Exhibits A.2.3 and A.2.4** below). The fault cut for Fault A can be picked at a depth of approximately Claimed as PBI in the Claimed as PBI and at a depth of approximately Claimed as PBI in the Claimed as PBI [redacted]. As evidenced by the well logs presented on **Exhibit A.2.4**, none of the sands above the Claimed as PBI appear to be hydrocarbon productive, confirming that the fault is both a lateral and vertical seal, likely due to clay smearing (further discussed below).

Exhibit A.2.3. Structural Cross-Section B-B' Transect Map.

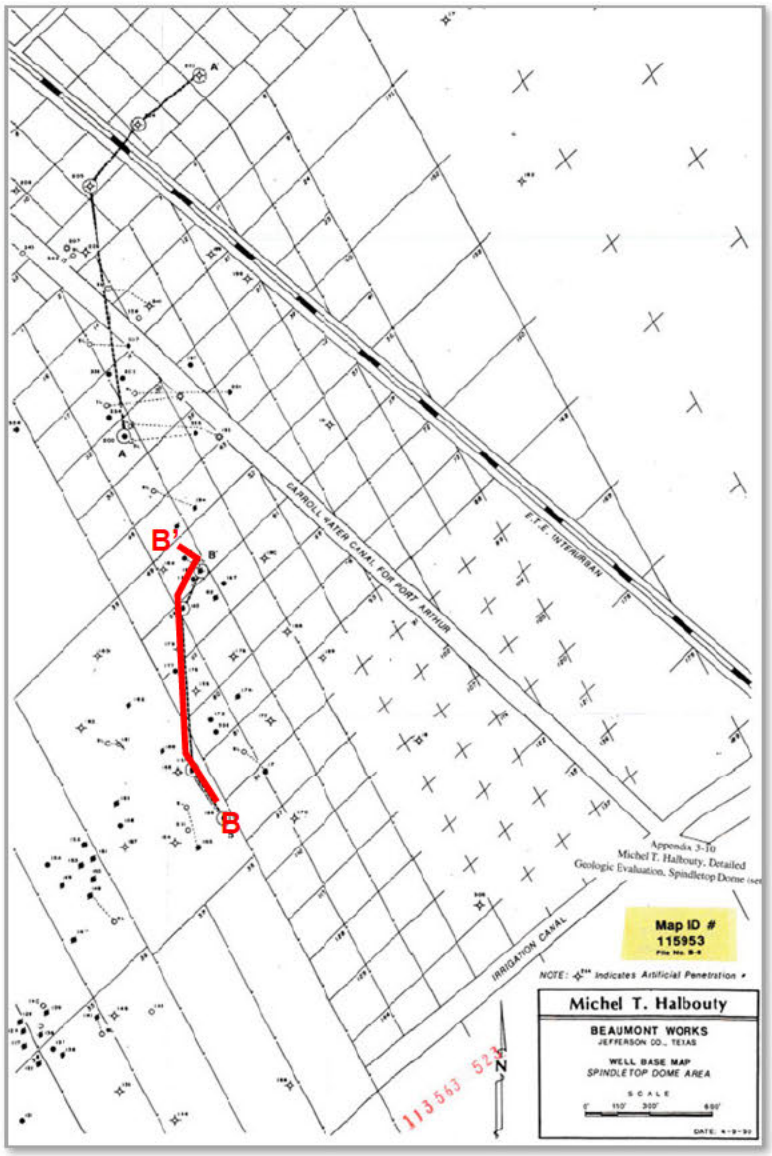

SOURCE: Modified from Halbouty, 1990.

Exhibit A.2.4. Structural Cross-Section B-B': Miocene 3700' Productive Sand near Spindletop Salt Dome.

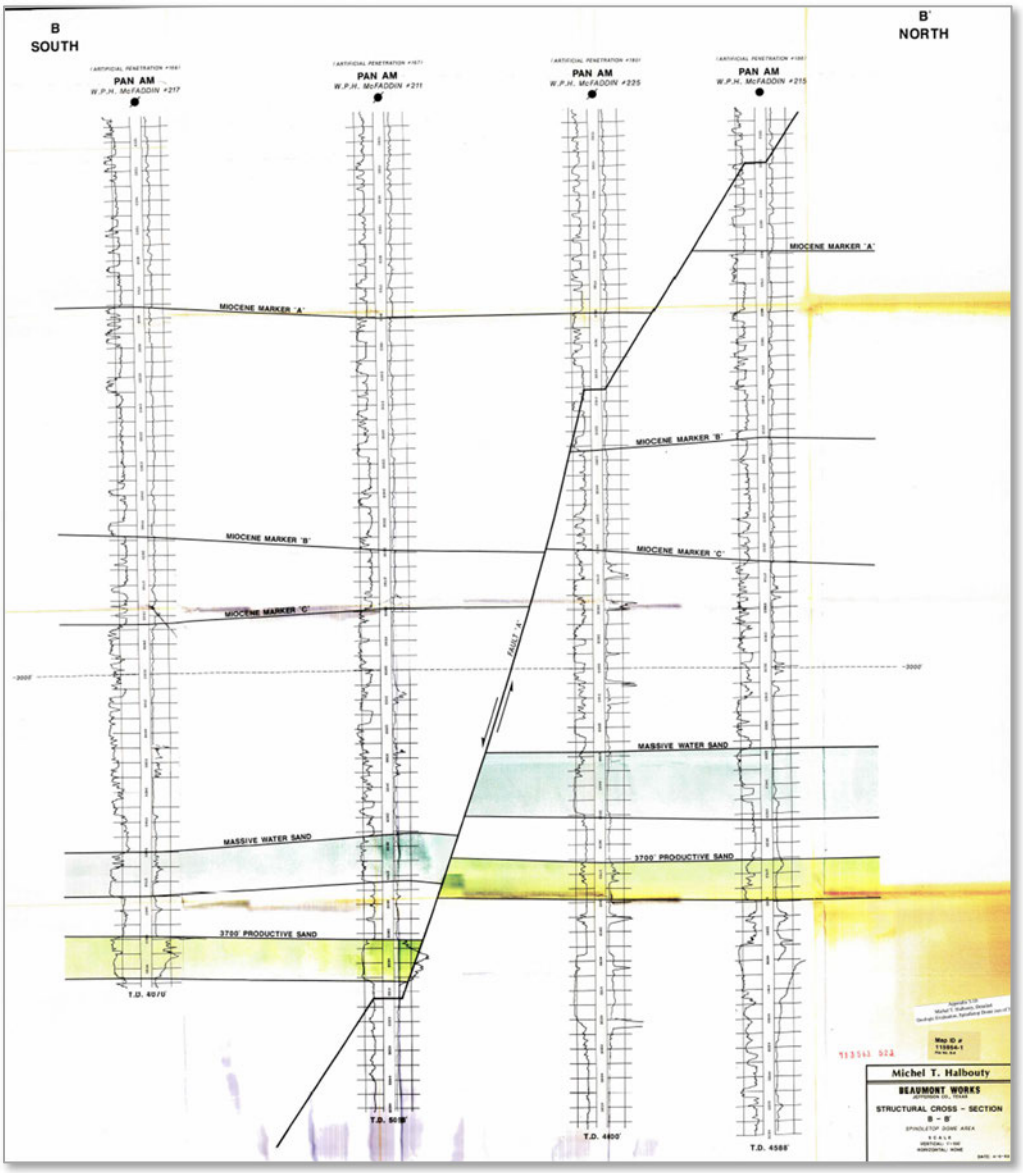

SOURCE: Halbouty, 1990.

A sequestration study evaluated the Frio and Anahuac formations just south of the Houston region and reported on the sealing potential of the thick, regional, ductile Anahuac Formation (Petra Nova, 2021). Also, if the Anahuac or other shale units in the section are intersected by a fault, they are not likely to generate open fractures, but to deform plastically by bending or smearing (Petra Nova, 2021).

Because the shales beneath the Caliche Beaumont Sequestration Project Site are ductile at depths of interest, the juxtaposition of shale beds or sand-to-shale beds across a fault will form a vertical barrier (seal) to fluid flow, due to their very low vertical permeability. This property of viscoelastic deformation behavior will cause any fractures and/or faults to close very rapidly in response to the in-situ compressive stresses within the surrounding sediments. This well-known

ductile (or plastic) behavior of the geologically young Gulf Coast shales is amply demonstrated by the presence of shale diapir structures and the natural closure of uncased boreholes with time (Johnston and Greene, 1979; Gray et al., 1980; Davis, 1986; Clark et al., 1987; Warner and Syed, 1986; Warner, 1988).

Jones and Haimson (1986) have found that due to the very plastic nature of Gulf Coast shales, faults will seal across shale-to-shale contacts, allowing no vertical fluid movement along the fault plane. E. I. DuPont de Nemours and Company conducted a borehole closure test at the Orange field salt dome which demonstrated the plastic nature of the Gulf Coast shales and the rapidity of shale movement to seal off open areas in the subsurface. The test conclusively demonstrated that the young Miocene shales of the Gulf Coast will flow and seal off an open area in the subsurface in a very short time period (test duration was approximately one week) (Clarke et al., 1991). Moreover, Doughty et al. (2008) found that block bounding faults in the Frio and Anahuac Formations at a nearby CO_2 injection site near Dayton, Texas were still sealed to fluid flow during CO_2 injection.

Smith (1980) presents a mechanism whereby shale may be emplaced along the fault plane to provide an effective seal against vertical fluid movement (see **Exhibit A.2.5** below). Shale can be deformed more readily prior to failure than sandstone in a sand-shale sequence. Continued deformation will eventually fault the shales, however, a zone of deformed shale may become greatly attenuated and trapped along the plane of the fault, resulting in a vertical seal.

Studies have shown that Gulf Coast faults also exhibit self-healing properties. When a fault develops within a low-porosity, clay poor rock, a fracture zone can occur along the plane. Several factors are involved when considering fault and fracture zone healing including formation ductility, fluid salinity, mineral precipitation, etc. While fracture zones may exist for certain more sandy portions of the Frio, the Anahuac and the Upper Frio containment layer are not likely to develop a fracture zone due to their more ductile characteristics (Vialle et al., 2016). Vialle et al. (2016) summarize multiple studies that suggest the fracture zone and fault plane can self-heal over time, especially under the large formation stress at depth. While the timescale ranges substantially, in some instances, it could be as short as days to self-heal.

The vertical sealing nature of the faults in the area also can be demonstrated by looking at the original formation pressure gradients for sands in the early Miocene-aged Fleming Group and Oligocene sands of the Frio Formation. For example, at the Claimed as PBI [redacted] If nearby faults were vertically transmissive, formation pressure gradients in the Miocene and Frio would be expected to be more similar, having equalized over geologic time.

Exhibit A.2.5. Shale Emplacement along Fault Plane Preventing Vertical Fluid Movement.

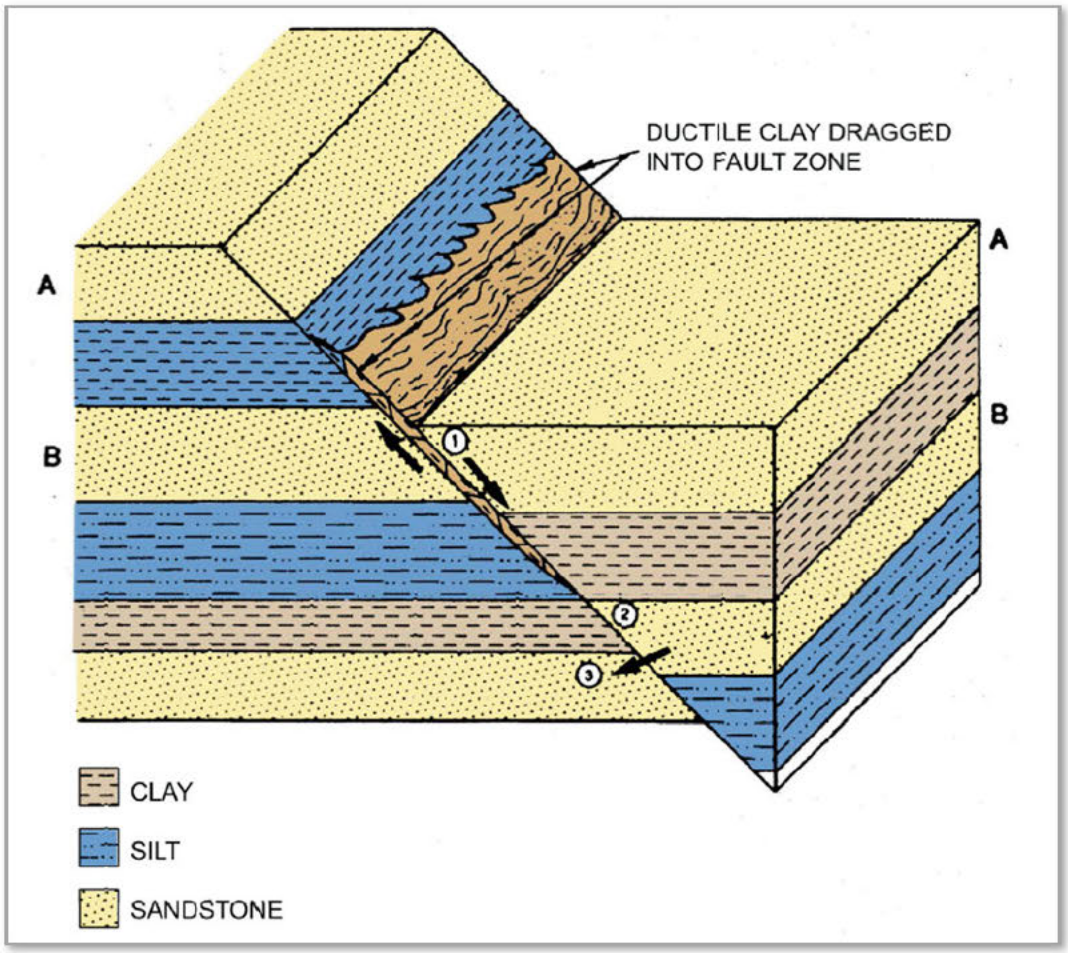

SOURCE: Modified from Smith (1980).

A similar differential in formation pressure gradients between the Fleming Group sands and Upper Frio Sands was observed at the recently completed Frio Brine Pilot – CO2 Sequestration Demonstration Project (run by the University of Texas Bureau of Economic Geology (UT-BEG)), located on the flank of Dayton Dome in nearby Liberty County, Texas. A Schlumberger Modular Dynamics Tester™ was used to take formation pressures in the Upper Frio test interval and in the overlying basal Fleming Group sands. At the Frio Brine Pilot Test Site, the basal Fleming Group sands had a formation pressure gradient of 0.448 psi/ft, while the underlying Upper Frio Sands had a lower formation pressure gradient of 0.436 psi/ft, thereby demonstrating hydraulic isolation.

Similarly, original formation pressure measurements at the Claimed as PBI located east of Houston, Texas and approximately nine miles south-southeast of the Claimed as PBI, showed pressure gradients in the range of Claimed as PBI to Claimed as PBI in Fleming Group sands versus the substantially lower pressure gradients measured in the Frio at the Claimed as PBI, which were on the order of Claimed as PBI

Therefore, the only mechanism available for vertical movement up along a fault is through "stair-stepping", whereby the fluid potentially moves laterally across juxtaposed sand-to-sand beds. However, beneath the Caliche Beaumont Sequestration Project Site, the preponderance of thick,

ductile shales within the Upper Frio, Anahuac, and Flemming Group above the Upper Frio Sand injection zone and notable fault offsets juxtaposing shale-to-shale or sand-to-shale beds will quickly restrict this type of movement.

Lateral Fault Transmissivity

Lateral fault seal can arise from juxtaposition of porous and permeable reservoir rock against nonporous or nonpermeable rock, or by the development of fault rock having a high entry pressure. Faults, in and of themselves, may not seal (Downey, 1984); however, faults that place porous intervals against impermeable rock form non-transmissive barriers (traps) (Swanson et al., 2013). Fault planes are normally inconsequential to migrating fluids, and generally are of significance only in the circumstance of shallow, near-surface faulting in an overall tensional regional stress environment. In such cases, field observations and theory (see Secor, 1965, for example) show that the fault plane may act as an open transmissive fracture. However, the process of faulting may result in a "disturbed" fault zone between the offset lithologies. Therefore, a two-tiered analysis approach may be required. First-order fault seal analysis involves identifying reservoir juxtaposition areas over the fault surface using mapping techniques. Second-order fault seal analysis ascertains whether the reservoir-to-reservoir contact is likely to support a pressure difference. A number of mechanisms have been recognized whereby fault planes can act as lateral seals (Knipe, 1992):

a) Juxtaposition, in which reservoir rock are juxtaposed against a low-permeability unit with a high entry pressure;

b) Clay smear or entrainment of clay/shale into the fault plane, thereby giving the fault "disturbed zone" a high entry pressure;

c) Catalysis, which is the crushing of sand grains to produce a fault gouge of finer grained material, giving the fault "disturbed zone" a high capillary pressure; and

d) Digenesis, where preferential cementation along a previously permeable fault plane may partially or completely remove porosity, creating a hydraulic seal.

Juxtaposition seals can be recognized explicitly by mapping the contact of the various units across a fault (such as an "Allen" cross-section, that shows the reservoir stratigraphy of both the "hanging wall" and "footwall" locations superimposed along a fault plane, showing the juxtaposition relationships of the various reservoir units across the fault). Identifying or predicting sealing via clay smear, catalysis, or digenesis requires an ability to relate these mechanisms to measurable properties or processes in the subsurface. The initial host rock is an important control on the fault disturbed zone material and properties, and thus, on seals. The host-rock properties that exert the most influence are the clay or phyllosilicate content, porosity, and permeability (Knipe, 1997).

Each of the sealing mechanisms is described in more detail in the following subsections. Note that none of the attributes described is, in itself, a measure of the sealing capacity of the fault surface. Instead, these attributes are an estimate of the sealing nature or relative likelihood of a seal being developed along a fault surface. To be useful, they must be calibrated from known seal and non-seal situations.

Connectivity of Juxtaposed Lithologies

The initial consideration in the evaluation of lateral transmissivity across a fault is the determination of juxtaposition of porous lithologies across a fault plane and the connectivity of the juxtaposed porous lithologies. In a sand and shale geologic sequence, faulting will result in the juxtaposition of like and/or unlike lithologies across the fault plane in three manners: a) sand-to-sand, b) sand-to-shale, and c) shale-to-shale. Each fault case must be assessed separately for

the lateral transmissivity of the juxtaposition of lithologies across the fault. In the case of a sand and shale sequence, the connectivity considers that fraction of net sand that is in geometric contact with sand across the fault. The lower the connectivity, the more likely the fault will tend to act as a seal and therefore the greater the effect of the fault on impeding fluid flow, resulting in increased pressure buildup. The determination of the percentage of connectivity requires an accurate depiction of the stratigraphy on both sides of the fault for its entire length. For complex situations, a fault-plane section (a display of the geometry of the stratigraphy brought into contact by fault displacement, i.e., two sides of a fault juxtaposed) can be prepared to show relationships (Allen, 1989). The plane of the "Allen" Section is not vertical but dips along the plane of the fault. Alternatively, a "juxtaposition diagram" (Knipe, 1997) can be constructed from the stratigraphy on either side of the fault to evaluate lithological cross-contacts. High sand-to-sand connectivity at the fault plane will have minimal impact on the lateral transmissivity of the reservoir.

As stated above, fault planes are normally inconsequential to migrating fluids, and generally are of significance as sealing surfaces only because they may juxtapose rocks of differing capillary properties and fluid pressures (Smith, 1966; Downey, 1984). Much of the knowledge base for characterizing fault seal/non-seal emanates from studies in oil fields, which deal with unlike fluid phases (oil-water) juxtaposed across a fault. In these examples, where porous intervals are juxtaposed, significant additional pressure (displacement pressure) may be needed to overcome capillary properties and force hydrocarbon molecules into connate water-filled pore spaces through and across a fault that would otherwise be transmissive to like-phase fluids (Smith, 1966). The forces that need to be overcome include the hydrocarbon-water interfacial tension and wettability of the reservoir rock, prior to initiation of hydrocarbon fluid flow. The discounting of the existence of the pressure differential effect due to differing capillary properties has probably influenced field study conclusions where there are insufficient data to recognize this phenomenon as the cause for sealing. The significance of differing capillary properties and fluid pressures also will apply to the unlike fluid phases of the formation fluid and the supercritical CO_2 (CO_2(sc)).

For example, annual transient pressure testing since 1991 of the Claimed as PBI [redacted] located on the Claimed as PBI of Spindletop, confirm the lateral sealing nature of the local fault. Claimed as PBI [redacted] fault is observable on area 2D seismic lines (Dow, 2018) and is interpreted to cut the stratigraphic section over an interval from as shallow as Claimed as PBI [redacted]. Claimed as PBI [redacted] Throw of the fault at the Upper Frio Formation level is interpreted to be approximately Claimed as PBI making it an ideal analogue to Fault A cross-cutting the southern Caliche Beaumont Sequestration Project Site (Dow, 2018). Evaluation of the pressure fall-off curve in the Claimed as PBI [redacted] shows a "textbook" single boundary response at a distance of approximately Claimed as PBI from WDW-188 (Dow, 2018), indicating that this fault is a lateral barrier to flow. Additionally, the flowing and shut-in pressures from the historical falloff test results offer a good match and calibration to the modeled no-flow boundary within the site-specific reservoir system (Dow, 2018).

Clay Smear

In cases where thick, undercompacted clay shales are interspersed between porous intervals, "clay smears" can develop and be emplaced along a fault plane (Smith, 1980; Vrolijk et al., 2016). Undercompacted clays can be deformed much more readily prior to failure than sandstone can in a sand-clay sequence. Continued deformation will eventually fault the clay/shales; however, a zone of deformed clay/shale may become greatly attenuated and trapped along the plane of the fault, resulting in a vertical and horizontal seal. Such fault-plane clay smears are common small-scale features and have been reported in East Texas outcrops (Smith, 1980), coal mines in

Germany (Weber, 1978), and have been inferred from log interpretation of fault zones (Weber, 1978; Berg and Avery, 1995).

Conclusions from faulting case histories indicate that the fault-zone clay/shale thickness and petrophysical properties of the clay/shale, in the displaced section at the time of faulting, are the primary factors that govern whether or not a clay/shale will "smear" and form boundary fault-zone material for sealing. Lehner and Pilaar (1991) observed from fault outcrops that clay smear, as an effective sealing mechanism, is likely to occur only in soft sediments and at sufficiently slow fault slip velocities. Smith (1980) found that growth faults, which form relatively near the surface contemporaneously with deposition (i.e., syndepositional faults), have a greater potential to be sealing due to clay smear than post-depositional faults, forming when sediments are more indurated. Harding et al. (1989) and Jev et al. (1993) also concluded that syndepositional faulting usually favors clay smear sealing because the muds are generally uncompacted at the time of displacement and are more likely to smear along the fault plane. However, even in cases of initial fault seal, fault plane seal breakdown may occur along weak areas, as the result of increased pressure differentials (resulting from production or injection) from one side of the fault to the other (Bouvier et al., 1989).

Claimed as PBI

[redacted] increasing with proximity to Spindletop salt dome structure (Lucite International, 2008). Review of available oil and gas logs indicate the juxtaposition of sand-prone lithologies across from each other along the fault plane; however, pressure falloff testing confirm no lateral transmissivity and therefore the effectiveness of clay smear as a fault seal.

The following factors have been found to control the likelihood of clay/shale smearing: 1) thicker source beds can produce thicker clay smears; 2) shear-type smears decrease in thickness with increasing distance from the source layer; 3) abrasion-type smears decrease in thickness with increasing fault throw; and 4) multiple source beds can give a combined continuous smear (Yielding et al., 1997). Several algorithms have been proposed for providing a quantitative approach to clay smear prediction. Bouvier et al. (1989) presents a study of the Nun River field in the Niger Delta, describing the "Clay Smear Potential" (CSP) as a means of estimating the likelihood of clay smearing in areas of sand-to-sand juxtaposition. The CSP is a measure of the amount of clay that has been smeared from individual shale source beds at a certain point along a fault plane. The CSP equation (Equation 1) is shown below:

$$CSP = \sum \frac{(Shale - bed - thickness)^2}{(Dis\tan ce - from - source - bed)} \qquad \text{(Eq. 1)}$$

The CSP models the behavior of shear-type smears for distance tapering and additive effect of compound clay beds; therefore, multiple shale beds can be used and the thickness is additive as shown by the sigma in Equation 1. Yielding et al. (1997) calibrated CSPs at multiple sites against known sealing and non-sealing faults and showed that CSP values above approximately 5-30 were sealed faults. Yielding et al. (1997) also modified the CSP formula to a more general form, called "Smear Factor" (SF), as shown below in Equation 2:

$$SF = \sum \frac{(Shale - bed - thickness)^n}{(Dis\tan ce - from - source - bed)^m} \qquad \text{(Eq. 2)}$$

The exponents “m” and “n” can be determined via experimental or observational studies. Note that as “n” increases above a value of one, thicker source beds are proportionally weighted higher than are thin beds (i.e., a bed twice as thick is weighted by more than twice as much).

Lindsey et al. (1993) proposed a “Shale Smear Factor” (SSF) based on observations of abrasion smears in a lithified sequence, as shown below in Equation 3:

$$SSF = \frac{Fault - throw}{Shale - layer - thckness} \qquad \text{(Eq. 3)}$$

Note that the SSF remains constant between the offset terminations because it does not depend on smear distance. However, lateral changes in fault throw would have a corresponding change on the calculated SSF. Lindsey et al. (1993) concluded that shale smears with a SSF of up to 7 are likely to be continuous.

Yielding et al. (1997) (and later Hovorka et al. (2003)) also recognized that the CSP and SSF may be difficult to apply in thick heterogeneous sequences due to the complications inherent in mapping every shale bed and then considering its contributive effect at the fault surface. They suggested an approach that considers the bulk properties of the sequence at the scale of the reservoir mapping utilized, termed the “Shale Gouge Ratio” (SGR), as shown below in Equation 4:

$$SGR = \frac{\sum\left[\left(Zone - thickness\right) \times \left(Zone - clay - fraction\right)\right]}{Fault - throw} \times 100\% \qquad \text{(Eq. 4)}$$

The SGR represents the proportion of shale or clay that might be entrained in the fault zone by a variety of mechanisms. Wall rocks with a high shale content tend to produce greater proportions of shale or clay in the fault zone. Investigation of fields in three different basins (Niger Delta; Northern North Sea; and Offshore Trinidad) show seal threshold on the order of 10 to 20 percent SGR (Yielding et al., 1997).

Cataclasis

Cataclasis involves the fracture, crushing, and rotation of mineral grains along the plane of the fault (Spencer, 1977). As such, it is a mechanism of brittle deformation. When the degree of deformation is severe, cataclasis may result in a “gouge” or “destruction” zone along the fault that is comprised of a fine-grained matrix of crushed grains, which can form a seal even when sandstones are juxtaposed (Engelder, 1974; Pittman, 1981). A sealing mechanism is present because the petrophysical and textural characteristics of the disturbed zone material differ from the juxtaposed lithologies on either side of the fault.

Cataclasis can increase or decrease the porosity of the material in the disturbed zone of the fault relative to the material in the juxtaposed lithologies. In cases of severe cataclasis, the deformed zone material may consist of crushed grains that have a lower porosity, smaller mean grain size, and poorer sorting than the juxtaposed lithologies. These characteristics may result in reduced permeabilities in the disturbed zone due to the smaller pore throat size of the gouge material, thereby increasing the potential for seal, especially between immiscible fluids, where the capillary pressures would be significantly higher in the disturbed zone material (Berg, 1975). Knipe (1992) found that cataclastic fault gouge can have pore throat radii less than 0.001 millimeters. Antonellini and Aydin (1994) and Pitmann (1981) found that deformation bands within the fault gouge can have a porosity one order of magnitude and a permeability three orders of magnitude less than the undeformed surrounding host rock. Gouge due to cataclasis generally only forms under conditions of significant friction along a fault plane, under high effective confining pressures

(Smith, 1966). Therefore, permeability reduction and/or seal by grain crushing and/or fracturing effects at the Caliche Beaumont Sequestration Project Site are expected to be negligible or minor since the faulting occurred at a shallow depth when the sands of interest were essentially unconsolidated.

Cementation/Secondary Mineralization

Cementation of fractures along the fault plane and/or of the disturbed zone material by secondary mineral deposits from circulating subsurface formation fluids may produce a zone that forms a vertical barrier to lateral fluid flow. A high degree of cementation may completely infill the voids within the pore throats of the disturbed zone, reducing the transmissivity of the material to virtually zero. Evidence from case studies in the Gulf Coast show that cementation along fault planes tends to be a surficial feature, not generally formed at depths below the ground surface (Smith, 1980). At the Greens Bayou site, the depth of the faulting, inspection of the faulted well logs for tight streaks at the depth of faulting, and the unconsolidated to semi-consolidated nature of the injection interval sands demonstrates that cementation and/or secondary mineralization by circulation formations fluids has not occurred.

2.2.3.3 Demonstration of Fault Sealing Capacity at the Caliche Beaumont Sequestration Project Site

A detailed review of the fault of interest, Fault A, beneath the Caliche Beaumont Sequestration Project Site confirms the non-transmissive, self-sealing nature of the fault, as discussed in this section and summarized below:

1) ***Ductile Nature of Confining System Shales:*** The shales of the Upper Confining System (Lower Oakville, Anahuac, and Upper Frio) are ductile and therefore deform plastically by bending or smearing.
2) ***Low Sand-Shale Ratio:*** The sand-shale ratio of the faulted geologic section indicates a substantial amount of impermeable shale [redacted] or greater of shale beds) is present in the Upper Confining System (Lower Oakville, Anahuac, and Upper Frio containment layers) and in the Lower Confining Unit (Frio-Hackberry shale).
3) ***High Clay Smear Potential:*** As shown on **Figures A.2.27 and A.2.28**, the low sand-shale ratio (i.e., greater impermeable shales) results in a high CSP as more shale-to-shale and shale-sand juxtaposition is found along the fault plane. [redacted] (Yielding et al., 1997).
4) ***High Shale Gouge Ratio:*** [redacted] Yielding et al., 1997).
5) ***Structural Trapping Capacity:*** Most petroleum system traps along the Gulf Coast are due to growth faults, including Fault A, as evidenced by the [redacted] artificial penetrations within the Caliche AoR being located near and along the northeast-southwest trending Fault A.
6) ***Differential Formation Pressure Gradients:*** Higher formation pressure gradients measured in the Miocene-aged Flemming Group versus the Oligocene-aged Frio Formation confirm the vertical sealing nature of local growth faults in the area.

2.3 Hydrogeology

Per Section 2.3.8 Hydrology and Hydrogeology of the Area of Review of the USEPA UIC Program Class VI Well Site Characterization Guidance for Geologic Sequestration of Carbon Dioxide, this section provides a discussion of the regional and local hydrogeology and hydrostratigraphy, as required by 40 CFR §146.82 (a)(5) and §146.82(a)(3)(vi). The key objective of this section is to *"demonstrate the relationship between the proposed injection formation and any USDWs"* and to provide support to the *"understanding of the water resources near the proposed well"* (USEPA, 2013, p. 29).

2.3.1 Regional and Local Hydrogeology

The Caliche Beaumont Sequestration Project Site is located near the city of Beaumont in north-central Jefferson County in Southeast Texas. Publicly available information and data were evaluated to interpret the regional and local hydrogeology in the vicinity of the Caliche Beaumont Sequestration Project Site.

The predominant aquifer found along the Gulf Coast of Texas is the Gulf Coast Aquifer System, which parallels the coastline of the Gulf of Mexico from the Texas / Louisiana border to the Texas / Mexico border (see "Gulf Coast" in **Figure A.2.39**). The Gulf Coast Aquifer System has a total area of approximately 42,000 square miles and underlies all or parts of over 50 Texas counties, including Jefferson County (George et al., 2011, p. 45).

As shown in **Figure A.2.40**, the Gulf Coast Aquifer System is comprised of multiple hydrogeologic units including the Chicot, Evangeline, and Jasper aquifers, presented in descending order (Young et al., 2016, p. 3), which are alluvial aquifers composed of discontinuous sand, silt, clay, and gravel beds (George et al., 2011, p. 43), and a regional aquitard, the Burkeville Confining Unit, a lithostratigraphic unit of multiple clay units from formations of different geologic ages corresponding to the middle Lagarto Formation at the base of the Evangeline aquifer. A more detailed hydrostratigraphic column of the Texas Gulf Coast Aquifer System near Beaumont in Jefferson County is provided in **Figure A.2.1**, which shows how the local geologic units correspond with the hydrogeologic units of the system. The total sand thickness of the Gulf Coast Aquifer System averages 1,300 feet, with an average fresh water saturated thickness of up to 1,000 feet (George et al., 2011, p. 43).

Younger Pleistocene and Holocene formations corresponding to the upper Chicot aquifer of the Gulf Coast aquifer in Jefferson County exhibit generally good water quality with total dissolved solids (TDS) concentrations of less than 1,000 milligrams per liter (mg/L) (George et al., 2011, p. 43; Wesselman and Aronow, 1971). As shown in **Figure A.2.41**, in Jefferson County, smaller quantities of fresh water with TDS concentrations of Claimed as PBI [redacted] (Young et al., 2016, Figure 6-2). As shown in **Figure A.2.42**, in Jefferson County, the base of the potentially usable quality water with Claimed as PBI [redacted] (Young et al., 2016, Figure 6-5). General water quality of the Chicot, Evangeline, and Jasper aquifers deteriorates more so in vicinity of shallow salt domes (Wesselman and Aronow, 1971; Young et al., 2012, pp. 2-13 – 2-14), as dissolution introduces sodium chloride (NaCl) into the aquifer system. As shown on **Figures A.2.22 and A.2.23**, the Spindletop salt dome and up to five other salt domes are located near the Caliche Beaumont Sequestration Project Site, with the Spindletop salt dome located Claimed as PBI [redacted] the Caliche Beaumont Sequestration Project Site (see **Figure A.1.1**).

The Gulf Coast aquifer is a groundwater resource generally utilized for municipal, industrial, and irrigation purposes, and, in some areas, increased pumping has led to land subsidence (George et al., 2011, pp. 43, 45). However, in Jefferson County, this effect of groundwater pumping is not apparent, as fresh water supply is limited and therefore the predominant source of drinking water is surface water from the Neches, Trinity, and Sabine Rivers, as well as from the Sam Rayburn-Steinhagen Lake/Reservoir System, and from neighboring counties (TWDB, 2022a; Ryder and Ardis, 1991, p. 17; Wesselman and Aronow, 1971, p. 1).

Jefferson County falls within the Neches-Trinity Coastal River Basin (Young et al., 2016, Figure 4-3). Exposed formations which outcrop at the surface within Jefferson County are Pleistocene and Holocene in age, with the Beaumont Clay being the oldest and most extensive (Wesselman and Aronow, 1971, p. 1). The Beaumont Clay averages less than 100 feet thick and is more than 30,000 years old (Wesselman and Aronow, 1971, p. 1). Holocene-age deposits comprise the low-lying floodplains of the Trinity and Neches Rivers and consist of interbeds of alluvial and deltaic deposits and coastal marsh, mudflat, and chenier deposits (Wesselman and Aronow, 1971, p. 1).

The principal source of fresh groundwater in Jefferson County is rainfall; however, only a small fraction of rainfall infiltrates to the water table, and much of this small fraction is quickly returned to surface as spring flow/baseflow (Wesselman and Aronow, 1971, p. 11).

2.3.1.1 Chicot Aquifer

The Chicot aquifer is the uppermost hydrogeologic unit in the Gulf Coast Aquifer System. The Aquifer is approximately 1,500 feet thick in the vicinity of the Caliche Beaumont Sequestration Project Site (see **Figures A.2.19 and A.2.43**) and is generally divided into Upper and Lower hydrologic units by clay sediments at the base of the Beaumont Clay formation (see **Figure A.2.1**) (GeoHydroLogicPro, 2018, pp. 3-35; Young et al., 2012, Figure 6-6). The Upper hydrologic unit includes the undifferentiated Holocene alluvial sediments and the Pleistocene Beaumont Clay Formation, while the Lower hydrologic unit includes the Lissie and Willis Formations.

The transmissibility coefficients in the Upper and Lower hydrologic units of the Chicot aquifer in the vicinity of the Caliche Beaumont Sequestration Project Site vary between Claimed as PBI [redacted] respectively (Geostock, 2022, pp. 29-30). Historical aquifer tests indicate that the transmissivity for the Lower hydrologic unit of the Chicot aquifer ranges from Claimed as PBI [redacted] across Chambers, Jefferson, and Orange Counties, with storage coefficients ranging between Claimed as PBI [redacted] (Thorkildsen and Quincy, 1990, p. 13). The upper portion of the Lower hydrologic unit of the Chicot aquifer is the major source of potable water in the vicinity of the Caliche Beaumont Sequestration Project Site. Consequently, most domestic and public water supply wells in the Chicot aquifer in the vicinity are completed in the upper portion of the Lower hydrologic unit of the Chicot aquifer Claimed as PBI [redacted]. Claimed as PBI [redacted] (Geostock, 2022, p. 10; TWDB Database, accessed 2023). TDS values in the vicinity of the project site typically range from less than 1,000 mg/L to greater than 35,000 mg/L (fresh to brine water) (Young et al., 2016, Figure 6-13). Claimed as PBI [redacted] n below **Exhibits A.2.6 through A.2.8**, respectively).

Exhibit A.2.6. Approximate Water Level Elevations of Lower Hydrologic Unit of the Chicot Aquifer (1941 and 1966).

SOURCE: Texas Water Development Board Report:
https://www.twdb.texas.gov/publications/reports/numbered_reports/doc/R133/Report133.asp.

Exhibit A.2.7. Approximate Water Level Elevations of Lower Hydrologic Unit of the Chicot Aquifer (1971).

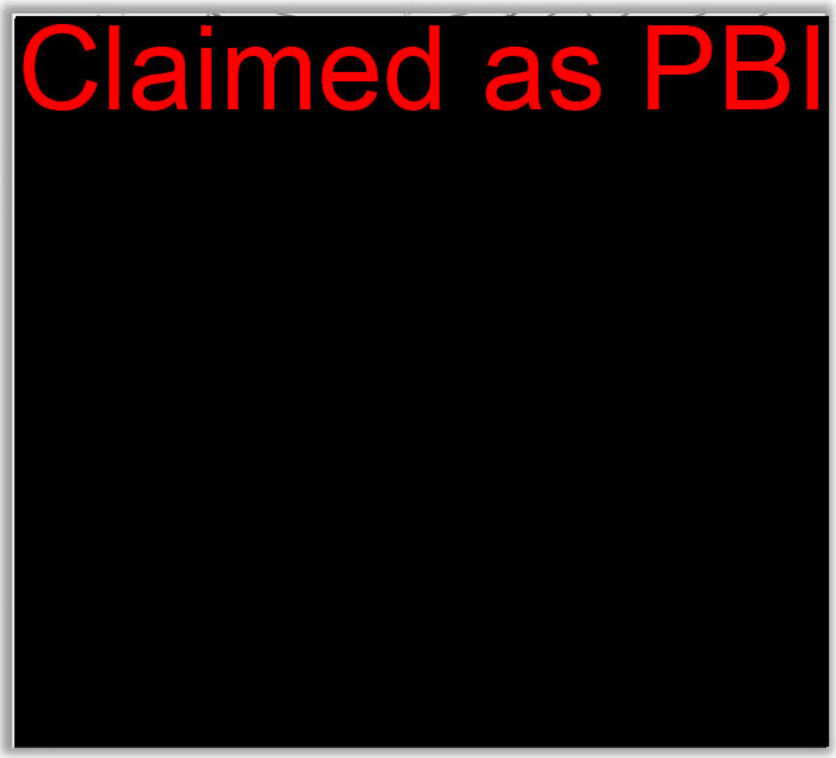

SOURCE: Texas Water Development Board Report:
https://www.twdb.texas.gov/publications/reports/numbered_reports/doc/R156/report156.asp.

Exhibit A.2.8. Approximate Water Level Elevations of Lower Hydrologic Unit of the Chicot Aquifer (1986).

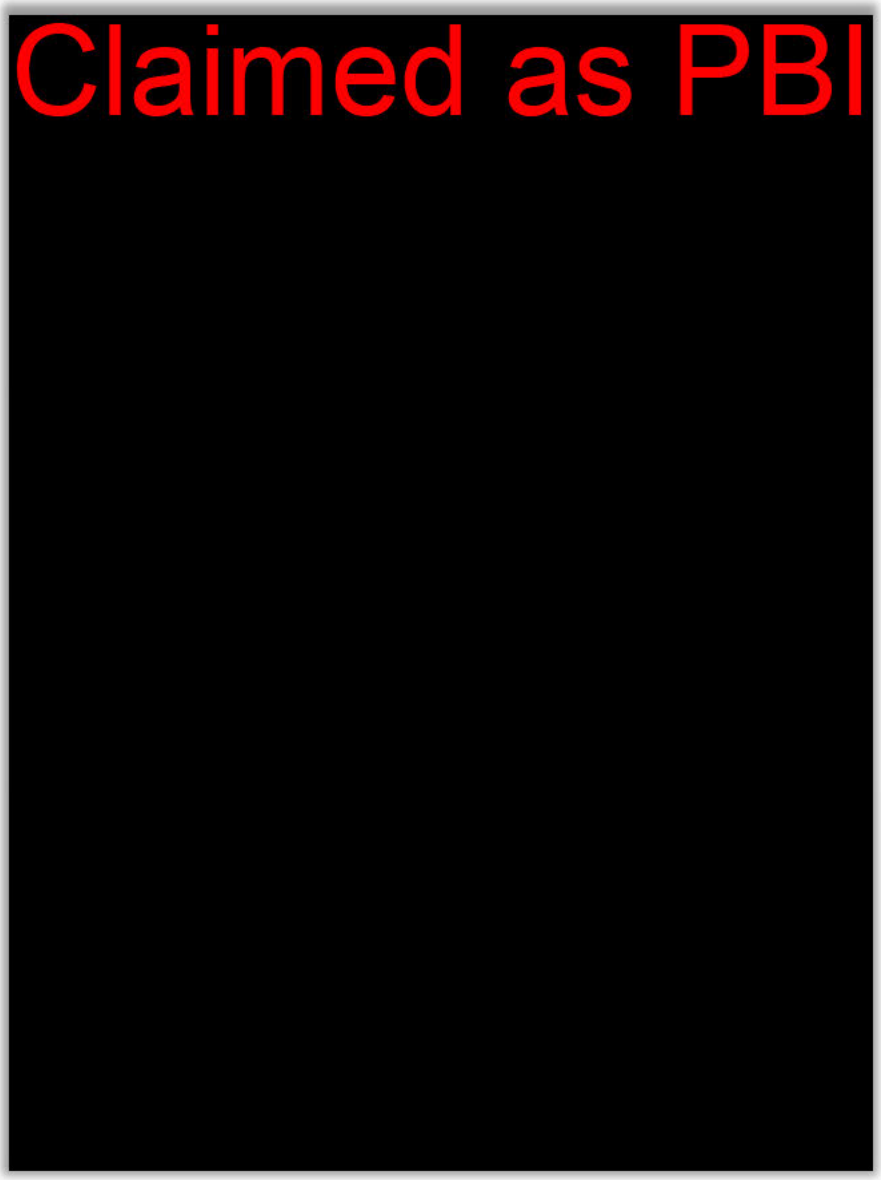

SOURCE: Thorkildsen and Quincy, 1990, Figure 7.

2.3.1.2 Evangeline Aquifer

In the vicinity of the Caliche Beaumont Sequestration Project Site, the Evangeline aquifer is approximately 2,000 feet thick (see **Figures A.2.19 and A.2.44**) and gradually thickens toward the coastline (Wesselman and Aronow, 1971, p. 7). The Evangeline aquifer includes the Upper and Lower Goliad Formation, consisting of interbedded fluvial and deltaic sandstone, and the Upper Lagarto Formation of the Fleming Group, consisting of mudstone and deltaic sandstone (see **Figures A.2.1, A.2.19, and A.2.40**) (Geostock, 2022, pp. 7, 9).

The estimated transmissibility coefficients in the Evangeline aquifer vary between 32,000 and 36,000 gpd/ft (Wesselman and Aronow, 1971, p. 13). Historical aquifer tests indicate that the transmissivity for the Evangeline aquifer ranges from 4,300 to 4,800 ft^2/day across Chambers and Jefferson Counties, with a storage coefficient of approximately 0.00003 (Thorkildsen and Quincy, 1990, p. 13). The Evangeline aquifer contains fresh water to a depth of more than 1,000 ft bgs in northern portions of Jefferson County (Wesselman and Aronow, 1971, p. 33); however, saltwater intrusion and proximity to salt domes has impacted water quality in the Evangeline aquifer. The Evangeline aquifer is underdeveloped in the area because of slightly saline conditions (Geostock, 2022, p. 10). TDS values in the vicinity of the project site typically range from 10,000 mg/L to greater than 35,000 mg/L (very saline to brine water) (**Figure A.2.54**; Young et al., 2016, Figure 6-13). As shown on **Figure A.2.45**, the estimated percentage of the total thickness of the Evangeline aquifer in Jefferson County with moderately saline or greater water quality (i.e., more than 3,000 mg/L TDS) is greater than 80% (Young et al., 2012, Figure 9-7). Note that although Young et al. (2012) indicates groundwater quality with TDS greater than 3,000 mg/L, it is understood that TDS concentrations in the Evangeline aquifer are greater than 10,000 mg/L (Young et al., 2016).

2.3.1.3 Burkeville Confining Unit

The lower confining layer of the Evangeline Aquifer is the Burkeville confining unit which primarily includes the middle portions of the Lagarto Formation (see **Figures A.2.1, A.2.19, and A.2.40**) (Young and Draper, 2020, p. 3) consisting of the medium to massively bedded shales with thin to medium bedded sandstones of the Bayfill/Lagoonal facies (Young et al., 2012, p. 8-6). The Burkeville confining unit typically ranges from 130 to 300 feet thick and exists only in the subsurface (Wesselman and Aronow, 1971, p. 7; Ryder and Ardis, 1991, p. 5). According to Young and Draper (2020), the Burkeville confining unit can be up to [redacted] thick near the Caliche Beaumont Sequestration Project Site (see **Figure A.2.46**), ranging from a depth of approximately 3,400 ft bgs to 4,000 ft bgs (see **Figure A.2.19**). The Burkeville confining unit acts as an aquiclude, as it is principally composed of silt and clay (Baker, 1979, p. 40), with an estimated average vertical hydraulic conductivity of $1X10^{-4}$ ft/day (Ryder and Ardis, 1991, Table 4) and clay fraction of 0.5 to 0.7 (see **Figure A.2.47**; Young and Draper, 2020, Figure 3-5). Some places contain minor amounts of sand, but the aquiclude is not a source of potable water in Jefferson County, as greater than 80% of the Burkeville confining unit contains TDS concentrations of greater than 3,000 mg/L (see **Figure A.2.48**; Young et al., 2012, Figure 9-10). TDS values in the vicinity of the project site typically exceed 35,000 mg/L (brine water) (Young et al., 2016, Figure 6-13). The Burkeville confining unit lies approximately 2,500 ft bgs near the Caliche Beaumont Sequestration Project Site (Geostock, 2022, p. 9; GeoHydroLogicPro, 2018, pp. 3-34).

2.3.1.4 Jasper Aquifer

The Jasper aquifer consists of the lower portions of the Lagarto Formation and the Oakville Formation sandstone (see **Figures A.2.1, A.2.19, and A.2.40**). The early Miocene Lower Lagarto Formation consists of prodelta mudstone and deltaic sandstone, and the early Miocene Oakville Formation sandstone consists of fluvial deposits of channel, meander-belt, and crevasse splay facies (Geostock, 2022, pp. 6, 9; Young et al., 2012, p. 1-1). In some places, the Jasper aquifer also includes the upper sandy intervals of Oligocene-age Catahoula Formation (Young et al., 2012, p. 1-1). However, near the Caliche Beaumont Sequestration Project Site, the Jasper aquifer is underlain by the Anahuac Formation (Young et al., 2016, p. 149), which is the primary confining unit above the target injection interval of the upper Frio Formation sands. The Jasper aquifer ranges in thickness from about 1,600 ft to about 2,400 ft, with a base elevation between -

6,000 and -8,000 ft MSL in the vicinity of the Caliche Beaumont Sequestration Project Site (see **Figure A.2.49**; Young et al., 2012, p. 6-6, Figure 6-11).

The Jasper aquifer lies unconformably over the Anahuac Formation confining unit which limits exchange of water between the Jasper aquifer and underlying units (Ellis et al., 2023, p. 18). The mean transmissivity of the Jasper aquifer is estimated at 10,400 ft^2/day (Ryder and Ardis, 1991, p. 6), with values of approximately 30,000 ft^2/day near the Caliche Beaumont Sequestration Project Site (Ryder and Ardis, 1991, Figure 11). The Jasper aquifer contains TDS concentrations of greater than 70,000 mg/L near the Caliche Beaumont Sequestration Project Site (Ryder and Ardis, 1991, Figure 20); and therefore, the Jasper aquifer is not used as a groundwater resource in Jefferson County (Ryder and Ardis, 1991, Figure 71). Underlying the Jasper aquifer in the vicinity of the Caliche Beaumont Sequestration Project Site is the massive shale-rich Anahuac Formation that is generally considered to form the base of the Gulf Coast Aquifer System (Geostock, 2022, pp. 11-12; Mace et al., 2006).

2.3.2 Determination of the Lowermost USDW

As defined in the Code of Federal Regulations (40 CFR §144.3), a USDW is *"an aquifer or its portion: (a)(1) Which supplies any public water system; or (2) Which contains a sufficient quantity of ground water to supply a public water system; and (i) Currently supplies drinking water for human consumption; or (ii) Contains fewer than 10,000 mg/l total dissolved solids; and (b) Which is not an exempted aquifer."*

In recent years, the TWDB has conducted extensive studies to characterize the availability of fresh, brackish, and saline groundwater resources in Texas. Young et al. (2016) document the extent of brackish water resources for the Gulf Coast Aquifer System. The TWDB has classified regional groundwater quality based on the following ranges of TDS and salinity:

- **Fresh Water:** TDS is less than 1,000 mg/L.
- **Slightly Saline:** TDS is between 1,000 and 3,000 mg/L.
- **Moderately Saline:** TDS is between 3,000 and 10,000 mg/L.
- **Very Saline:** TDS is between 10,000 and 35,000 mg/L.
- **Brine:** TDS is greater than 35,000 mg/L.

According to this classification, very saline and brine groundwaters would not be considered a USDW, whereas fresh, slightly saline, and moderately saline groundwater may be considered a USDW.

Young et al. (2012) provide a detailed analysis of the water quality in the Gulf Coast Aquifer System by estimating the specific conductivity of aquifer formation water using geophysical resistivity logs. In Jefferson County, the percentage of fresh water in the Chicot aquifer is estimated to be less than 20% (see **Figure A.2.50**; Young et al., 2012, Figure 9-2). In addition, Young et al. estimated the following for each hydrogeologic unit of the Gulf Coast Aquifer System in the vicinity of the Caliche Beaumont Sequestration Project Site:

- ***Chicot Aquifer:*** The percentage of slightly saline water is estimated at approximately 80% (see **Figure A.2.51**; Young et al., 2012 p. 9-11). The percentage of moderately saline water is estimated at approximately [redacted] in the vicinity of the Caliche Beaumont Sequestration Project Site (see **Figure A.2.52**; Young et al., 2012, Figure 9-4).

- ***Evangeline Aquifer:*** The percentage of fresh water and slightly saline water is estimated to be below [redacted] (Young et al., 2012, Figures 9-5 and 9-6), while the percentage of moderately saline water is estimated between [redacted] (see **Figure A.2.45**; Young et al., 2012, Figure 9-7).
- ***Burkeville Confining Unit:*** The percentage of fresh water and slightly saline water is estimated to be [redacted] (Young et al., 2012, Figures 9-8 and 9-9), while the percentage of moderately saline water is estimated between [redacted] (see **Figure A.2.48**; Young et al., 2012, Figure 9-10).
- ***Jasper Aquifer:*** The percentage of fresh water and slightly saline water is estimated to be [redacted] (Young et al., 2012, Figures 9-11 and 9-12), while the percentage of moderately saline water is estimated between [redacted] (see **Figure A.2.49**; Young et al., 2012, Figure 9-13).

Figure A.2.41 shows the depth to the base of the fresh water zone (TDS < 1,000 ppm) in the Gulf Coast Aquifer System. At the Caliche Beaumont Sequestration Project Site, this depth is between [redacted]. **Figure A.2.45** shows the depth to the base of the lowermost USDW (TDS < 10,000 ppm) in the Gulf Coast Aquifer System. At the Caliche Beaumont Sequestration Project Site, this depth is between [redacted]. It also is noted in Young et al. (2012) that most of the water well locations with at least one measurement of TDS concentrations in Jefferson County were in the Chicot aquifer.

The inset map located within **Figure A.2.53** shows the location of [redacted] that Young et al. (2016) utilized to estimate the depth to the base of the USDW (here defined as 10,000 mg/L TDS). **Figure A.2.53** shows the salinity zone profile through the cross-section adjacent to the Caliche Beaumont Sequestration Project Site. Note that the well log for [redacted] shown on **Figure A.2.53** is located [redacted] from the Caliche Beaumont Sequestration Project Site. At approximately the location of the Caliche Beaumont Sequestration Project Site, little to no fresh groundwater is found. [redacted]

Figure A.2.54 shows the salinity zone profile versus the geologic formations through the cross-section that runs adjacent to the Caliche Beaumont Sequestration Project Site. Note that the well log for [redacted] shown on **Figure A.2.54** is located [redacted] from the Caliche Beaumont Sequestration Project Site. This figure also indicates that fresh, slightly saline, and moderately saline water are only found in the Chicot aquifer with very saline water in the Evangeline aquifer, and very saline and brine water occurring through the Burkeville confining unit and into the Jasper aquifer.

2.3.2.1 Apparent Water Resistivity (R_{wa}) Method

As described in Section 2.4.1.3, in the absence of taking direct samples of formation fluids, geophysical log data can be used to estimate the groundwater salinity (i.e., TDS) by determining the resistivity of the formation fluid and converting that resistivity value to a salinity value. This can be accomplished by using the apparent water resistivity (R_{wa}) method, referred to as the "R_{wa} Minimum method" (Young et al., 2016). This methodology determines the formation fluid resistivity by using the Archie (1942) Equation and measured formation resistivity data from geophysical logs. As described by Young et al. (2016) and in Section 2.4.1.3, the method requires certain

assumptions to be made about formation porosity, geothermal gradient, the cementation exponent, and the specific conductance to TDS conversion factor.

2.3.2.2 *Methodology used in the Site Evaluation*

As described in Section 2.4.1.3, the Apparent Water Resistivity (R_{wa}) Method was used to calculate the formation resistivities that would correspond to a TDS of 10,000 mg/L at varying depths. Furthermore, the Apparent Water Resistivity (R_{wa}) Method was used to estimate depths corresponding to a TDS of 10,000 mg/L using resistivity data from Claimed as PBI located within an approximately Claimed as PBI radius of the Caliche Beaumont Sequestration Project Site. Assumptions of formation porosity, cementation exponent, and specific conductance to TDS conversion factor were obtained from Young et al. (2016). A geothermal gradient of Claimed as PBI was assumed using temperature log data acquired from the Claimed as PBI, as discussed in Section 2.4.1.1.

As shown in **Table A.2.4** in Section 2.4.1.3, formation waters with resistivities below Claimed as PBI at a depth of Claimed as PBI, or below Claimed as PBI, would be expected to have TDS concentrations exceeding 10,000 mg/L and thus should not be considered USDWs. As shown in **Table A.2.5** in Section 2.4.1.3, the depth to the base of the USDW is estimated to be approximately Claimed as PBI using the Apparent Water Resistivity (R_{wa}) Method with resistivity data from the four geophysical logs located within an approximately Claimed as PBI of the Caliche Beaumont Sequestration Project Site.

2.3.3 *Local Water Usage*

2.3.3.1 *Local Water Supply*

According to water budget modeling conducted by Wade (2022) for Jefferson County, which includes the Caliche Beaumont Sequestration Project Site, the Chicot aquifer contains nearly the entirety (~99%) of the 15,425 acre-feet of modeled available groundwater for the county. Hence, the Chicot aquifer is the predominant groundwater fresh water supply source. This is consistent with Wesselman and Aronow (1971) who found that only small quantities of fresh groundwater were available in Chambers and Jefferson counties (p. 1). No groundwater conservation district has been formed in Jefferson County (TWDB, 2023).

However, most of the fresh water used in the area is supplied by surface water sources. According to data contained in the Texas State Water Plan (TWDB, 2022a), surface water supplies in Jefferson County amounted to over 350,000 acre-feet in 2020, while groundwater supplies reportedly totaled less than 12,000 acre-feet. Surface water is supplied to Jefferson County from the Neches, Trinity, and Sabine Rivers, as well as from the Sam Rayburn-Steinhagen Lake/Reservoir System and neighboring counties (TWDB, 2022a; Ryder and Ardis, 1991, p. 17; Wesselman and Aronow, 1971, p. 1).

2.3.3.2 *Public Water Supply Boundaries*

The Caliche Beaumont Sequestration Project Site is predominantly located within the West Jefferson County Municipal Water District (MWD) (PWS ID TX1230021); however, the northern portion of the Caliche Beaumont Sequestration Project Site is located within the City of Beaumont Water Utility Department (PWS ID TX123001).

The West Jefferson County MWD serves approximately 9,298 individuals at 3,266 service connections with surface water purchased from the Lower Neches Valley Authority sourced from

the Sam Rayburn Reservoir. During the most recent TWDB Water Use Survey in 2022, the West Jefferson County MWD reported a total use of 344,260,000 gallons (TWDB, 2022b).

The City of Beaumont Water Utility Department serves approximately 115,282 individuals at over 59,000 service connections with a combination of groundwater supplied from the Gulf Coast Aquifer System and surface water obtained from the Neches River. During the most recent TWDB Water Use Survey in 2022, the City of Beaumont Water Utility Department reported a total use of 6,710,650,000 gallons of surface water and 1,889,980,958 gallons of groundwater (TWDB, 2022b).

2.3.4 Water Wells and Data Sets

Four TWDB databases were used to obtain all wells within an Claimed as PBI of the City of Beaumont Acreage including the entirety of the AoR (see **Exhibit A.2.9 below**). These databases include:

- TWDB Groundwater Database Well Locations
- TWDB Submitted Driller's Reports Database (SDRDB) Well Locations
- TWDB SDRDB Plugging Report Well Locations
- TWDB Brackish Resources Aquifer Characterization System (BRACS) Database

Results of the TWDB database searches are shown on **Figure A.2.55** and summarized below.

The TWDB Groundwater Database Well Locations indicated Claimed as PBI of the City of Beaumont Acreage:

- Claimed as PBI

The TWDB SDRDB Well Locations Database indicated Claimed as PBI of the City of Beaumont Acreage:

- Claimed as PBI
- 12 test wells installed to depths between 25 and 30 ft bgs

The TWDB SDRDB Plugging Report Database indicated Claimed as PBI of the City of Beaumont Acreage:

- Claimed as PBI

- Claimed as PBI

The TWDB BRACS Database indicated Claimed as PBI related to oil or gas within a Claimed as PBI of the City of Beaumont Acreage e. One well installed to Claimed as PBI, and the second well installed to Claimed as PBI, the third and fourth wells Claimed as PBI, installed to Claimed as PBI; and therefore, none are for public or private water supply.

Exhibit A.2.9. TWDB Well Database Search Area.

The well data above indicates that most wells are for monitoring, domestic, stock, and rig supply operations. These wells are all screened in the Chicot aquifer, except for the Claimed as PBI wells. No water supply wells appear to have been installed to a depth greater than Claimed as PBI within a Claimed as PBI of the City of Beaumont Acreage. These depths are consistent with the maximum well depths reported by Young et al. (see **Figure A.2.56**; Young et al., 2016, Figure 6-33), also based on well information obtained from the TWDB SDRDB. Additionally, Young et al. (2012) produced maps of water well locations with at least one TDS measured concentration installed within the Chicot aquifer, Evangeline aquifer, Burkeville confining unit, and Jasper aquifer (see **Figures A.2.57 to A.2.60**; Young et al., 2012, Figures 9-14 to 9-17), which show water wells installed within the Chicot aquifer only in all of Jefferson County.

Thus, all available data reviewed indicate that only the Chicot aquifer is being utilized as a groundwater resource in the Caliche Beaumont Sequestration Project Site.

2.3.5 Injection Depth Waiver

The targeted injection zones are deeper than the base of the lowermost USDW by more than Claimed as PBI and separated from it by the Burkeville and Anahuac Confining Units; therefore, an Injection Depth Waiver is not required for the Caliche Beaumont Sequestration Project Site.

2.4 Geochemical Characterization

Site specific data have not been collected specifically for this permit; however, core analyses, temperature logs, and water chemistry data from conventional hydrocarbon wells and saltwater disposal wells (SWDs) located proximal to the project site and throughout Jefferson County were evaluated as analogues in lieu of site-specific data at this time. Jefferson County has an extensive history of oil and gas development dating back to the early 1900s, and sample data presented in this permit application were obtained from numerous industry, agency, and academic sources. These include the United States Geological Survey (USGS) National Produced Waters Geochemical Database, which houses a compilation of geochemical and related information for fluids from oil and gas wells throughout the United States. Water chemistry data were also obtained from published literature on Frio Formation fluids in Jefferson County, as well as resistivity logs from four local SWDs, from which TDS content could be inferred. Information on the mineralogy of the targeted formation and overlying confining unit, as well as the local temperature gradient, were provided by operators of proximal SWDs to the project site. In combination, these data were utilized to better predict possible rock-fluid interactions in the Frio Sand and Anahuac Shale following CO_2 injection.

Because these data originate from a number of different sources and time periods, they are subject to some limitations and uncertainties. These are largely related to differences in the parameters analyzed and/or analytical methods, some of which were not comprehensively documented. For example, fluid chemistry data in the USGS database from the Upper Frio Formation originate from as early as 1946 and are reported through 1979. For some samples, certain ions were not analyzed, or were analyzed in combination with other ions (e.g., K and Na together). Where possible, fluid data were evaluated to ensure quality assurance (i.e., a cation-anion balance <±10%, which is the threshold commonly applied to brines (Reed and Mariner, 1991).

Other data provide best approximations in lieu of direct measurements. These include estimates of salinity based on wireline spontaneous potential and resistivity logging measurements, as well as estimates of temperature within the targeted interval that were inferred from a locally calculated temperature gradient. Where available, multiple datasets were evaluated to better understand data trends and outliers (e.g., temperature deviations associated with different geologic features).

To better characterize site-specific aqueous chemistry, formation fluid samples will be collected in-situ (i.e., under pressure) and analyzed at designated laboratories (*Module D – Pre-Operational Testing Plan*). Similarly, open hole wireline measurements will be recorded during the drilling of the injection well into the Frio Sand and other deep monitoring wells. These data will facilitate estimates of vertical salinity and temperature profiles within the targeted injection interval as well as overlying formations. Collectively, site-specific data will be compared to the larger regional dataset discussed herein and utilized to adjust geochemical and transport models (as discussed in *Module B – Area of Review and Corrective Action Plan*) to best reflect site-specific conditions.

2.4.1 Baseline Geochemical Characterization

Site-specific geochemical data were not available at the time of this permit application. However, mineralogy data for the Frio Sands and overlying Anahuac Shale were evaluated from core samples originating from the Claimed as PBI This well is located approximately Claimed as PBI of the project area. In addition, temperature logs acquired Claimed as PBI located approximately Claimed as PBI of the northeastern portion of project area boundary, respectively, were utilized to estimate the local temperature gradient (**Appendix A.D**).

Estimates of the range of TDS concentrations within major aquifers in or proximal to the project area were based on available information from the literature, as well as formation resistivity logs obtained Claimed as PBI (**Appendix A.E**). Resistivity logs for these wells were available for depths ranging between Claimed as PBI. These wells are located within an approximate Claimed as PBI radius of the northeastern portion of the project area boundary.

Additional information on TDS content, and major and trace ion chemistry within the Frio Formation, which includes the proposed injection zone (Claimed as PBI depth at the project site), was obtained from the following sources:

1) Laboratory analysis of fluid chemistry obtained during drilling (and prior to saltwater injection) of the Claimed as PBI Although information was not provided on the specific depth interval from which fluid originated, the sample likely originated from the perforated interval between Claimed as PBI within the Frio Formation.
2) Fluid chemistry data in the USGS National Produced Waters Geochemical Database originating from 17 conventional hydrocarbon wells in Jefferson County targeting the Frio Formation between 6,000- and 9,000-foot depth. This is consistent with the range of depths corresponding to the top of the Frio Formation throughout the majority of Jefferson County (Bebout et al., 1976).
3) Fluid chemistry data presented in the manuscript *"Waters from the Frio Formation, Texas Gulf Coast"* (Jessen and Rolhausen, 1944) for 10 conventional hydrocarbon wells from Jefferson County targeting the Frio Formation between 6,000- and 9,000-foot depth.

The locations of source wells for these data, where coordinates were reported, are shown on **Figure A.2.61**, and the analytical data are presented in attached **Table A.2.1**.

2.4.1.1 Temperature

The local temperate gradient was estimated from the temperature logs acquired Claimed as PBI (**Appendix A.D**). Specifically, a linear regression was fit to the temperature data from the Claimed as PBI (Claimed as PBI to yield an estimated geothermal gradient of Claimed as PBI This value is similar to the estimated temperature gradient of Claimed as PBI calculated from the Golden Claimed as PBI temperature log (corresponding to depths of Claimed as PBI (Note that the Claimed as PBI exhibits a significant temperature anomaly from Claimed as , likely associated with sulfur solution mining; therefore, the temperature gradient was estimated based only on measurements corresponding to depths Claimed as PBI.

Assuming an average local temperature gradient of Claimed as PBI, and an initial average annual temperature of Claimed as PBI at ground surface, the temperature is estimated to be Claimed as PBI at the

targeted injection interval within the Frio Sand between approximately Claimed as PBI .

2.4.1.2 Mineralogy

The bulk mineralogy and porosity of the Frio Sand and overlying Anahuac Shale were evaluated in core samples collected from Claimed as PBI , respectively, in the Claimed as PBI . Specifically, thin section petrographic and scanning electron microscope analyses were performed on whole, small fragments of the core collected from the wellbore to characterize mineralogy and porosity. In addition, sorted sand and silt fractions were assessed using X-Ray Diffraction (XRD) for mineralogy.

For the Frio Sand sample, bulk mineralogy was composed of Claimed as PBI (attached **Table A.2.2**). The clay fraction consisted of Claimed as PBI (**Table A.2.2**). Thin section petrographic analysis indicated that the Frio Sand sample is a poorly lithified, medium-grained arkosic sandstone, and confirmed that the minor clay fraction was predominantly interlayered illite/smectite. Petrographic analysis showed visible permeability owing to the relative absence of lithification and interconnectedness between the sand grains.

For the Anahuac Shale sample, bulk mineralogy was composed of Claimed as PBI (attached **Table A.2.3**). The clay fraction consisted of Claimed as PBI (**Table A.2.3**). Thin section petrographic analysis indicated that the Anahuac Shale sample was a well laminated silty shale. Claimed as PBI

2.4.1.3 Base of USDW

Literature Review

USDW is defined in the Code of Federal Regulations (40 CFR §144.3) as:

> *an aquifer or its portion: (a)(1) Which supplies any public water system; or (2) Which contains a sufficient quantity of ground water to supply a public water system; and (i) Currently supplies drinking water for human consumption; or (ii) Contains fewer than 10,000 mg/l total dissolved solids; and (b) Which is not an exempted aquifer.*

In recent years, the Texas Water Development Board (TWDB) has conducted extensive studies to characterize the available fresh, brackish, and saline groundwater resources in Texas. Young et al. (2016) document the extent of brackish water resources for the Gulf Coast Aquifer System, a major aquifer system paralleling the Gulf of Mexico coastline from the Louisiana border to the border of Mexico. The methodology used by Young et al. (2016) was developed and implemented by the TWDB to estimate the vertical profile of TDS concentrations from geophysical logs at a total of approximately 600 wells located across the Gulf Coast Aquifer System in Texas.

The TWDB has classified regional groundwater quality based on the following ranges of TDS and salinity:

- Fresh Water – TDS < 1,000 mg/L
- Slightly Saline – TDS is between 1,000 and 3,000 mg/L
- Moderately Saline – TDS is between 3,000 and 10,000 mg/L

- Very Saline – TDS is between 10,000 and 35,000 mg/L
- Brine – TDS > 35,000 mg/L

According to this classification, very saline and brine groundwaters would not be considered an USDW, whereas fresh, slightly saline, and moderately saline groundwater would be considered an USDW.

Young et al. (2016) compiled groundwater data from the Gulf Coast Aquifer and reported measured TDS concentrations collected from 9,227 wells and calculated TDS concentrations using resistivity curves from 600 well logs throughout the aquifer. They found:

- Chicot Aquifer: TDS values in the vicinity of the project site typically range from less than 1,000 mg/L to greater than 35,000 mg/L (fresh to brine water).
- Evangeline Aquifer: TDS values in the vicinity of the project site typically range from 10,000 mg/L to greater than 35,000 mg/L (very saline to brine water).
- Burkeville Confining Unit: TDS values in the vicinity of the project site typically exceed 35,000 mg/L (brine water).
- Jasper Aquifer: TDS values in the vicinity of the project site typically exceed 35,000 mg/L (brine water).

Previous studies (Aronow, 1971) have noted that, in Jefferson County, the Evangeline Aquifer only contains fresh water in the northern parts of the County. Conversely, the Chicot aquifer is the most widespread containing fresh water in Jefferson County (Aronow, 1971). Geophysical logs in the area indicate relatively high salinities within the Evangeline Aquifer compared to the Chicot Aquifer (Young et al., 2016); furthermore, in the proximity of the project site, water quality deteriorates quickly with depth, and reaches TDS values greater than 35,000 mg/L at depths above ~2000 ft bgs (Aronow, 1971; Young et al., 2016).

Exhibit A.2.10 shows the location of 600 geophysical well logs that Young et al. (2016) utilized to estimate the depth to the base of the USDW (here defined as 10,000 mg/L TDS). **Exhibit A.2.11** shows the base of the moderately saline zone where TDS < 10,000 mg/L, which corresponds to the base of the USDW. Claimed as PBI [redacted]

Exhibit A.2.12 shows the location of the project site projected onto a cross-section developed by Young et al. (2016) that runs north-south adjacent to the site (see **Exhibit A.2.11**). As can be seen, shallower groundwater in the Beaumont and Lissie Formations (Chicot Aquifer) is slightly to moderately saline before salinity increases near the top of the Willis Formation and into the Upper Goliad (Evangeline Aquifer). At depths around Claimed as PBI TDS exceeds 10,000 mg/L, and groundwater can no longer be considered a USDW. This occurs in the upper portion of the Willis Formation (Chicot Aquifer) and TDS remains greater than 10,000 mg/L into the Goliad Formation (Evangeline Aquifer), Lagarto Formation (Burkeville Confining Unit) and into the Oakville Formation (Jasper Aquifer). In addition, it is apparent on the cross-section that within a particular formation, salinities generally increase towards the south (i.e., towards the coast).

On the **Exhibit A.2.13** cross-section (location of cross-section shown in **Exhibit A.2.10**), the depth to the base of the USDW can be represented by the orange line (10,000 mg/L TDS), which in this area is approximately Claimed as PBI. This is within the Chicot Aquifer, as interpreted by the TWDB (Young et al., 2016).

Exhibit A.2.10. Locations of 600 Geophysical Logs Used by Young et al. (2016) to Map Depths to Various Salinity Zones.

SOURCE: Modified from Young et al. (2016); Figure 6-1. Note: Claimed as PBI

Exhibit A.2.11. Location of Base of Moderately Saline Zone (TDS <10,000 mg/L; i.e., Base of USDW).

SOURCE: Modified from Young et al. (2016); Figure 6-5.

Exhibit A.2.12. Calculated Salinity Zones Near the AoR.

SOURCE: Modified from Young et al. (2016); Figure 6-13. Claimed as PBI

Exhibit A.2.13. Subsurface Boundaries for Freshwater, Slightly Saline, Moderately Saline, and Very Saline Groundwater Near the AoR.

SOURCE: Modified from Young et al. (2016); Figure 6-12. Claimed as PBI

Calculation of the Base of the USDW Using Resistivity Profiles

For the purposes of determining the base of the deepest USDW, vertical resistivity profiles from Claimed as PBI also evaluated to estimate the TDS profiles from approximately 750 to 1,400 foot-depth (**Appendix A.E**).

Geophysical log data can be used to estimate the groundwater salinity (i.e., TDS) by using the apparent water resistivity (R_{wa}) method, referred to as the "R_{wa} Minimum method" (Young et al., 2016). This methodology determines the formation fluid resistivity of sand units using the Archie (1942) Equation. (Note that the Archie Equation cannot be applied to conductive materials such as clays.)

In the situation where a sand aquifer is saturated with water, the Archie Equation can be written as:

$$R_{we} = \varphi^{m} \cdot R_{o}$$

where:

R_{we} = resistivity of water equivalent (ohm-meters) at 25 degrees Celsius (77 degrees Fahrenheit);

φ = porosity (porosity can be estimated in the Gulf Coast Aquifer using the following equation: $\varphi = 36.64 - 0.001 \cdot d$, where d is depth in feet (Young et al., 2016));

m = the cementation exponent (assumed to be 1.3 for the Gulf Coast Aquifer (Young et al., 2016));

R_o = the resistivity of a 100% water saturated formation at 25 degrees Celsius (77 degrees Fahrenheit) in ohm-meter; and

F = formation factor = φ^{m}.

The resistivity of the water equivalent, R_{we}, can be converted to the specific conductance (SC), and subsequently to TDS, with the following two equations:

$$C_{\mathrm{w}} = \frac{10{,}000}{R_{we}}$$

and,

$$\mathrm{TDS} = \mathrm{ct} \cdot C_{\mathrm{w}}$$

where:

C_{w} = specific conductance at 25 degrees Celsius (77 degrees Fahrenheit) in µmhos/cm;

ct = specific conductance to TDS concentration conversion factor (Young et al. (2016) applied a ct value of 0.57 for the Gulf Coast Aquifer); and

TDS = total dissolved solids concentration (mg/L).

Rearranging these equations and applying the Gulf Coast Aquifer relationships identified by Young et al. (2016) leads to the following equation:

$$R_0 = \frac{0.57 \cdot 10{,}000}{((36.64 - 0.001 \cdot d)/100)^{1.3} \cdot TDS}$$

In addition, it is necessary to apply a temperature adjustment to measured electrical resistivity values, as resistivity changes with temperature. The Arp equation (below) can be used to correct for temperature (Young et al., 2016).

$$R_w{}^{2} = R_w{}^{1} \frac{(T_1 + 6.77)}{(T_2 + 6.77)}$$

Where:

R_w^1 is water resistivity at temperature T_1

R_w^2 is water resistivity at temperature T_2

Following the local temperature gradient established in Section 2.4.1.1, it can be assumed that shallow groundwater is 78 degrees Fahrenheit (F) and the geothermal gradient is approximately 1.1 degrees F per 100 feet of increased depth. For example, at a depth of 2,000 ft bgs, the groundwater temperature is expected to be 100 degrees F.

Table A.2.4 below shows the formation resistivity within a sand unit that would correspond to a TDS of 10,000 mg/L (base of the USDW) in the four available resistivity logs from Claimed as PBI This exhibit was calculated using the equations above, the assumed parameters for the Gulf Coast Aquifer (from Young et al., 2016), and making the temperature adjustments using the Arp equation based on an assumed thermal gradient of Claimed . For example, formation waters with resistivities below Claimed as PBI would be expected to have TDS concentrations exceeding 10,000 mg/L and would not be considered USDWs.

Table A.2.4. Formation resistivity cutoff values for the Rwa Minimum Method that produces measured TDS concentration values of 10,000 mg/L.

Claimed as PBI

Following this approach, geophysical logs from Claimed as PBI were reviewed to evaluate the depth of the base of the deepest USDW at each location (**Table A.2.5**). Of importance, the resistivity log for Claimed as PBI is only available for depths greater than Claimed as PBI. At the top what appears to be the uppermost sand unit of this log Claimed as PBI), a resistivity of Claimed is recorded, corresponding to a TDS concentration of approximately Claimed as PBI. Below Claimed as PBI measured resistivities in the Claimed as PBI consistently correspond to groundwater with Claimed as PBI therefore, the base of the USDW is estimated to be present at a shallower depth Claimed as PBI at this location. This assumption is consistent with findings from the evaluation of resistivity logs from Claimed as PBI, which begin at depths of Claimed as PBI respectively. At these three wells, the depth to the USDW is estimated to be approximately Claimed as PBI ft bgs, corresponding to the shallowest interpreted sand units with measured resistivities below the thresholds listed in **Table A.2.4**. This is consistent with the depth to the base of Claimed as PBI groundwater in the vicinity of the project site as reported by Young et al. (2016) of slightly less than Claimed as PBI (see **Exhibit A.2.11**). Based on a cross-section from Young et al. (2016), the base of the USDW appears to occur within the Lissie Formation, which is within the Lower Chicot aquifer (see **Exhibit A.2.12**).

Table A.2.5. Depth Corresponding to 10,000 mg/L TDS in Resistivity Logs for Nearby Brine Disposal Wells.

Claimed as PBI

2.4.1.4 Salinity of Frio Formation Fluids (6,000 – 9,000-foot depth)

Geochemical Analyses

Based on fluid chemistry data from the Claimed as PBI the USGS National Produced Waters Geochemical Database and published literature, the TDS content in Frio Formation fluids ranged from Claimed as PBI, with a median concentration of Claimed as PBI (**Table A.2.1**). The wide variation in salinity among these fluid samples could reflect a number of factors, including differences in formation temperature and pore pressure with depth, the presence of major growth faults which act as barriers to fluid movement (e.g., Morton et al., 1981), the influence of salt dissolution (e.g., Kharaka et al., 2006), and contribution of low-salinity water condensing out of the gas phase (e.g., Kharaka et al., 1977).

Estimation of TDS in Frio Formation Using Resistivity Profiles

TDS of formation fluids within the portion of the Frio Formation targeted for injection (Claimed as PBI was also estimated based on resistivity profiles from the Claimed as PBI located in the approximate vicinity of the planned injection location (Claimed as PBI). As described in Section 2.1.1.3 of this permit application, TDS was estimated using the "R_{wa} Minimum method" presented by Young et al., 2016. The method used by Young et al. (2016) was modified, however, using a cementation exponent (*m*) of 2 (Schlumberger, 1987), which is more representative for deeper, consolidated sandstones, such as those located within the Frio Formation, as opposed to near-surface sandstones. Based on this approach, calculated TDS values for sandstones within the Claimed as PBI depth within the Claimed as PBI ranged from Claimed as PBI, with median values ranging between Claimed as PBI (**Table A.2.6**).

Table A.2.6. Estimated Minimum and Maximum TDS Concentrations in Upper Frio Sands.

Claimed as PBI

2.4.1.5 Water Composition of Frio Formation Fluids (6,000 – 9,000-foot depth)

Chemical analyses of major ions and select trace elements from Frio Formation fluids were evaluated for fluid samples from Claimed as PBI conventional wells with Frio fluid chemistry data in the USGS Produced water Database, and the Claimed as PBI with Frio chemistry data from the manuscript "*Waters from the Frio Formation, Texas Guld Coast* (Jessen and Rolhausen, 1944). Combined, these chemical analyses (**Table A.2.1**) show that the Frio formation fluid between 6,000- and 9,000-foot depth is typically Na-Cl-type water. For samples where bromide data are available, fluids exhibited relatively high Cl/Br mass ratios (600-976), suggesting that salinity is influenced by dissolution of halite (rock salt) (Davis et al., 1998). Halite, which is comprised of Cl and Na but negligible Br, is present in proximate salt domes (Morton et al., 1981). Other evidence for halite dissolution includes Na/Cl molar ratios between 0.9 and 1, indicating similar molar concentrations of Na and Cl, as expected from the dissolution of halite.

With respect to other geochemical parameters, fluids within the Frio Formation exhibit a wide range of variability depending on location. The range and median concentrations of major ions for the samples for which we have data are presented in **Table A.2.7**. Fluids at the subject location will be characterized as part of future sampling.

2.4.2 Compatibility of Injected CO2 with Frio Formation Fluids and Bulk Mineralogy

The potential for CO_2-rock-water interactions following CO_2 injection is important for understanding the short-term (i.e., immediately following injection), as well as long-term (i.e., 100 years or more) fate of CO_2 in the targeted reservoir. Additionally, these reactions may alter fluid chemistry or matrix mineralogy and porosity in other ways that can impact long-term storage capabilities and associated risks. Carbon dioxide is typically injected into deep formations as CO_2(sc). However, once in the subsurface, some fraction of the injected CO_2(sc) is likely to undergo a series of phase changes and chemical reactions.

These chemical reactions are, first and foremost, governed by the dissolution of CO_2(sc) into formation fluid. This dissolution depends on the solubility of CO_2 in the formation fluid under in-situ conditions (temperature and pressure), as well as the contact area between CO_2(sc) and brine. The latter can vary depending on formation porosity, geometry, and injection strategy, and is expected to evolve over time, from a dynamic phase of contact during injection, to a slower and steadier phase of dissolution once the CO_2(sc) plume is stable (Hovorka et al., 2006).

Table A.2.7. Range and Median Concentrations of Major Ion Concentrations based on Available Upper Frio Formation Fluid Data.

Once dissolved, important rock-water-CO_2 chemical reactions include dissolution of existing minerals, as well as precipitation of new minerals. To evaluate the potential chemical reactions that could occur in the Frio Sand following CO_2 injection at the project site, findings from the University of Texas Bureau of Economic Geology (BEG) Frio Brine Pilot Test Site were evaluated. The Frio experimental site is located within the South Liberty oil field in Liberty County, Texas, which abuts Jefferson County to the northeast. At this location, the Frio "C" Sandstone was perforated between 5,055 to 5,073 feet deep, and approximately 1600 tons of CO_2 were injected over a 10-day period. The mineralogy of the Frio "C" sandstone within the South Liberty oil field is similar to that anticipated for the project site. Specifically, the Frio "C" sandstone unit is poorly cemented, subarkosic sandstone predominantly comprised of quartz, with minor amounts of illite/smectite, feldspar, and calcite (Kharaka et al., 2006).

Following CO_2 injection, chemical analysis from observation wells shows an immediate decrease in pH (6.5 to 5.7), and dramatic increases in alkalinity (e.g., 100 to 3,000 mg/L) and Fe (e.g., 30 to 1,100 mg/L). In addition, the team observed notable changes in the stable isotopic compositions of dissolved inorganic carbon (DIC) and H_2O. Geochemical modeling suggested that buffering associated with the dissolution of calcite and Fe oxyhydroxides prevented a more significant pH drop, while simultaneously accounting for the increase in HCO_3, Ca, Mg, and Fe concentrations observed (Kharaka et al., 2006). Based on these findings, Kharaka et al. (2005) , Kharaka et al. (2009) and Xu et al. (2010) present a list of important mineral-water-gas interactions in the Frio Formation following CO_2 injection (**Table A.2.8**).

Table A.2.8. Important Mineral-Water-Gas Interactions in Upper Frio Formation, from the Frio Brine Test Site.

Mineral	Reaction	Reference
--	$CO_{2(gas)} + H_2O \rightleftharpoons H_2CO_3$	Kharaka et al. 2005
--	$H_2CO_3 \rightleftharpoons HCO_3^- + H^+$	Kharaka et al. 2005
Calcite	$CO_{2(gas)} + H_2O + CaCO_3 \rightleftharpoons Ca^{2+} + 2HCO_3^-$	Kharaka et al. 2005; Kharaka et al. 2009
Calcite	$H^+ + CaCO_3 \rightleftharpoons Ca^{2+} + HCO_3^-$	Kharaka et al. 2005
Siderite	$H^+ + FeCO_3 \rightleftharpoons Fe^{2+} + HCO_3^-$	Kharaka et al. 2005
--	$4Fe^{2+} + O_2 + 10H_2O \rightleftharpoons 4Fe(OH)_3 + 8H^+$	Kharaka et al. 2005
--	$2Fe(OH)_{3(s)} + 4H_2CO_3 + H_{2(g)} \rightleftharpoons 2Fe^{2+} + 4HCO_3^- + 6H_2O$	Kharaka et al. 2009
Dolomite	$2H^+ + CaMg(CO_3)_2 \rightleftharpoons Ca^{2+} + Mg^{2+} + 2HCO_3^-$	Kharaka et al. 2005
Plagioclase feldspar	$4.8H^+ + Ca_{0.2}Na_{0.8}Al_{1.2}Si_{2.8}O_8 + 3.2H_2O \rightleftharpoons 0.2Ca^{2+} + 0.8Na^+ + 1.2Al^{3+} + 2.8H_4SiO_4$	Kharaka et al. 2005
Plagioclase feldspar	$0.4H^+ + Ca_{0.2}Na_{0.8}Al_{1.2}Si_{2.8}O_8 + 0.8CO_2 + 1.2H_2O \rightleftharpoons 0.2Ca^{2+} + 0.8NaAlCO_3(OH)_2 + 0.4Al(OH)_3 + 2.8SiO_2$	Kharaka et al. 2005; Kharaka et al. 2009
Dawsonite	$NaAlCO_3(OH)_2 + 3H^+ \rightleftharpoons Al^{3+} + HCO_3^- + Na^+ + 2H_2O$	Xu et al. 2010; Søvik 2012
Ankerite	$CaFe(CO_3)_2 + 2H^+ \rightleftharpoons Ca^{2+} + Fe^{2+} + 2HCO_3^-$	Xu et al. 2010; Søvik 2012
Kaolinite	$Al_2Si_2O_5(OH)_4 + 5H_2O + 6CO_{2(g)} \rightleftharpoons 2Al^{3+} + 6HCO_3^- + 2H_4SiO_4$	Xu et al. 2010; Harvey et al. 2012
Illite	$K_{0.6}Mg_{0.25}Al_{2.3}Si_{3.5}O_{10}(OH)_2 + 8H^+ \rightleftharpoons 5H_2O + 0.6K^+ + 0.25Mg^{2+} + 2.3Al^{3+} + 3.5SiO_{2(aq)}$	Xu et al. 2010; Fatah et al. 2022

SOURCE: Kharaka et al., 2005; Kharaka et al., 2009; and Xu et al., 2010. Note: Note that Xu et al. (2010) only provide modelling results in their work, so the reaction equations provided above are sourced from other cited literature.

As a first step in the modeling of geochemical reactions during CO_2 injection and transport at the project site, the reactions presented in **Table A.2.8** have been incorporated into the multiphase transport simulator TOUGHREACT®, and further discussed in *Module B - Area of Review and Corrective Action Plan*. In addition, the TOUCHREACT simulation incorporated reactions provided in the TOUGHREACT software package for the minerals identified in the Frio core samples from the Dow Injection Well No. 3 (**Tables A.2.2 and A.2.3**).

Following the collection of site-specific formation fluid and bulk solid phase samples from the target injection zone in the Frio Sand and overlying Anahuac Shale, these reactions will be updated to reflect local aqueous geochemistry and mineralogy. Specifically, a geochemical modeling program such as PHREEQC will be used to further evaluate the distribution of aqueous species, mineral saturation indices, and reactions anticipated to occur within the targeted formation. The results of the geochemical modeling will be incorporated into reactive transport models to assess potential changes in the chemistry of formation fluids within the targeted formation and relevant mineral dissolution and precipitation reactions over near-term and longer-term timeframes. These models will inform potential changes in porosity and permeability, and the recalcitrance or lability of relevant carbonate minerals during and following injection. The impact of physiochemical model input parameters on modeling results will be evaluated to quantify uncertainties.

2.5 Geomechanical Characterization

Regional and local geology, respectively, at the Caliche Beaumont Sequestration Project Site are described in detail in Sections 2.1 and 2.2 of this *Module A*. Per 40 CFR §146.82(a)(3)(iv), this section details i) the mechanical rock properties and in-situ fluid pressures, including ductility, stress, pore pressures, and fracture gradients, of the Caliche Beaumont Sequestration Project sequestration complex, and ii) the results of a stress evaluation of local Fault A.

Site-specific geomechanical data, including laboratory analyses of recovered core samples, will be collected during the drilling and testing of the injection and monitoring wells (as detailed in *Module D – Pre-Operational Testing Plan*, and the geomechanical characterization will be updated accordingly.

2.5.1 Ductility

Site-specific data will be acquired and tested on cores collected during the drilling of the injection well. Although there are no site-specific brittleness or ductility/creep measurements available for the Anahuac Formation, assumptions have been made based on information in published literature and from nearby sites. Claimed as PBI [redacted] **Exhibit A.2.14** below shows the relationship between ductility and bulk density observed for 68 shales by Hoshino et al. (1972). The geomechanical behavior of the Anahuac Formation is expected to be ductile (yellow shaded range in **Exhibit A.2.14**), meaning that it will deform to large strains by diffuse deformation without macroscopic fracturing (i.e., lacking a discrete fault plane). The stress-strain relationship would not show a sharp stress drop after peak stress. Moreover, the confining pressures increase ductility.

Exhibit A.2.14. Density Effects on Shale Ductility.

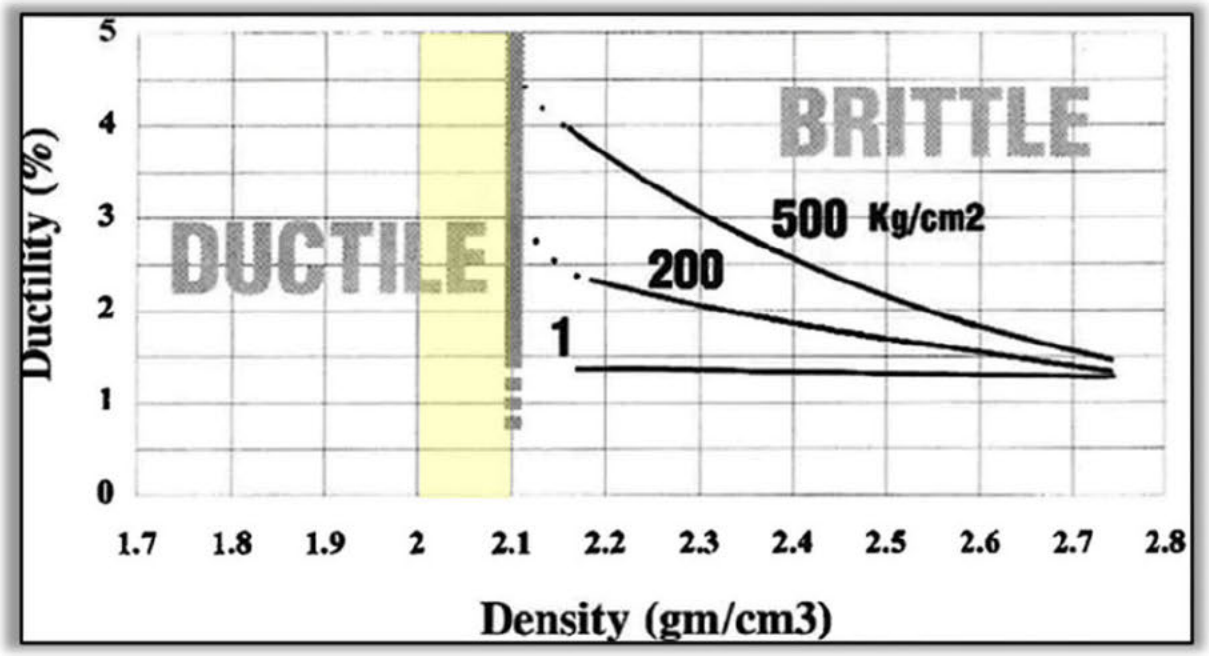

SOURCE: Hoshino et al., 1972; modified by GSI.

2.5.2 Pore Pressures

Changes in pore pressure resulting from CO_2 injection activities can disrupt the natural stress conditions in the subsurface, potentially leading to fault or fracture movements. This occurs due to a decrease in the normal effective stress and an increase in shear stress.

Pore pressure data from each Upper Frio Sand (Orange, Green, Yellow, and Gold) layer was extracted from the computational model. Static pore pressure was determined at the start of the pre-injection period. Pressure changes during and after CO_2 injection were estimated. These induced pressure values were used to set maximum injection pressures and calculated safety factors at the fault line.

2.5.3 Stress

Regional literature from Eaton (1969) indicates that the overburden stress gradient for normally compacted Gulf Coast sediments ranges from about 0.85 psi/ft near the surface to about 1.00 psi/ft at depths of about 20,000 feet. Sedimentary rocks along the central portion of the Gulf Coastal Plain experience predominantly normal faulting, with a maximum horizontal stress oriented sub-parallel to the coastline (Lund Snee and Zoback, 2020b) and a minimum horizontal stress (i.e., the least principal stress) oriented orthogonal to the coastline.

Published data have been used to set the orientation of the principal horizontal stresses (Meckel et al., 2017; Nicholson, 2012; Zoback and Zoback, 1980) using regional fault-strike statistics (see **Exhibit A.2.15** below). The geomechanical properties of the primary Upper Confining Unit (Anahuac Formation) will be further measured during the drilling and completion of the project's injection and monitoring wells.

Exhibit A.2.15. Principal Horizontal Stresses along the Gulf Coast Region.

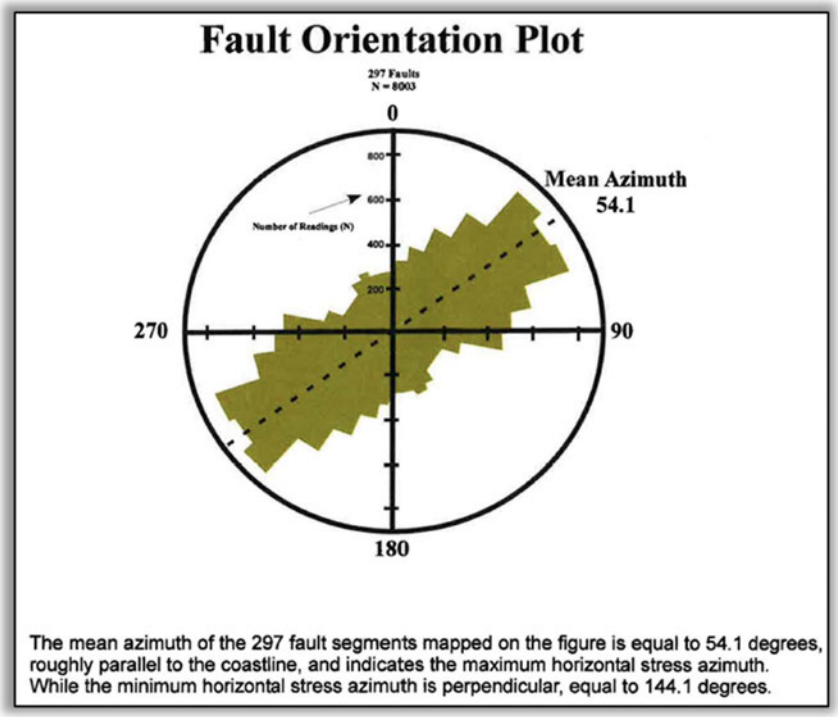

SOURCE: Nicholson, 2012.

2.5.3.1 Vertical Stress

An overburden pressure gradient was estimated using the composite overburden stress gradient for all normally compacted Gulf Coast sediments (Mohr, 1986, Figure 13-10) (see **Exhibit A.2.16**).

Exhibit A.2.16. Composite Overburden Stress Gradient for All Normally Compacted Gulf Coast.

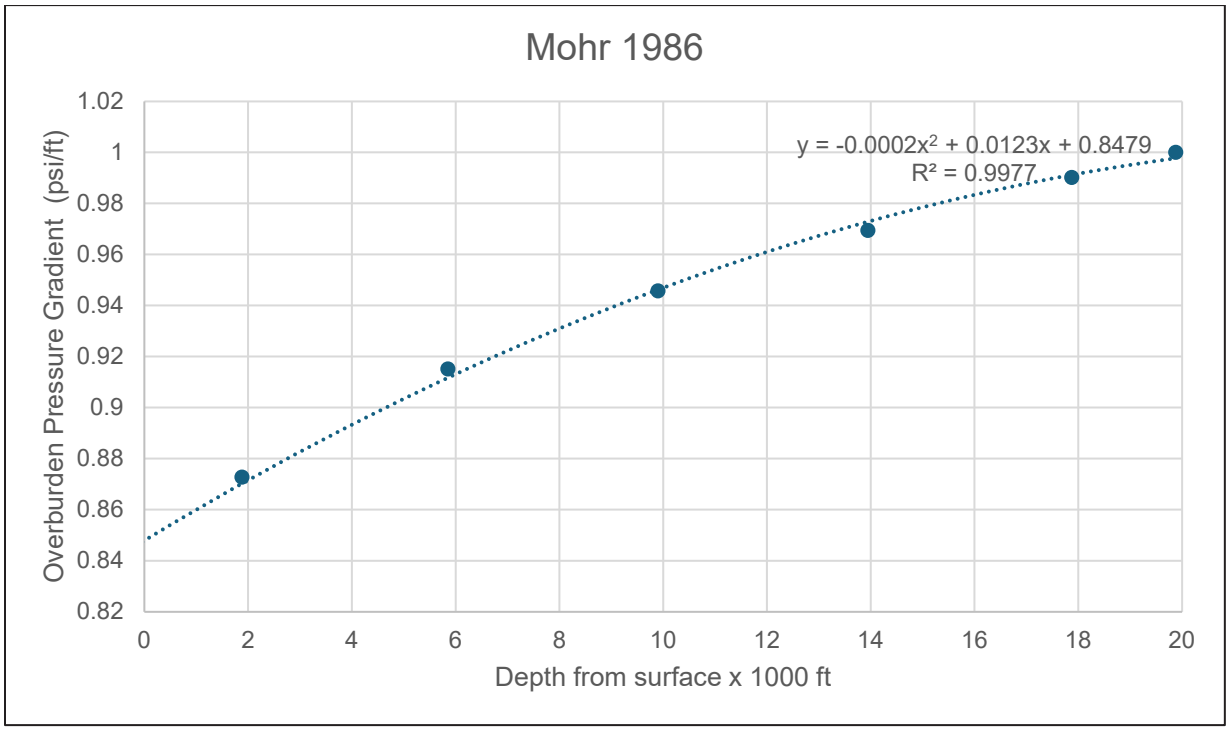

SOURCE: Mohr, 1986, Figure 13-10; modified by GSI.

The vertical stress (psi) was calculated based on the approximate depth of each Upper Frio Sand layer at the injection well locations and the overburden pressure (psi/ft). The results are tabulated below in **Table A.2.9**.

Table A.2.9. Summary of the Estimated Range of Vertical Stress Distribution at the Caliche Beaumont Sequestration Project Site.

Note: Lower Frio Formation range is the bottom of Frio Gold Sand.

2.5.3.2 Maximum and Minimum Horizontal Stress

Maximum and minimum horizontal stresses were derived from the vertical stress and pore pressure estimates from above using the following equation.

$$\sigma_h = \frac{\nu}{1-\nu}(\sigma_v - P_p) + P_p$$

Where:

σ_h= horizontal stress (psi)
ν = Poisson's ratio(-)
σ_v = vertical stress (psi)
P_p = pore pressure (psi)

Results of the maximum, minimum, and best estimate horizontal stresses at the CO_2 injection wells are tabulated in **Table A.2.10** below.

Table A.2.10. Summary of the Estimated Range of Minimum Horizontal Stress Distribution at the Caliche Beaumont Sequestration Project Site.

Note: Lower Frio Formation range is the bottom of Frio Gold Sand.

The maximum horizontal stress was estimated using a Poisson's ratio of 0.45, while the minimum horizontal stress was estimated at 0.25. The best estimate horizontal stress was also calculated based on the Poisson's ratio obtained from Figure 13-11 Variations of Poisson's Ratio with Depth in Mohr (1986) (see **Exhibit A.2.17**).

Exhibit A.2.17. Variations of Poisson's Ratio with Depth.

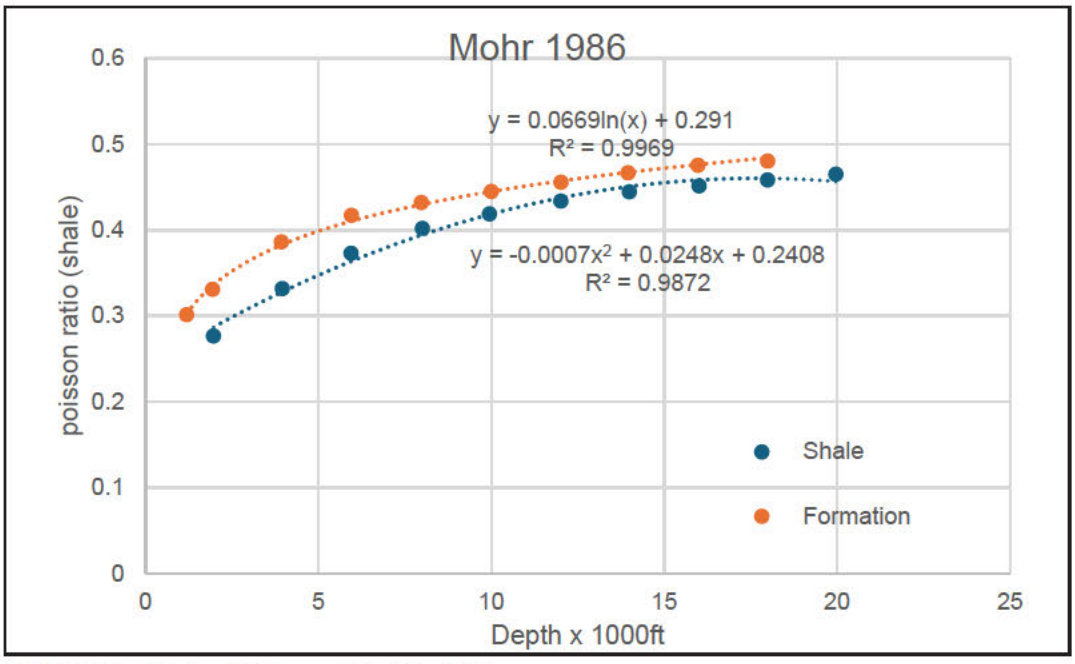

SOURCE: Mohr, 1986; modified by GSI.

The pore pressure of the formation was estimated from the linear regression line fitted to the observed pressure at each depth. The data for **Exhibit A.2.18** were obtained from work done by Geostock Sandia in the Upper Frio Formation at nearby Dow and BASF Class I injection well sites.

Exhibit A.2.18. Relationship between Depth and Aquifer Pressure in Upper Frio Formation.

Note: Grey data points are from Frio Sands, and orange data points are from Miocene Sands.

2.5.4 Fracture Gradients

The fracture gradient (FG) was estimated from the horizontal stress (σ_h) calculated above.

$$FG = \sigma_h / B$$

where B is the depth of the injection zone from the elevation surface. The estimated fracture gradient varies between 0.60 and 0.84 psi/ft (see **Table A.2.11** below).

For the maximum pore pressure, the best-estimated value of horizontal stress was used. To be conservative, the depth of the well perforation tops at each layer was selected to calculate the maximum pore pressure.

Table A.2.11. Fracture Gradient within Each Upper Frio Formation Sand Interval.

2.5.5 Elastic Moduli

The geomechanical properties of the primary Upper Confining Unit (Anahuac Formation) will be further measured during the drilling and completion of the project's injection and monitoring wells.

Compressive wave velocity measurements were used to compute the elastic moduli. The relationship between compressive wave velocity v_p, bulk modulus K and shear modulus G is:

$$v_p = \sqrt{\frac{K+\frac{4G}{3}}{\rho}},$$

where $\rho = 127.9\ \frac{lb}{ft^3}$ is the average density of the formation. Similarly, the shear modulus G is related to the shear wave velocity v_s by:

$$v_s = \sqrt{\frac{G}{\rho}}$$

Shear wave velocity measurements at the site were not available, but were derived from the relationship to compressive velocity velocity and Poisson's ratio ν:

$$\nu = \frac{\left(\frac{v_p}{v_s}\right)^2 - 2}{2\left(\left(\frac{v_p}{v_s}\right)^2 - 1\right)},$$

where ν was computed according to Figure 13-11 Variations of Poisson's Ratio (Mohr, 1986). Finally, the Young's Modulus was calculated by:

$$E = 3K(1 - 2\,\nu)$$

From measurements of v_p provided by Geostock Sandia, the elastic moduli were computed for the average formation depth and are listed below in **Table A.2.12**.

Table A.2.12. Elastic Moduli by Upper Frio Formation Sand Interval.

Compressibility (deformation change per stress increase) is the inverse of elastic modulus (stress change per strain increase). Young's Modulus is 2.9 x 10^5 psi, which is derived from the rock compressibility of soil in the feasibility study (2021 RAZZA Feasibility Study).

2.5.6 Fault Stress Condition

The fault Factor of Safety (FOS) was computed using the Mohr-Coulomb failure envelope, which is described as the shear stress τ parallel to the fault plane as (Jaeger and Cook, 1969; Byerlee, 1978):

$$\tau = C + \mu(\sigma_n - p_f) = C + \mu\sigma_n',$$

Where:

C = fault cohesion
μ = friction angle
σ_n = total stress normal to the fault
p_f = fluid pore pressure
σ_n' = effective rock stress

The failure envelope is a line on the Mohr-Coulomb diagram. The effective stress normal to the fault can also be found by construction of the Mohr's circle, whose diameter is the difference of the effective principal stresses σ_1' and σ_3', and which intersects the x-axis of the Mohr-Coulomb diagram at σ_1' and σ_3', respectively. An example Mohr-Coulomb diagram is shown below in **Exhibit A.2.19**. $\sigma_1 > \sigma_2 > \sigma_3$ are defined as the stresses in vertical and two horizontal directions, respectively. $\sigma_1 = P_{ob} * z$, where z is the depth below ground surface at which the pressure is measured, and P_{ob} is based on Moore (1986, **Exhibit A.2.18**). Jung et al. (2018) compute σ_3 by:

$$\sigma_3 = \frac{\nu}{1-\nu}(\sigma_1 - p_f) + p_f$$

where ν is calculated after Moore (1986, **Exhibit A.2.17**). Following Nicholson et al. (2014), we also assume that $C = 0$ and $\mu = 0.6$, which corresponds to a fault friction angle of about 30°. Using these relationships, the normal and shear effective stresses on the fault, σ' and τ', are computed, which then provide the associated friction angle as $\phi = \tan^{-1}\frac{\tau'}{\sigma'}$. The ratio of the available friction angle of the failure envelope to ϕ is the FOS. **Exhibit A.2.20** shows the Mohr-Coulomb diagrams for the pre-injection (dark blue line) and post-injection (light blue line) stress conditions by Upper Frio Sand layer and the assumed failure envelope at Fault A. The dot on the Mohr's circle signifies the respective σ'/ τ' pair. The lowest FOS is 3.21 at Fault A.

Exhibit A.2.19. Mohr-Coulomb Diagram.

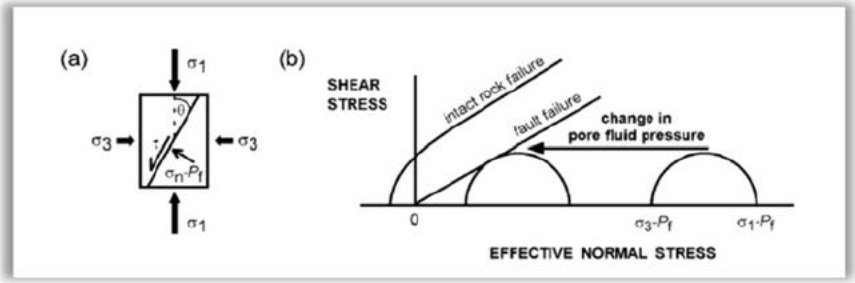

SOURCE: Streit and Hillis, 2004.

Claimed as PBI

Claimed as PBI

2.6 Seismic History and Risk

The Caliche Beaumont Sequestration Project Site is in the coastal region of the West Gulf Coastal Plain where the seismic hazard is low. According to the 2018 US seismic hazard map (**Exhibit A.2.21**), published by the USGS (USGS, 2019a), the project site is near the southern boundary of a region where the earthquake peak ground acceleration (PGA) that has a 5% chance of being exceeded in 50 years (i.e., return period of 975 years) has a value between 4% and 8% g. **Exhibit A.2.22** shows the 2014 US Seismic hazard map (former version of the map), which indicated that the 975-year PGA at the site was previously estimated to be below 0.04 g (USGS, 2019b). Therefore, the most recent estimate of the 975-year PGA at the project site is expected to be slightly over 0.04 g. Additionally, according to Texas Almanac (2021) which included data from the U.S. Geological Survey and the Institute for Geophysics at the University of Texas at Austin, the seismic hazard at the project site is low (**Exhibit A.2.23**).

Exhibit A.2.21. 2018 U.S. Seismic Hazard Map.

SOURCE: USGS, 2019a.

Exhibit A.2.22. 2014 U.S. Seismic Hazard Map.

SOURCE: USGS, 2019b.

The regional faulting system and local faults are described in detail in Section 2.2 of this *Module A*. Natural seismicity in the West Gulf Coastal Plain is primarily due to the movement along normal faults which extend to the basement (**Exhibit A.2.24**). This faulting is a result of continental rifting with down to the basin extension during the opening of the Gulf of Mexico; in combination with extreme sediment loading creating down warping of previously deposited sediments. Both extension and sediment loading remained active through the deposition of Tertiary sediments in the region. Extensional tectonic stress driven by the vertical stresses of the overlying sediment has caused persistent subsidence of the seafloor and extension of the basin, resulting in graben zones. Contemporaneous extensional faulting with sedimentation has generated growth faults. Thicker sediments are observed on the downthrown side of faults. Throw tends to decrease up section and away from the origin of the fault. Although grabens and growth faults can store and release seismic energy, they are weak and ineffective at generating intense ground motion. Echelon of grabens and syn-depositional growth faults have resulted in the regional faulting systems. The maximum horizontal stress is subparallel to the coastline, following the strikes of the growth faults.

Exhibit A.2.23. Major Earthquakes of Texas.

SOURCE: Texas Almanac, 2021.

As discussed in Section 2.2 of this *Module A*, the Caliche Beaumont Sequestration Project Site is in a structural low or syncline. In the vicinity of the project site, one large down-to-the-southeast fault, designated as Fault A, extends from the southwestern margin of Spindletop salt dome (as a domal radial and growth fault – extending and influencing regional strata) and passes through the subsurface in a northeast to southwest trending direction, transecting the southernmost portions of the Caliche Beaumont Sequestration Project Site and terminating into Lovells Lake Field (where it is the master field fault). The fault has Claimed as PBI of displacement along its length at the top of the Frio Formation and transects approximately 10 wells across the project area. A small throw antithetic fault (Fault A') is associated with Fault A; however, the antithetic fault does not appear to intersect any of the wellbores in the area. In addition, two domal radial faults, Faults B and C, extend from the western and northern margins, respectively, of the Spindletop salt dome, but neither fault intersects the Caliche Beaumont Sequestration Project Site; and therefore, Faults A', B, and C are not further considered.

Exhibit A.2.24. Location of Project Caliche Site in Regional Tectonic Setting of the East Texas Basin.

SOURCE: Jackson and Wilson, 1982.

As further discussed in Section 2.2 of this *Module A*, several lines-of-evidence (LOEs) demonstrate that Fault A is a self-healed, non-transmissive fault that prevents vertical or lateral fluid migration:

1. Shales beneath the Caliche Beaumont Sequestration Project Site are ductile at the depths of interest.
2. Juxtaposition of ductile shale beds or sand-to-shale beds across a fault forms a vertical barrier to fluid flow.
3. Zones of deformed clay/shale can become greatly attenuated and trapped along fault planes.
4. Fault slippage generally “self-heals” over time.
5. Numerous oil and gas accumulations are trapped by the Gulf Coast faults and are targeted for oil and gas production.
6. Miocene formation pressure gradients exceed Oligocene formation pressure gradients.

Plastic flowage of salt rupturing adjacent sedimentary layers has caused salt domes in the coastal region. These sediments have low density, poor cementation, low shear strength and shear modulus. As shown in **Exhibit A.2.25**, the project site is approximately Claimed as PBI of the Spindletop Salt Dome. **Exhibit A.2.26** below shows the domal radial Faults A, B, and C, extending from the Spindletop salt dome near the project site. Earthquakes triggered by a salt dome are expected to have magnitudes less than 3.0 on the Richter scale, which might be felt locally but incapable of propagating damaging ground motions. However, there is no evidence that the faults near the project site are seismically active, and no induced earthquake has been recorded within 100 miles of the project site. Furthermore, as discussed in *Module B – Area of Review and Corrective Action Plan*, maximum injection pressures anticipated for the Caliche Beaumont Sequestration Project Site are not predicted to exceed the 80% fracture gradient and therefore injection operations will not initiate or propagate existing fractures in the sequestration zone.

Exhibit A.2.25. Coastal Texas and Louisiana Salt Dome Locations.

SOURCE: Looff and Looff, 2000.

Exhibit A.2.26. Radial Faults Associated with Salt Domes in the Gulf Coastal Region.

SOURCE: Modified from Ewing 1986.

USGS (2023a) reported an increase in seismicity in the Central United States since 2009. **Exhibit A.2.27** shows the annual number of earthquake events with magnitude greater than 3 from 1973 to 2023. **Exhibit A.2.28** (USGS, 2016) shows 21 areas with earthquake events that were interpreted to be related to oil and gas activities. These areas are more than 100 miles from the project site. Induced earthquakes in these areas are not expected to impact the project site.

Exhibit A.2.27. Seismicity of Central United States: 1973 through August 2023.

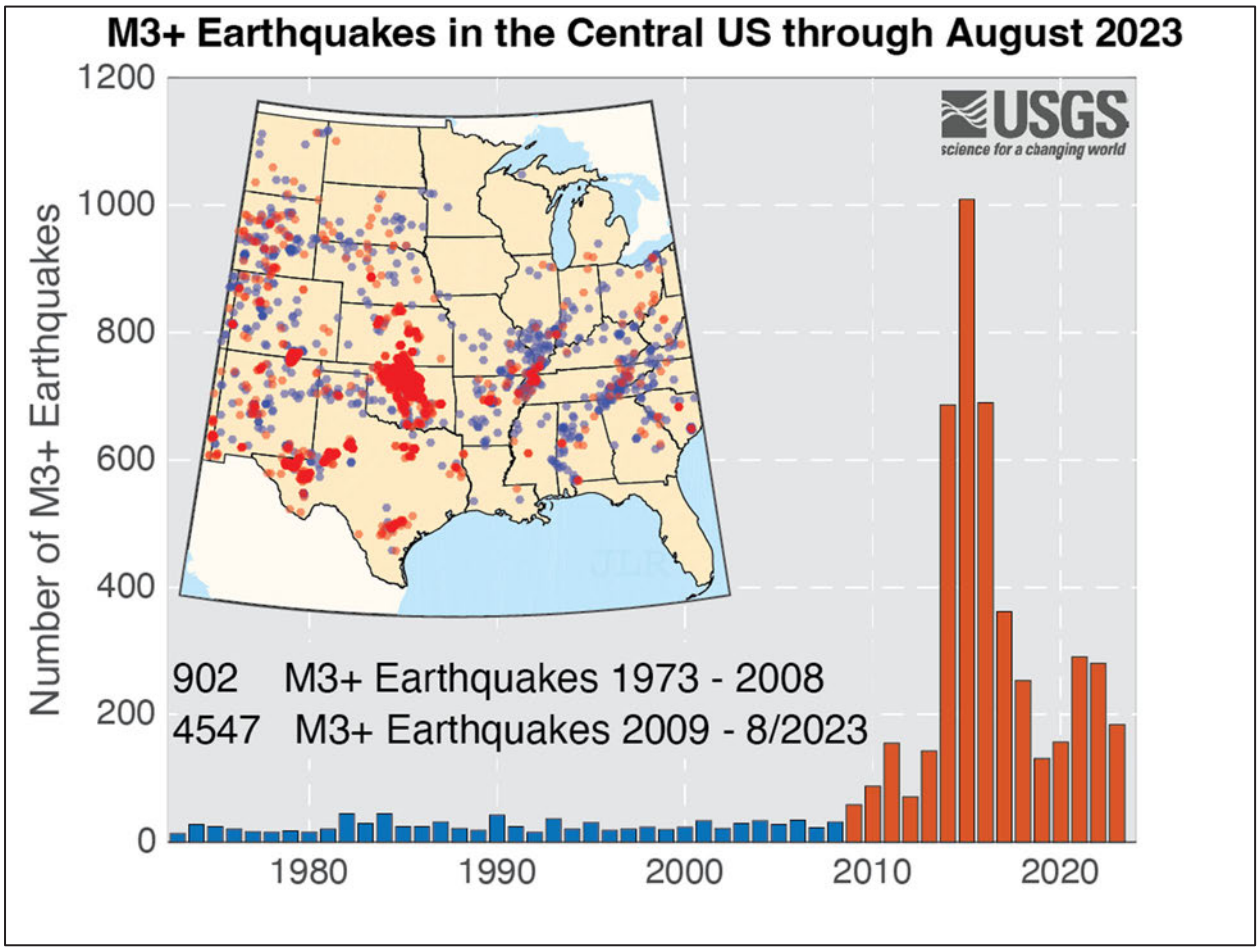

SOURCE: USGS, 2023a.

Exhibit A.2.28. Seismicity Related to Injection Wells.

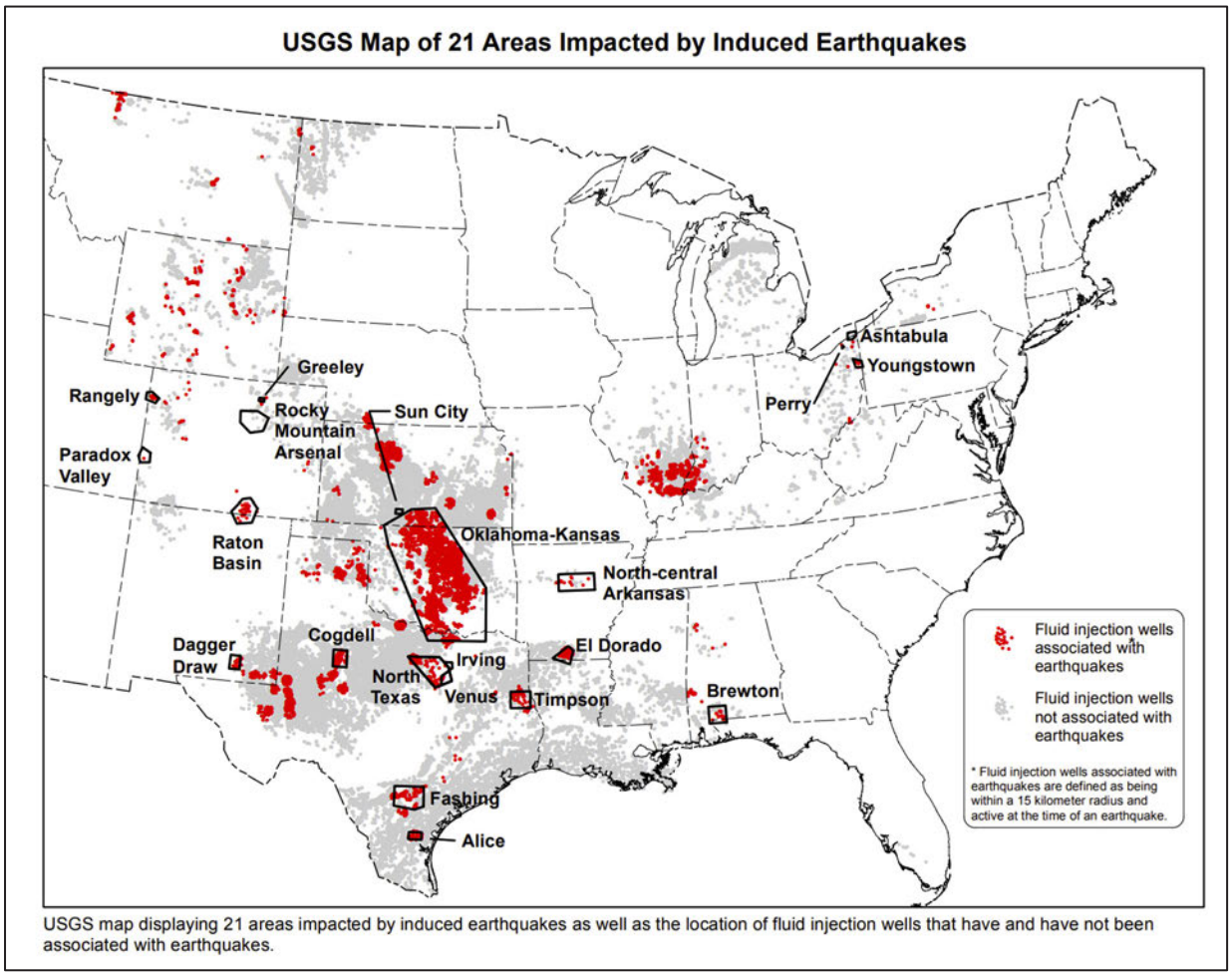

USGS map displaying 21 areas impacted by induced earthquakes as well as the location of fluid injection wells that have and have not been associated with earthquakes.

SOURCE: USGS, 2016.

Exhibit A.2.29 shows the identified earthquake events in the coastal region from 1843 through 1989. None of the recorded earthquakes within 100 km radius from the project site have a magnitude greater than 4.0.

Exhibit A.2.29. Identified Gulf Coast Earthquakes from 1843 to 1989.

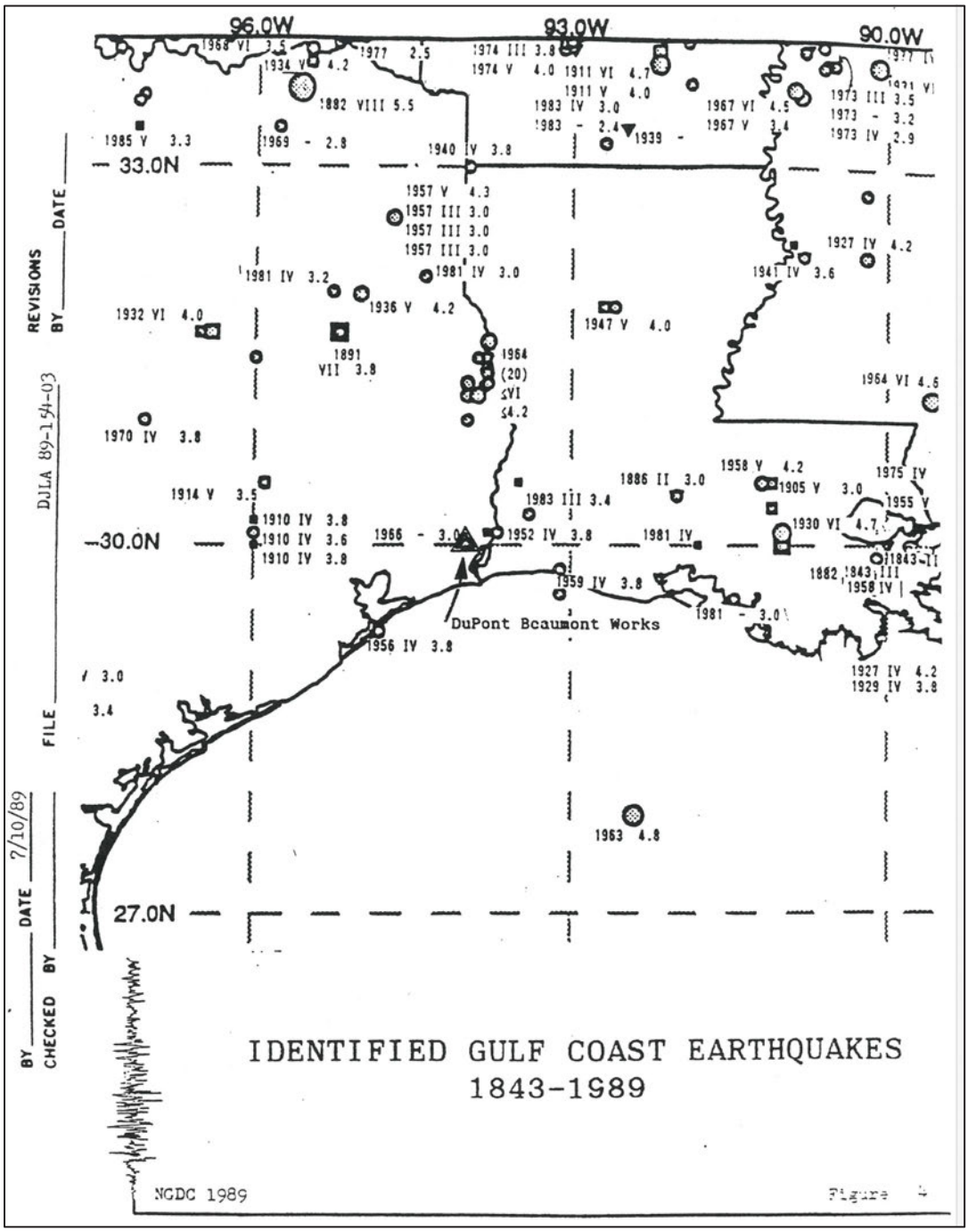

SOURCE: NOAA publication 'Earthquake History of the Gulf Coast Region

Proximal seismicity data also have been downloaded from several sources, as described below:

- **SOURCE:** USGS (https://earthquake.usgs.gov/earthquakes/search/)

  The available dataset includes seismic events from 8 January 1891 through 29 January 2021. Two events were found within a [redacted]-mile radius of the project site. The magnitudes

of these earthquakes are less than 4.0. **Exhibit A.2.30** shows the locations of the two earthquake events identified and summarizes the date, magnitude, and depth of these earthquakes.

Exhibit A.2.30. Seismicity Data from USGS: 1891 to 2021.

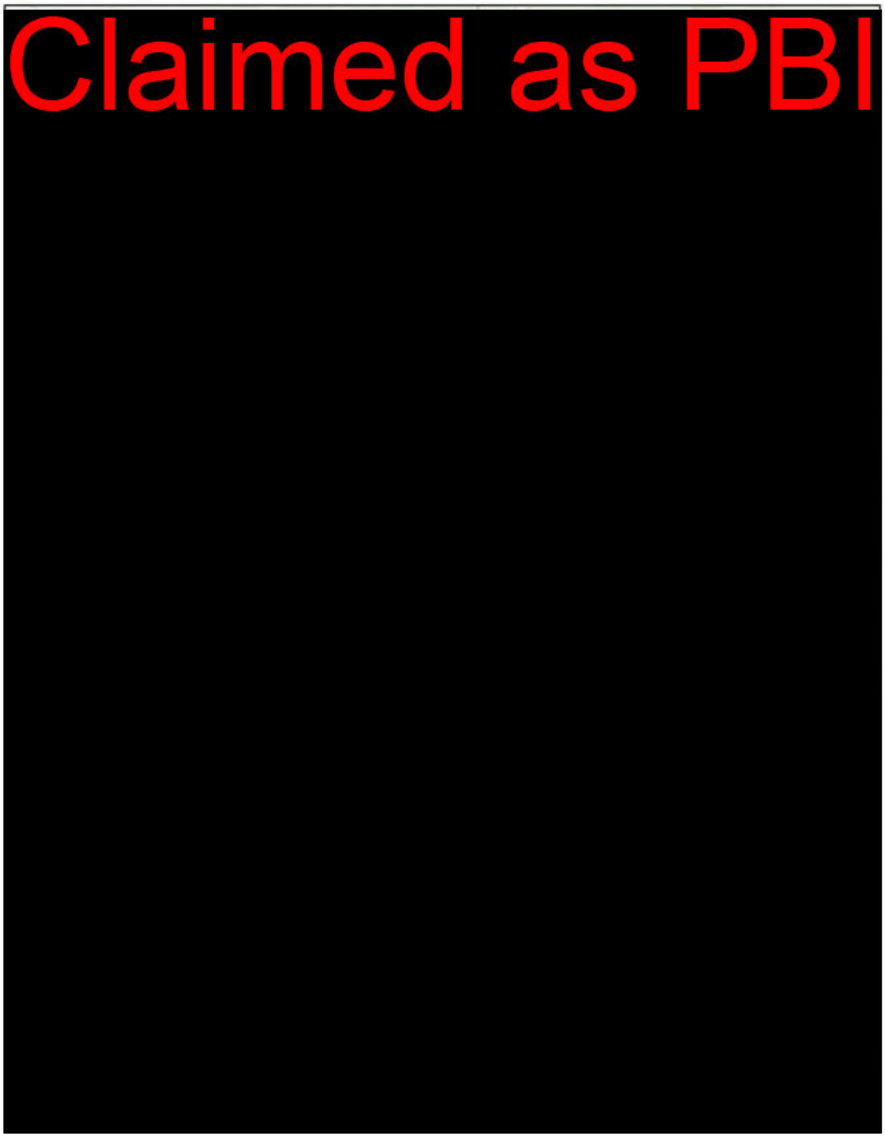

SOURCE: USGS, 2023b.

Event Date	Magnitude	Depth
10/16/1983	3.8 mblg	5.0 km
01/20/2019	3.3 ml	5.0 km

- **SOURCE:** The Human-Induced Earthquake Database (*HiQuake*) (https://inducedearthquakes.org/)

Eight induced earthquake events within [redacted] miles of the project site were recorded in this data set. The locations of these events are shown in **Exhibit A.2.31**. Magnitude information is available for only one of these events. The recorded magnitude is less than 4.0. It is expected that the magnitudes of the other events are also less than 4.0.

Exhibit A.2.31. Seismic Data from Human-Induced Earthquake Database.

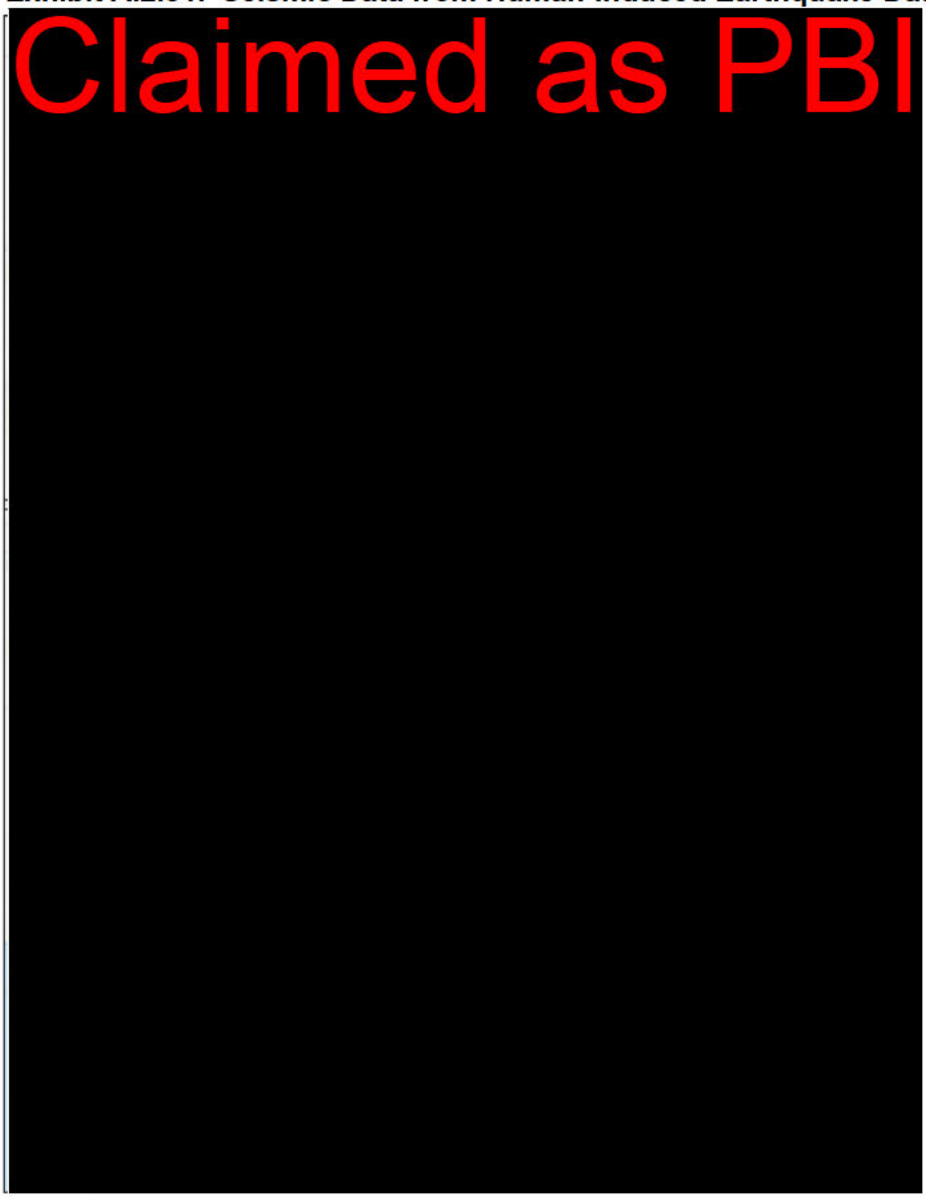

SOURCE: HiQuake, 2023.

Point	Earthquake cause	Date	Magnitude
A-F	Oil and gas extraction	-	-
G	Waste disposal	1993	-
H	Waste fluid disposal	1983	3.8 ml

- SOURCE: University of Texas (TexNet) (https://www.beg.utexas.edu/texnet-cisr/texnet/earthquake-catalog)

  This data set includes earthquake events from 1 January 2017 through 7 August 2023. Sixteen earthquake events were found within a [redacted] radius of the project site. **Exhibit A.2.32** shows the locations and magnitudes of these events. The magnitudes of these events are less than 4.0. The earthquake event with a magnitude between 3.5 and 4 is likely to be the 2019 earthquake event obtained from the USGS data set described above.

Exhibit A.2.32. Seismic Data from Human-Induced Earthquake Database.

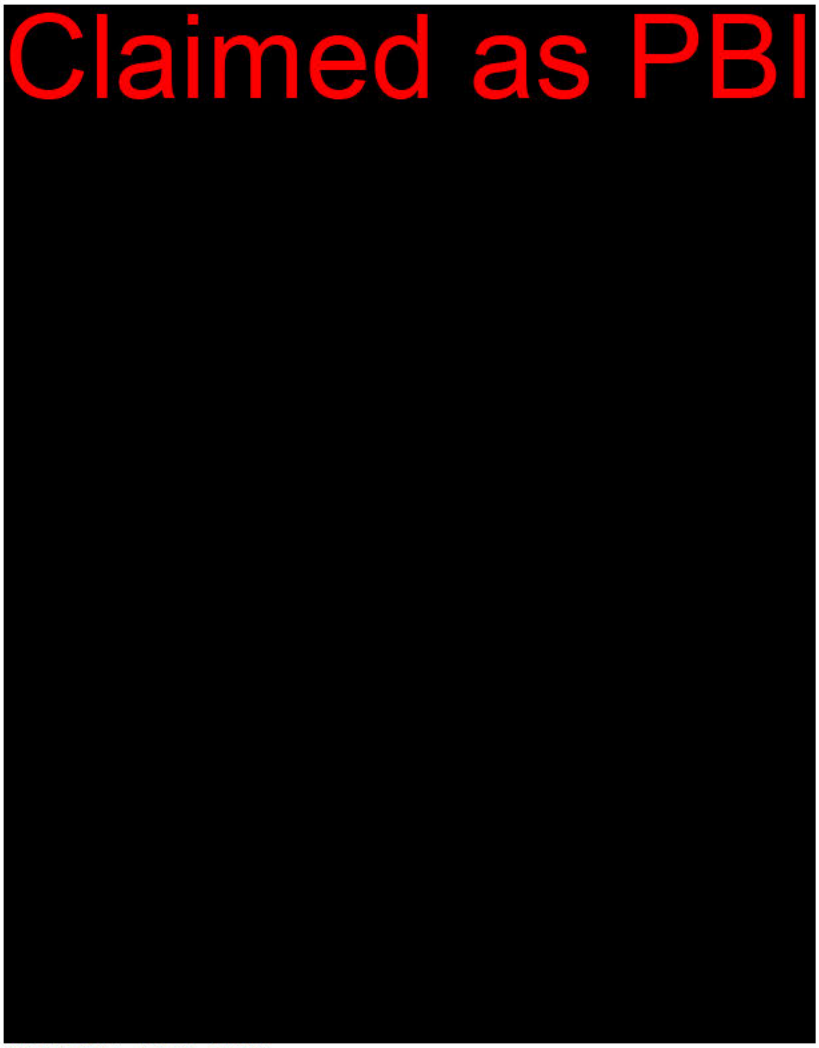

SOURCE: BEG, 2023.

- **SOURCE:** Seismological Facility for the Advancement of Geoscience (SAGE) (http://ds.iris.edu/wilber3/find_event)

  Two seismic events were found within Claimed as PBI of the project site. **Exhibit A.2.33** shows the locations, magnitudes, dates, and depths of these earthquakes. They are the same events recorded in the USGS data set; however, the magnitudes of these earthquakes in the SAGE database are less than the magnitudes recorded in the USGS database.

Exhibit A.2.33. Seismicity data from the SAGE.

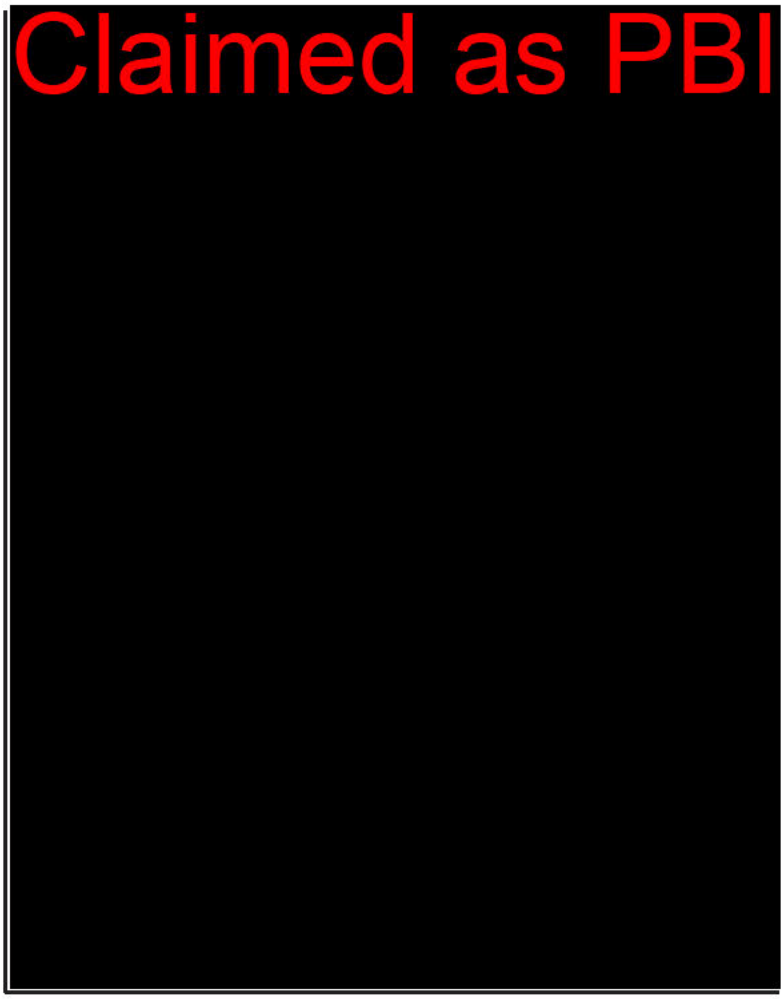

SOURCE: SAGE, 2023.

Event Date	Magnitude	Depth
10/16/1983	3.5 mblg	5.0 km
01/20/2019	3.2 ml	5.0 km

None of the earthquake events found from these sources are associated with the local faults identified near the project site. In summary, the overall seismic risk and the potential of significant fault rupture in the project area is rated low because:

- The 975-year PGA is estimated to be approximately 4% g.
- Only a few low magnitude (< 4.0) earthquakes have been recorded within 100 miles of the project site.
- There is no evidence that the faults near the project site are seismically active.
- No induced earthquake has been recorded within 100 miles of the project site.

As a result, the liquefaction risk and its potential damage at the project site is expected to be insignificant.

2.7 Local Economic Geology

Pursuant to 40 CFR §146.82(a)(2) and CARB LCFS Subsections C.2.3(a)(1)(A) & C.2.3(a)(10), a brief description of the major known mineral deposits and their relevance to the Caliche Beaumont Sequestration Project Site is discussed below. Caliche identified three main natural resources or activities which are typically encountered in the vicinity of Caliche Beaumont Sequestration Project Site and include: 1) oil and gas resources, 2) deep geology storage for injection and disposal of waste typically associated with oil and gas activities, and 3) mineral resources.

2.7.1 Oil and Gas Resources

Texas has a long history of oil and gas (O&G) exploration and production (E&P) with the first E&P activities dating back to the mid-1860s near Nacogdoches, East Texas (Hinton and Olien, 2002, Chapter 1). However, the early oil productions were considered "modest" by the standard of their time until the discovery of the Spindletop Oilfield in 1901 near Beaumont, Texas, which revolutionized the oil industry (Hinton and Olien, 2002, Chapter 1). Since this major oilfield discovery, as well as many other oilfields, Texas has been one of the major O&G producers in the US, contributing to over 40% of total US crude oil production in 2022 (US EIA, 2023a, see website). The US Energy Information Administration predicts that the total US production of crude oil and condensate will generally remain stable (US EIA, 2023b, Annual Energy Outlook 2023b Table 1); and therefore, as this carbon intensive industry remains generally stable, the need for capturing and sequestering CO_2 will remain important for meeting net carbon emission targets to help reduce the effects from climate changes.

The Caliche Beaumont Sequestration Project Site is located near historical and active oilfields, including the Spindletop, Lovells Lake, and Amelia Oilfields (see attached **Figure A.2.62**). The City of Beamont Acreage, where the injection wells will be located, is approximately Claimed as PBI of the Spindletop Oilfield, 4 miles northeast of the Lovells Lake Field, and Claimed as PBI of the Amelia Field. A short description of the oilfields is included below. A detailed discussion of nearby artificial penetrations including O&G and waste disposal wells within the Caliche Beaumont Sequestration Project Site AoR is provided in Section 3.0 of this *Module A* and in *Module B – Area of Review and Corrective Action Plan*.

2.7.2.1 Spindletop Oilfield

Located in the southern portion of Beaumont, Texas, the Spindletop Oilfield was first discovered in January 1901, with the first well drilled to 1,139 ft bgs in the flank of the Spindletop salt dome (TSHA, 2019). The rush to this oilfield followed soon after the report of the famous "Lucas Gusher," which blew a stream of oil more than 100 feet high before being capped and was estimated to produce up to 100,000 barrels/day (TSHA, 2019). According to the RRC database, there are records of over 1,000 wells drilled in the Spindletop Oilfield for O&G productions (RRC, 2023, GIS website output). The majority of O&G wells in the Spindletop Oilfield were constructed between 500 and 6,300 ft bgs with some wells installed deeper than 15,000 ft into underlying formations.

2.7.2.2 Lovells Lake Oilfield

The Lovells Lake Oilfield was first discovered in 1938, with multiple zones discovered between 1938 and 1956 (Kraye, 1962, p. 1). As of 1962, the total productive area was estimated to be approximately 3,600 acres (Kraye, 1962, p. 1). Most of the wells in this oilfield were constructed between 7,200 and >10,000 ft bgs (RRC, 2023, GIS website output).

2.7.2.3 Amelia Oilfield

In 1936, the Amelia Oilfield was discovered approximately 5 miles west of Beaumont, Texas (Hammer, 1939, Abstract). The relatively thin producing sands were found within the Frio Formation of nearly 1,200 acres (Hammer, 1939, Abstract). The RRC database indicates that the majority of the wells were constructed between 6,500 and 6,800 ft bgs, with some of the wells installed deeper than 8,700 ft bgs (RRC, 2023, GIS website output).

2.7.2 Other Resources from Oil and Gas Activities: Hydrocarbon Production Stimulation and Underground Disposal and Storage

The production of O&G often comes with large volumes of produced water (i.e., production water), which can contain very high levels of salinity, making the water unfit for potable water use without treatment. Common reuses or recycling of produced water associated with O&G E&P activities include hydraulic fracturing and water flooding (also known as secondary recovery) by stimulating the producing reservoir (US DOE, 2020, website). These processes involve the injection of produced water commonly treated with additives or proppants. The nearest injection well (Total Vertical Depth of 12,676 ft bgs) to the Caliche Beaumont Sequestration Project Site used for hydraulic fracturing is located Claimed as PBI and was operated last in January 2013 (FracFocus, 2023, Disclosure(s) for Gulf Terrace 'B' No. 1). Additionally, several nearby wells at various depths listed in the RRC database are used for water flooding (secondary recovery) purposes, under the authorization of USEPA UIC Class II injection well permits.

Nearby salt domes, including the Spindletop salt dome, are commonly associated with O&G E&P. In Jefferson County, nearby salt domes are also associated with sulfur production and storage of petroleum products and other gases. Utilizing USEPA UIC Class III injection wells, salt caverns, regulated by the RRC, are constructed via the dissolution of salt with fresh- or low-salinity water during the salt mining process, which creates underground spaces of generally inert composition – ideal for storing fluids and gases (Seni et al., 1984, p. 7). In the vicinity of the Caliche Beaumont Sequestration Project Site, large salt caverns in the Spindletop Oilfield are operated by Caliche (formerly Golden Triangle Storage, Inc), Centana Intrastate Pipeline LLC, and WSP USA Inc (RRC, 2022).

Additionally, the boom of the O&G industry in the early twentieth century in southeast Texas promoted the construction and operation of many petrochemical and chemical facilities. In Jefferson County, many facilities use deep injection wells to dispose of waste into various deep geologic formations, including saline reservoirs, under the authorization of USEPA UIC Class I hazardous waste injection well permits. Two such facilities with active Class I hazardous waste injection wells are located near the Caliche Beaumont Sequestration Project Site, approximately 5 miles to the southeast (BASF Beaumont Facility) and east (Dow Beaumont Facility).

As mentioned above, a detailed discussion of nearby artificial penetrations including O&G and waste disposal wells within the Caliche Beaumont Sequestration Project AoR is provided in Section 3.0 of this *Module A* and in *Module B – Area of Review and Corrective Action Plan*.

2.7.3 Mineral Resources

Although Jefferson County is well known for its hydrocarbon fuel production (i.e., oil and gas primarily), other nonfuel minerals and industrial minerals are also produced, predominantly including salt, sulfur, and construction sand and gravel (see **Figures A.2.63 and A.2.64**).

Salt (sodium chloride; NaCl) is used in various industries but is mostly used in chemical facilities for manufacturing of hydrochloric acid (Kyle and Elliott, 2019, Section 5.1). In Jefferson County, salt is produced primarily from salt domes such as the Spindletop salt dome by excavation of salt caverns within the domes (Kyle and Elliott, 2019, Section 5.1). One of the major salt-producing companies in Jefferson County is Texas Brine Corporation (Callaghan, 2019, p 46.3).

Sulfur, which was once produced from natural deposits from microbial processes in the Coastal Plain salt-dome cap rocks, is an essential compound in many industries as it is used to manufacture sulfuric acid (Kyle and Elliott, 2019, Section 5.3). Due to the depletion of natural sulfur deposits, low economical value of the sulfur production from those deposits, and requirements of the Clean Air Act, most of the sulfur is now produced from O&G production from "sour" fields with a high hydrogen sulfide (H_2S) content (Kyle and Elliott, 2019, Section 5.3).

Sand and gravel production is important to sustain population growth and urbanization as sands and gravels are used as construction material for roads, highways, buildings and various other structures. In Texas, most production facilities are located in the Coastal Plains (Kyle and Elliott, 2019, Section 4.2). The closest sand and gravel prospect to the Caliche Beaumont Sequestration Project Site is located approximately 4 miles east (BGE, 2023, Texas Mineral Resources Map).

2.8 Site Suitability

In this section, Caliche demonstrates that the proposed injection wells at the Caliche Beaumont Sequestration Project Site will be constructed and operated within a *"suitable geologic system,"* as required by 40 CFR §146.83 Minimum Criteria for Siting. As summarized below, Caliche has confirmed through detailed site characterization and computational modeling that the Caliche Beaumont Sequestration Project Site exhibits the following conditions:

- ***Sufficient Injection Zone:*** The Upper Frio injection zone contains three laterally extensive injection intervals Claimed as PBI [redacted] which exceeds the minimum injection depth of 2,600 ft. Isopach maps indicate that the injection intervals range in thickness from Claimed as PBI within the AoR, with a total thickness of Claimed as PBI . Estimated porosity and permeability within the injection intervals range between approximately Claimed as PBI and approximately Claimed as PBI, respectively.

Key Finding: *The Upper Frio Sand is of "sufficient areal extent, thickness, porosity, and permeability to receive the total anticipated volume" (40 CFR §146.83(a)(1)) of 18 to 24 MMt of CO_2(sc) over the anticipated* Claimed as PBI .

- ***Sufficient Upper and Lower Confining Zones:*** The Upper Frio Sand is confined below by the Upper Hackberry shales (Lower Confining Unit) and above by the Upper Confining System, which includes the shale containment layers of the Upper Frio (above the Upper Frio Green Sand), the Anahuac Formation, and the Lower Oakville Formation. The Upper Confining System and Lower Confining Unit are *"free of transmissive faults or fractures"* (40 CFR §146.83(a)(2)), as further discussed below. In addition, a low vertical permeability, approximately Claimed as PBI -thick shale interval is present between both the Green and Yellow Sands and between the Yellow and Gold Sands, which provide for hydraulic isolation of each of the three Sands from each other.
  Key Finding: *The Upper Confining System and Lower Confining Unit are of "sufficient areal extent and integrity to contain the injected carbon dioxide stream and displaced formation fluids" and to "allow injection at [the] proposed maximum pressures and volumes without initiating or propagating fractures in the confining zones" (40 CFR §146.83(a)(2)).*

- ***Non-Transmissive Fault A:*** A detailed review of the fault of interest, Fault A, beneath the Caliche Beaumont Sequestration Project Site confirms the non-transmissive, self-sealing nature of the fault thereby preventing vertical or lateral fluid movement. Several lines-of-evidence confirm that the local growth Fault A is not vertically or laterally transmissive, due to the ductile nature of the confining shales, the low sand-shale ratio, the high clay smear potential, the high shale gauge ratio, the structural trapping capacity, and the differential formation pressure gradients between Miocene- and Oligocene-aged formations.

- ***Key Finding:*** *The confining zone is free of transmissive faults or fractures and of sufficient areal extent and integrity to contain the injected carbon dioxide stream and displaced formation fluids and allow injection at proposed maximum pressures and volumes without initiating or propagating fractures in the confining zone(s). (40 CFR §146.83(a)(2)).*

- ***Buffer Aquifer/ Aquiclude System:*** The Upper Confining System and the first transmissive zone above the Upper Confining System (the Middle and Upper Oakville Formation), along with secondary and tertiary containment layers in the Middle Oakville and Lagarto Formations, respectively, provide layered intervals of low and moderate permeability rocks that allow for bleed-off of excess pressure, impede the vertical migration of CO_2 and or formation fluids, and provide opportunities for testing and monitoring; and therefore, are adequate reservoirs capable of detecting and containing any CO_2 or other fluids leaks that may occur.
  Key Finding: *The Buffer Aquifer/ Aquiclude System provides an additional safeguard of protection for the Caliche Beaumont Sequestration Project Site.*

- ***Minimal Artificial Penetration Risk:*** Of the Claimed artificial penetrations with the AoR that penetrate through the Upper Frio Sand injection zone, Claimed have been identified for further field investigation as part of the Corrective Action Plan, of which only three have been identified as posing a potential concern of leakage pathways.
  Key Finding: *Caliche has developed a Corrective Action Plan to further investigate these APs and perform corrective action, as needed.*

- ***Low Seismic Hazard:*** The Caliche Beaumont Sequestration Project Site is in the coastal region of the West Gulf Coastal Plain where the seismic hazard is low. There is no evidence that the faults near the Caliche Beaumont Sequestration Project Site are seismically active, and no induced earthquake has been recorded within Claimed as PBI of the Caliche Beaumont Sequestration Project Site.
  Key Finding: *The overall seismic risk and the potential of significant fault rupture in the project area is rated low. No seismic events are reasonably expected to occur during the course of the Caliche Beaumont Sequestration Project, and as such, seismic activity will not compromise subsurface containment of injected carbon dioxide.*
- ***Environmental Justice (EJ) Review:*** The results of the EJScreen analysis indicate the Claimed as PBI (as identified in Section 13.0 of this *Module A*); however, Caliche Beaumont Sequestration Project activities Claimed as PBI The majority of the Caliche EJ Area is within undeveloped land and has a low population density and effects from drilling and maintenance are expected to be brief, localized, and minimal.
  Key Finding: *Disproportionately high adverse impacts on minority or low-income populations are not expected as a result of the Caliche Beaumont Sequestration Project Site.*

3.0 AOR AND CORRECTIVE ACTION

Caliche has uploaded the *"Area of Review and Corrective Action Plan"* to *Module B* of the USEPA GSDT Portal, which abides by all requirements of 40 CFR §146.82(a) and §146.84(b). The report contains the details of the computational modeling as required by 40 CFR §146.84(c) and optional CARB LCFS protocol Subsections C.1.1.2, C.2.4.1, and C.2.4.3(a). Pressure front and CO_2(sc) plume extents are presented at Claimed as PBI during injection and 50- and 100-years post-injection for the simulated operation. Regional data, which include wells in reasonable proximity to the Caliche Beaumont Sequestration Project Site, were used as the basis for the model data. Once obtained, model parameters will be replaced with site-specific data and used to predict the critical pressure and CO_2(sc) plume extent.

The technical report also includes the tabulation of all artificial penetrations (APs) within the delineated Area of Review (AoR), per 40 CFR §146.82(a)(4). There is a total of Claimed as PBI which penetrate the Upper Confining System. Caliche performed a thorough records search for all Claimed as PBI within the AoR utilizing the best available methods: historical well records, scout tickets, and logs obtained from publicly available state and local databases. Hard files at the Texas Railroad Commission also were searched for historical well records by a subcontractor agency that specializes in researching historical well records. A well schematic was constructed for each of the Claimed as PBI that were determined to penetrate the Upper Confining System and used to determine if the AP may serve as a potential conduit of CO_2 or formation fluid into the USDW and warrant corrective action. Of the Claimed as PBI were determined to warrant additional field investigation to determine whether the well showed any evidence of well integrity concerns. A phased approach will be conducted for APs that are determined to require corrective action, these APs will be mitigated accordingly to protect the USDW.

Per the USEPA Class VI monitoring and operating requirements under 40 CFR §146.84(e) and Subsection C.2.4.4 of CARB LCFS (CARB, 2018, p. 37), the AoR, including the maximum extent of both the CO_2(sc) and the pressure front, will be reevaluated at least once every five years, or when monitoring or operational conditions warrant reevaluation per CARB LCFS Subsection C.2.4.4.1. This plan will be updated as the project develops to consistently match geological, testing, and operational data received from injection and monitoring wells during the life of the project.

AoR and Corrective Action GSDT Submissions

GSDT Module: AoR and Corrective Action
Tab(s): All applicable tabs

Please use the checkbox(es) to verify the following information was submitted to the GSDT:
☒ Tabulation of all wells within AoR that penetrate confining zone ***[40 CFR §146.82(a)(4)]***
☒ AoR and Corrective Action Plan ***[40 CFR §146.82(a)(13) and §146.84(b)]***
☒ Computational modeling details ***[40 CFR §146.84(c)]***

4.0 FINANCIAL ASSURANCE DEMONSTRATION

Caliche has submitted the *"Financial Assurance Demonstration"* (FAD) to *Module C* of the USEPA GSDT Portal, per 40 CFR §146.82(a) and §146.85, which ensures resources are available to cover the cost of the corrective action plan, injection well plugging plan, post-injection site care and site closure, and the emergency and remedial response plan. Costs include the CARB LCFS requirements for a 100-year PISC, site closure, and emergency and remedial response. The FAD also covers monitoring and reporting activities during the post-injection and closure operations.

Total cost estimates for the activities are provided in **Table C.1.1** of *Module C*. These estimates include project management, administrative costs, overhead, and contingency.

Detailed cost estimates for each FAD component are available in the "Cost Estimates" tab of *Module C* of the GSDT Tool. Actual values may change as the project is finalized, including inflation and additional charges to the final project, etc. If changes to the cost estimate occur, Caliche will adjust the value of the FAD and submit this to the authorized regulatory body for review on an as-needed basis.

Financial Responsibility GSDT Submissions

GSDT Module: Financial Responsibility Demonstration
Tab(s): Cost Estimate tab and all applicable financial instrument tabs

Please use the checkbox(es) to verify the following information was submitted to the GSDT:
☒ Demonstration of financial responsibility ***[40 CFR §146.82(a)(14) and §146.85]***

5.0 INJECTION WELL CONSTRUCTION

Caliche is applying for a permit for three new Class VI CO_2 sequestration wells for the Caliche Beaumont Sequestration Project (**Figure A.1.1**). Injection Well Nos. 1, 2, and 3 will be completed in the "Green," "Yellow," and/or "Gold" Sands of the Upper Frio Formation (see **Figures A.5.1, A.5.2, and A.5.3**).

The following sections address the procedures to drill, sample, complete, operate, and test the proposed injection wells, as well as specifications of the construction materials. The construction and completion of the injection wells will be conducted to i) prevent the movement of fluids into or between USDWs or other unauthorized zones, ii) permit the use of appropriate testing devices and workover tools, and iii) permit continuous monitoring of the annulus space between the injection tubing and the long string casing (CARB, 2018, p. 69). Construction of each of the wells is substantially similar, except for the perforation depths, which will be specific to each well and based upon the results from the open hole logging runs. Specification of maximum instantaneous rate of injection; average rate of injection; and the total monthly and annual volumes requested are also included.

All construction data meet the requirements for Class VI injection wells under 40 CFR §146.86, 40 CFR §146.82(a)(9), (11), and (12) and CARB LCFS – Section 3. Well Construction and Operating Requirements and Subsection C.1.1.2. Procedures for the plugging and abandoning of the injection wells are contained in *Module E.2 – Injection Well Plugging Plan*. The regulatory agency will be provided the opportunity to witness all open and cased hole logging acquisitions for each of the injection wells per 40 CFR §146.87(f).

5.1 Proposed Stimulation Program

Pursuant to 40 CFR §146.82(a)(9), a detailed stimulation plan will be developed for the Caliche Beaumont Sequestration Project, which will be employed after the drilling and completion of the injection wells. The stimulation program will consist of an acidization and wellbore flowback (utilizing nitrogen on coiled tubing) to remove formation skin damage due to invasion of solids during drilling and any perforation damage. The acid treatment will most likely consist of the following acids, with acid treatment chemicals and actual volumes to be determined based on core analysis, evaluation of open hole logs, and footage of interval to be treated at the time of placement:

- 15% Hydrochloric Acid (HCl)
- 7.5% HCl + 1.5% Hydrofluoric (HF) Acid
- 15% Hydrochloric Acid (HCl) Flush

Best practices for recommended volumes for acid stimulations generally range from 25 to 100 gallons per foot of completion, depending on the severity of the suspected near wellbore formation damage. Chemicals will be added to the acid blends to limit clay swelling, reduce emulsions, and inhibit reaction to the completion equipment. The type and quantity of these chemicals will be determined based on formation characteristics determined from core and wireline log evaluation. Stimulation will not interfere with confinement of the reservoir per 40 CFR §146.82(a)(9).

Additional acids and the use of diverter fluids may be considered at the time of placement. The acid fluids will be displaced from the wellbore using non-hazardous treating water or brine.

Additional stimulation treatment may be necessary if the injection performance of the well remains unacceptable following treatment.

5.2 Construction Procedures – Injection Well Nos. 1, 2, and 3

Caliche plans to complete the injection wells into the "Green," "Yellow," and/or "Gold" Sands of the Upper Frio Formation from a depth of approximately Claimed as PBI to a maximum depth of approximately Claimed as PBI. All three proposed injection wells will be located within the City of Beaumont Acreage (see proposed locations in **Figure A.1.1**). The new injection wells will be constructed in accordance with 40 CFR §146.86 standards for Class VI injection wells and will meet the requirements of CARB LCFS – Section 3. Well Construction and Operating Requirements and Subsection C.1.1.2.

The proposed completion schematics for Injection Well Nos. 1, 2, and 3 are included as attached **Figures A.5.1, A.5.2, and A.5.3**, respectively. The schematics include well casing specifications and setting depths, cementing data, and completion details. Note, unless specified, all depths in this section are relative to the ground level. As shown, Injection Well Nos. 1 and 3 will be completed in the "Green" and "Yellow" Sands of the Upper Frio Formation, while Injection Well No. 2 will be completed in the "Green," "Yellow," and "Gold" Sands of the Upper Frio Formation. Well completion intervals for each injection well will be adjusted based on the depths of the "Green," "Yellow," and/or "Gold" Sands of the Upper Frio Formation encountered during the drilling operations.

5.2.1 Casing String Details

Casing specifications for the proposed Injection Well Nos. 1, 2, and 3 are detailed in **Tables A.5.1, A.5.2, and A.5.3**, respectively, below, which consider factors listed under 40 CFR §146.86(b)(1). Tubular stress calculations for all well casing and tubing are included in **Appendix A.F**. All components of the surface and protection casings will be manufactured to API standards and are designed for the proposed active life of the Caliche Beaumont Sequestration Project, based on the materials of construction and the environment of use. The casing and cementing program has been designed to prevent the movement of fluids into or between USDWs, into unauthorized zones, or out of the injection zone and into the subsurface that is likely to reach the overlying USDW or the atmosphere.

Each well will employ at least one long string casing, using a sufficient number of centralizers, per 40 CFR §146.86(b)(3). The wells will use both carbon steel (non-CO_2 stream contact) and martensitic stainless steel (22Cr for CO_2/H_2S/Cl contact usage) to ensure structural strength and the longevity of the wellbore (40 CFR §146.82(a)(9), (11), and (12); CARB, 2018, p. 69). Carbon steel will be used for the conductor and surface casing and a mixed string of carbon steel and 22Cr steel will be utilized for the completion casing. Surface casing will extend through the base of the lowermost USDW, per 40 CFR §46.86(b)(2). Additionally, all casing strings will be fully cemented to surface, which will provide additional isolation of the casing string from external formation fluids along the borehole path, per 40 CFR §146.86(b)(2).

Prior to running the casing in the hole, each string will be visually inspected and drifted to ensure that no defects are present. The connections will be cleaned, and the manufacturer's recommended thread compound will be applied to the pin of each connection before make-up.

Table A.5.1. Casing Details – Injection Well No. 1.

Claimed as PBI

Table A.5.2. Casing Details – Injection Well No. 2.

Claimed as PBI

Table A.5.3. Casing Details – Injection Well No. 3.

Claimed as PBI

5.2.2 Tubing and Packer Details

Tubing and packer materials used in the construction of each Class VI well will be compatible with the fluids with which the materials may be expected to come into contact. The materials will meet or exceed standards developed for such materials by the API, ASTM International, or comparable

standards acceptable to the USEPA, per 40 CFR §146.86(c)(1). Tubing specifications for proposed Injection Well Nos. 1, 2, and 3 are detailed in **Table A.5.4, A.5.5, and A.5.6**, respectively. Tubular stress calculations for all well casing and tubing are included in **Appendix A.F**. Consistent with 40 CFR §146.86(c), the proposed injection wells will be completed with 22Cr injection tubing to provide resistance to corrosion from CO_2 injection (CARB, 2018, p. 70). The tubing will extend from the surface (wellhead) to the injection packer, with a slip-and-seal assembly installed to provide engagement with the surface wellhead.

The proposed injection packer will be set in the completion casing just above the top of the Upper Frio Injection Zone at a depth of approximately Claimed as PBI within the Anahuac primary confining unit (CARB, 2018, p. 71). The proposed packer will be a retrievable injection packer and will be constructed with all the parts that will be in contact with the injection stream ("wetted parts") constructed out of 22Cr steel or better. The packer assembly will include a Polished Bore Receptacle (PBR) of sufficient length to account for potential tubing movement during well operation.

Prior to running the tubing in the hole, each string will be visually inspected and drifted to ensure that no defects are present. The connections will be cleaned, and the manufacturer's recommended thread compound will be applied to the pin of each connection before make-up. Each connection of the injection tubing will be externally pressure tested to ensure no leaks exist upon makeup.

The injection packer will also be visually inspected to ensure no defects are present. A pressure test of the annulus will be conducted during installation of the packer to confirm proper setting and absence of leaks.

Table A.5.4. Tubing Details – Injection Well No. 1.

Claimed as PBI

Table A.5.5. Tubing Details – Injection Well No. 2.

Claimed as PBI

Table A.5.6. Tubing Details – Injection Well No. 3.

Claimed as PBI

5.2.3 Centralizers

Each casing string will have hinged bow type centralizer attached to the casing at intervals along the entire well path (CARB, 2018, p. 70). The centralizers will be placed to maximize the casing standoff from the well bore to enhance the cementing of the wells. The centralizers will be placed as follows:

- 1 Centralizer 8 ft above the float shoe, straddling a stop collar;
- 1 Centralizer 8 ft above the float collar, straddling a stop collar;
- 1 Centralizer every other joint, to surface on the surface and intermediate casing.
- 1 Centralizer every other joint to the to the stage collar at approximately 6,100 ft on the completion casing;
- 1 centralizer above and below the stage collar, straddling a stop collar;
- 1 Centralizer every third joint, up to the surface on the completion casing; and,
- 1 Centralizer approximately 10 ft below ground level.

Actual placement of centralizers will be determined once the drilling of each well section is completed, and logs have been reviewed. Additional centralizers may be used as needed.

5.2.4 Annular Fluid

The annular fluid designed for the wells is 9.0 lb/gal (1.08 Specific Gravity) sodium chloride brine with corrosion inhibitor and oxygen scavenger additives or equivalent. An annulus monitoring and pressurization system will always maintain the annulus at a pressure greater than the injection tubing pressure.

5.2.5 Cement Details

The surface and completion casing strings will be cemented using current cementing technology and practices. Cementing standards detailed in 40 CFR §146.86(b)(4) and (5) and CARB LCFS Section 3 (CARB, 2018, pp. 69-70) will be used during the construction of the wells. The wells will use both standard cement (Class A or Class H) and CO_2 resistant cement (e.g. Halliburton's CORROSACEM™, or equivalent) to ensure the longevity of the wellbore. All casing strings will be fully cemented to surface with cement and cement additives of sufficient quality and quantity, which will provide isolation of the casing string from external formation fluids along the borehole path over the design-life of the project (40 CFR §146.86(b)(1); CARB, 2018, p. 70). For the completion casing strings, the CO_2 resistant cement will be brought above and into the Anahuac

confining unit in each well. A service company recommendation on cementing of the surface and protection casing strings is included in **Appendix A.G**.

The expected downhole temperature at total depth is Claimed as PBI, which is not considered detrimental to the cement program planned for this well. The cement will increase in hardness over time and reach a value close to its maximum compressive strength soon after setting.

5.2.6 Proposed Drilling Program

The surface and completion casing strings will be cemented using current cementing technology and practices. Cementing standards detailed in 40 CFR §146.86(b) (4) and (5) will be used during the construction of the wells.

The drilling program for Injection Well Nos. 1, 2, and 3 at the Caliche Beaumont Sequestration Project Site contains three phases: a conductor hole, surface hole, and protection hole. All depths in the outlined procedure are referenced to the KB, which is estimated at 20 feet above ground level.

Conductor Hole

1. Prepare surface location and mobilize drilling rig. Drill mousehole and rathole.
2. Pick up casing hammer and drive 30-inch conductor pipe to approximately Claimed as PBI or until 100 blows per foot penetration rate is reached. (alternate is to auger the conductor hole and grout the casing).

Surface Hole

3. Drill 17-1/2-inch surface hole to Claimed as PBI using drilling fluid as detailed in the Drilling Fluids section of this procedure. Take deviation surveys every 500 feet. Maximum deviation from vertical should be no more than 3 degrees.

17-1/2-INCH BOREHOLE DRILLING LOST CIRCULATION AND DEVIATION CONTINGENCY PLAN

If circulation is lost (high probability) while drilling the 17-1/2-inch surface casing borehole, lost circulation material pills will be pumped to re-establish circulation. Depending upon the severity of lost circulation encountered, lost circulation material may need to be blended with the drilling fluid in concentrations dictated by hole conditions to maintain circulation to the surface casing point. Should lost circulation occur while drilling from the base of conductor to the surface casing point, paper, cottonseed hulls, or other forms of standard lost circulation material may be used to remedy the loss condition. A cement truck may be mobbed to location and placed on "standby" to minimize "wait time" if severe loss of circulation is encountered.

17-1/2-INCH BOREHOLE DRILLING OVERPRESSURED ZONE CONTINGENCY PLAN

If an over-pressured zone is encountered (not expected) while drilling the 17-1/2-inch surface casing borehole, drilling fluid pump rate down the drill pipe will be increased while the drill fluid density is increased. The increased pumping rate will continue until the well stops flowing.

17-1/2-INCH BOREHOLE DEVIATION AND CONTINGENCY PLAN

Take inclination surveys minimum every 500 feet and at the TD for the hole size to monitor the well path. A maximum allowable deviation from vertical is 3 degrees, and the targeted deviation between surveys is 1 degree. If the maximum recommended deviation is exceeded, an evaluation will be made to determine whether remedial action is necessary.

4. Run open hole electric logs as listed in *Module D – Pre-Operational Testing Plan*.

5. Run 13-3/8-inch surface casing to Claimed as PBI Refer to Section 5.2.1 – Casing String Details for a detailed description of the casing.
6. Cement the casing in place using the stab-in method. Refer to Section 5.2.5 – Cement Details.
7. If no cement returns are observed at surface, a temperature or similar diagnostic survey will be run to determine the top of cement. Grout the un-cemented annular space to the surface if necessary.
8. After waiting on cement for a minimum of 12 hours, cut off the surface and conductor pipe and install a 9-5/8-inch x 3,000 psi casing head and pressure test.
9. Nipple up Blowout Preventers (BOP) and ancillary equipment and pressure test to a low pressure of 250 psig and a maximum pressure of 3,000 psig. Pressure test the surface casing to 1,000 psi for 30 minutes.
10. Rig up wireline unit and log differential temperature survey and cement bond log.

Protection Hole

11. Pick up a 12-1/4-inch drilling assembly and trip into the wellbore.
12. Displace the fresh water from cementing with a potassium-based drilling fluid to improve hole cleaning and stability. Drill out casing float equipment.
13. Drill a 12-1/4-inch protection hole to Claimed as PBI into the Hackberry Shale Formation. The actual total depth of the wells will be contingent on the subsurface depth of the base of the Frio sand. Take inclination surveys every 500 feet to monitor well path.
14. Attempt to collect conventional whole cores at selected geologic intervals within the Anahuac confining unit and Upper Frio injection zones. Note core may be taken in one or more of the injection wells. Refer to *Module D – Pre-Operational Testing Plan* for details on the coring program.

12 ¼-INCH BOREHOLE DRILLING LOST CIRCULATION AND DEVIATION CONTINGENCY PLAN

If circulation is lost (low probability) while drilling the 12-1/4-inch borehole, lost circulation material pills will be pumped to re-establish circulation. Depending upon the severity of lost circulation encountered, lost circulation material may need to be blended with the drilling fluid in concentrations dictated by hole conditions to maintain circulation to the surface casing point. Should lost circulation occur while drilling from the base of conductor to the surface casing point, paper, cottonseed hulls, or other forms of standard lost circulation material may be used to remedy the loss condition.

12-1/4-INCH BOREHOLE DRILLING OVERPRESSURED ZONE CONTINGENCY PLAN

If an overpressured zone is encountered (not expected) while drilling the 12-1/4-inch borehole, drilling fluid pump rate down the drill pipe will be increased while the drill fluid density is increased. The increased pumping rate will continue until the well stops flowing.

12-1/4-INCH BOREHOLE DEVIATION AND CONTINGENCY PLAN

Take inclination surveys minimum every 500 feet and at the TD for the hole size to monitor the well path. A maximum allowable deviation from vertical is 3 degrees, and targets allowable deviation between surveys is 1 degree. If the maximum recommended deviation is exceeded, an evaluation will be made to determine whether remedial action is necessary.

15. Run electric wireline logs and collect rotary sidewall core samples (if needed) over the open hole interval. Refer to *Module D – Pre-Operational Testing Plan* for details.
16. Run 9-5/8-inch casing (mixed string), with casing packer and stage tool, (and fiber optic cable: DTS/DAS, and perforation markers, if required) to the planned casing point (7,750 feet). Refer to Section 5.2.1 – Casing String Details for a detailed description of the casing.

    Note: Caliche is evaluating "smart well" completion technologies to monitor Differential Temperature, Acoustic, and Bottomhole Pressure.
17. Rig up cementing equipment and cement the protection casing in place. Cement will be placed in stages with the lower cement being CO_2 resistant cement and the upper being a lightweight cement blend. Refer to Section 5.2.5 – Proposed Cementing Program.
18. In the event cement returns are not observed at the surface, a temperature or similar diagnostic survey will be run to determine the top of cement. After the cement top is located, a procedure to grout in the un-cemented annular space will be provided.
19. After waiting on cement for a minimum of 12 hours, nipple down the BOP, pick up the BOP, set the 9-5/8-inch casing slips and nipple down the BOP's. Nipple up the casing/tubing spool and test the seals. Set night cap and secure well.
20. Rig down the drilling rig, and associated equipment.

5.2.7 Proposed Completion Procedure

The completion procedure has been developed to utilize the "Green," "Yellow," and/or "Gold" Sands of the Upper Frio Formation for sequestration of the injected CO_2 (see **Figures A.5.1, A.5.2, and A.5.3**). The following is a proposed completion procedure for the Caliche Beaumont Sequestration Project injection wells.

1. Move in and rig up the completion rig and associated equipment.
2. Check for pressure, remove the night cap and nipple up and test the 11-inch BOP from 250 low to 3,000 psi high.
3. Pick up an 8-1/2-inch bit and casing scraper for 9-5/8-inch casing and trip into the wellbore.
4. Drill out the cement in the casing to Claimed as PBI (50 feet above the casing shoe).
5. Rig up and run differential temperature and radial cement bond and casing evaluation logs as detailed in the *Module D – Pre-Operational Testing Plan*.
6. Pressure-test the casing string to 2,000 psi for 30 minutes.
7. Displace the drilling fluid in the wellbore with completion fluid.
8. Rig up wireline unit and perforate 9-5/8-inch casing (directionally perforate if fiber optic cable is installed) as detailed in **Tables A.5.7, A.5.8, and A.5.9**, respectively, for Injection Well Nos. 1, 2, and 3.

   Note: Perforating depths are approximate and will be determined after reviewing open hole logs. Note, oriented perforating will be required if DTS/DAS cable run on casing through the Injection Zone.

Table A.5.7. Completion Intervals – Injection Well No. 1.

Perforation Interval	Formation/Lithology
Claimed as PBI	

Table A.5.8. Completion Intervals – Injection Well No. 2.

Perforation Interval	Formation/Lithology
Claimed as PBI	

Table A.5.9. Completion Intervals – Injection Well No. 3.

Perforation Interval	Formation/Lithology
Claimed as PBI	

9. Lower the workstring into the wellbore to the bottom of the protection casing and circulate solids from the wellbore.
10. Pick up 9-5/8-inch x 5-1/2-inch injection packer (packer constructed using CO_2 resistant 22Cr materials) on workstring and lower into wellbore.
11. Set injection packer at approximately Claimed as PBI Conduct preliminary pressure test to verify pressure integrity of the well annulus. Note: Caliche is investigating “smart well” completion technology for flow allocation control.
12. Retrieve the workstring from the wellbore while laying it down.
13. Pick up the seal assembly on 5-1/2-inch 22Cr injection tubing and lower into the wellbore. Externally pressure test each connection.
14. Circulate inhibitive packer fluid through the tubing-casing annulus until completion brine is fully displaced.
15. Land the tubing in the packer and wellhead and conduct preliminary annulus pressure test to verify pressure integrity.
16. Nipple down well control equipment and install tubing head adapter.
17. Rig down drilling rig and demobilize from site.
18. Rig up coiled tubing and nitrogen equipment. Conduct formation backflow with nitrogen to develop well and collect native formation brine samples. An acid stimulation treatment

may also be required and may be followed by either a wellbore flowback to remove drilling/completion solids from near-wellbore interval or displacement of the acid into the formation.

19. Conduct mechanical integrity test and ambient pressure test per *Module D – Pre-Operational Testing PLan*.
20. Return well to site for installation and connection of surface equipment and piping.

General Notes

- All depths referenced are approximate and are based on the expected log depth.
- Actual depths may vary based on lithology of local formations.

5.2.8 Proposed Well Fluids Program

Lost circulation material (LCM) will be on location to treat for fluid losses in top hole sands above the potential injection intervals. The fluid system will be pre-treated with LCM before encountering any known or suspected fluid loss zones. High-viscosity sweeps will be used to assist hole cleaning. Sodium chloride (NaCl) is planned for use as the completion fluid. The fluid weight will be maintained to contain reservoir pressures without inducing flow to the wellbore. **Tables A.5.10, A.5.11, and A.5.12**, respectively, are provided to show the proposed well fluids per hole.

Table A.5.10. Proposed Well Fluids – Injection Well No. 1.

Claimed as PBI

Table A.5.11. Proposed Well Fluids – Injection Well No. 2.

Claimed as PBI

Table A.5.12. Proposed Well Fluids – Injection Well No. 3.

Claimed as PBI

5.2.9 Proposed Cementing Program

The surface and protection casing strings will be cemented using current cementing technology and practices. Cementing standards defined in 40 CFR §146.86(b)(4) and (5) will be used during the construction of the wells. The wells will use both standard cement (Class A or Class H) and CO_2 resistant cement (Halliburton CORROSACEM™ or equivalent) to ensure the longevity of the wellbore. All casing strings will be fully cemented to surface, which will provide additional isolation of the casing string from external formation fluids along the borehole path [40 CFR §146.86(b)]. For the protection casing string, the CO_2 resistant cement will brough to above the top of the Anahuac confining unit in each injection well. A service company recommendation on cementing of the surface and protection casing strings is included in **Appendix A.G**.

5.2.9.1 Surface Casing

The following cementing program is proposed for installation of the surface casing string:

- 13-3/8-inch in 17-1/2-inch borehole at Claimed as PBI
- Float shoe;
- Float Collar, 1 joint above the float shoe;
- Cement to surface;
- Cement volumes are estimated 100% excess over bit size in open hole interval;
- Actual volume to be calculated from caliper log plus 20% excess; and
- In the event the hole diameter exceeds the scale of a 2-dimensional caliper, a minimum of 150 percent of the annular space between the casing and the maximum caliper reading will be used for calculating cement volume for that section of the wellbore.

Tables A.5.13, A.5.14, and A.5.15, respectively, are provided to show the proposed cementing details of the surface casing at Injection Well Nos. 1, 2, and 3.

Table A.5.13. Cementing Details – Surface Casing – Injection Well No. 1.

Claimed as PBI

*** Or equivalent based on selected vendor**

Table A.5.14. Cementing Details – Surface Casing – Injection Well No. 2.

Claimed as PBI

*** Or equivalent based on selected vendor**

Table A.5.15. Cementing Details – Surface Casing – Injection Well No. 3.

Claimed as PBI

*** Or equivalent based on selected vendor**

5.2.9.2 Protection Casing

The following cementing program is proposed for installation of the protection casing string:

- 9-5/8-inch in 12-1/4-inch hole at Claimed as PBI
- Two-stage cement job with cement to surface, with stage tool and external casing packer;
- Estimated 50% excess over bit size in open hole sections only;
- Actual volume to be calculated from caliper log plus 20% excess; and
- In the event the hole diameter exceeds the scale of a 2-dimensional caliper, a minimum of 150 percent of the annular space between the casing and the maximum caliper reading will be used for calculating cement volume for that section of the wellbore.

Tables A.5.16, A.5.17, and A.5.18, respectively, are provided to show the proposed cementing details of the protection casing at Injection Well Nos. 1, 2, and 3.

Table A.5.16. Cementing Details – Protection Casing – Injection Well No. 1.

*** Or equivalent based on selected vendor**

Table A.5.17. Cementing Details – Protection Casing – Injection Well No. 2.

*** Or equivalent based on selected vendor**

Table A.5.18. Cementing Details – Protection Casing – Injection Well No. 3.

*** Or equivalent based on selected vendor**

5.2.10 Casing Float Equipment and Jewelry

Surface Casing

13-3/8-inch Float Equipment and Jewelry

1. Float shoe with receptacle for stab-in cementing technique.
2. 20 hinged bow spring centralizers:
    - 1 Centralizer 8 ft above the float shoe, straddling a stop collar;
    - 1 Centralizer straddling the first casing collar above the float shoe; and
    - 1 Centralizer every other collar up to the surface.

Protection Casing

9-5/8-inch Float Equipment and Jewelry

1. Float shoe.
2. Float collar, 2 joints above the float shoe.
3. 1 bottom wiper plug.
4. 1 top wiper plug.
5. External Casing Packer (if fiber optic cable is not installed).
6. Stage Tool.
7. 1 bottom wiper plug.
8. 1 top wiper plug.
9. Approximately 58 hinged bow spring centralizers:
    - 1 Centralizer 8 feet above the float shoe, straddling a stop collar;
    - 1 Centralizer 8 feet above the float collar, straddling a stop collar;
    - 1 Centralizer every other joint, to 3,900 ft;
    - 1 Centralizer every third joint, from 3,900 ft to the surface; and
    - 1 Centralizer approximately 10 ft below ground level.

5.2.11 Well Logging, Coring, and Testing Program

Details on the proposed logging program are contained in *Module D - Pre-Operational Testing Plan*. All tools will be run on a wireline and will be compatible with open hole and cased hole diameters, allowing for successful testing runs (40 CFR §146.87).

6.0 PRE-OPERATIONAL TESTING PLAN

Caliche has uploaded the *"Pre-Operational Testing and Logging Plan"* to *Module D* of the USEPA GSDT Portal. Caliche is proposing to inject CO_2 using three injection wells, which will inject into one or more of the Upper Frio Sand injection intervals described in Section 5.0. All injection wells will abide by all logging and testing requirements under federal standards outlined under 40 CFR §146.87(a)-(d) and CARB LCFS Subsections C.3.2(a)-(e).

As each well is drilled, coring will adapt to drilling parameters, wellbore conditions, overall core recovery, and core quality. The UIC Program Director and CARB Executive Officer will be provided the opportunity to witness all operations for the drilling and testing of the injection wells, per the 40 CFR §146.87(f) and CARB LCFS Subsection C.3.2(g). Prior to injection authorization, all three Caliche wells will demonstrate mechanical integrity.

The logging and testing data obtained in this plan will be used to update, if necessary, the *"Area of Review and Corrective Action Plan"* (*Module B*), as well as define and reduce uncertainties regarding site characterization. The *"Testing and Monitoring Plan"* (*Module E.1*) will be revised as needed using the acquired data to determine the final operational limits and procedures of the Caliche Beaumont Sequestration Project. All logging and well testing plans will be submitted to the UIC Program Director and CARB Executive Officer 30 days prior to commencing construction operations.

Pre-Operational Logging and Testing GSDT Submissions

GSDT Module: Pre-Operational Testing
Tab(s): Welcome tab

Please use the checkbox(es) to verify the following information was submitted to the GSDT:
☒ Proposed pre-operational testing program ***[40 CFR §146.82(a)(8) and §146.87]***

7.0 OPERATING PLAN

40 CFR §146.82(a)(7) requires a description of the proposed operating data, including the source of the CO_2 stream, the chemical and physical characteristics of the CO_2 stream, the average and maximum injection pressures, and the average and maximum daily rate and volume and/or mass of injection, and the total anticipated volume and/or mass of the CO_2 stream. 40 CFR §146.82(a)(10) requires the description of the proposed procedure to outline steps necessary to conduct injection operations. 40 CFR §146.88 requires description of the injection well operating requirements.

Caliche will operate all three Class VI injection wells under all requirements of the USEPA, as well as the CARB LCFS protocol. Caliche will ensure injection pressure, annulus pressure, and planned down-hole shut-off systems comply with the Class VI regulations. Caliche will ensure the protection of any USDWs throughout all operating procedures and conditions.

7.1 Proposed Operating Conditions

Caliche Class VI injection wells will operate under all requirements of the USEPA and CARB LCFS in order to protect the surrounding community, environment, and the applicable USDW (i.e., the Chicot aquifer).

Except during stimulation, Caliche will ensure that injection pressures do not exceed 80% of the fracture pressure (per CARB LCFS) of the injection zone so as to ensure that the injection does not initiate new fractures or propagate existing fractures in the injection zone. In no case will the injection pressures initiate fractures in the primary Upper Confining Unit or cause the movement of injectied CO_2 or formation fluids that endangers the overlying USDW. Pursuant to requirements at 40 CFR §146.82(a)(9), all stimulation programs must be approved by the UIC Program Director as part of the permit application and incorporated into the permit.

Caliche will not, under any circumstances, inject CO_2 between the outermost casing and the formation, per 40 CFR §146.88(b). Caliche will cement the space between the casing and the injection formation (Subsection C.3.1(c)(3)) with non-corrosive fluid to ensure protection of the USDW (i.e., the Chicot aquifer) against any drilling or formation fluid or CO_2 migration.

Caliche will ensure that the annulus between the tubing and the long string casing will be filled with a non-corrosive fluid. The mechanical integrity of this annulus space will be constantly monitored and maintained except under specific circumstances of disassembly for maintenance or corrective measures. A positive pressure will be maintained on the annulus of at least 100 psi greater than the injection tubing pressure to prevent leaks from the well into unauthorized zones and to detect well malfunctions.

The temperature, pressure, rate, and volume of the CO_2 stream will be continuously monitored at the injection wellhead (40 CFR §146.88(e)(1)). Per CARB LCFS requirements, the maximum injection pressure at the Caliche wells will not exceed 80% of the calculated fracture pressure of the injection zone (CARB, 2018, p. 74); this will be monitored continuously throughout the injection period. Site-specific in-situ fracture gradients will be taken into consideration and applied as needed after the stratigraphic well drilling and testing is completed.

The Caliche wells will be equipped with an automatic warning and shut-off system. Caliche will immediately begin shutdown procedures when a well enters an unallowable state, i.e. loss of mechanical integrity is discovered, or injection pressures approach the limits shown below in **Tables A.7.1, A.7.2, and A.7.3** (see *Module E.4 – Emergency and Remedial Response Plan*

(ERRP)). Shutdown procedures will ensure the equipment is de-energized quickly and safely, meaning gradual shutdown may be used in cases where a quick shutdown may cause more harm.

Caliche will immediately investigate and identify as expeditiously as possible the cause of the shutoff. If, upon such investigation, the well appears to be lacking mechanical integrity, or if monitoring equipment and procedures otherwise indicate that the well may be lacking mechanical integrity, Caliche will:

1. Immediately cease injection;
2. Take all steps reasonably necessary to determine whether there may have been a release of the injected carbon dioxide stream or formation fluids into any unauthorized zone;
3. Notify the Director within 24 hours;
4. Restore and demonstrate mechanical integrity to the satisfaction of the Director prior to resuming injection; and
5. Notify the Director when injection can be expected to resume.

If no release of CO_2 has occurred, well conditions will be monitored to decide on steps to return to full rate injection. In cases where return to full injection is not possible, additional troubleshooting steps may be required.

7.2 CO_2 Stream Source and Composition

The source and location of the CO_2 stream as well as the percentage of impurities present will be considered. The CO_2 stream is expected to come from industrial, power operation/utility, and/or chemical manufacturing or refinery processes. A detailed analysis of the CO_2 stream composition and characteristics will be performed and provided to the UIC Program Director prior to initiating injection operations (40 CFR §146.82(a)(7)(iii) and (iv)). For the purpose of the AoR modeling, the CO_2 composition is expected to be Claimed as PBI [redacted] During operations, Caliche will analyze the composite CO_2 stream to confirm its chemical and physical characteristics (40 CFR §146.90(a)).

7.3 Demonstration of Appropriateness of Operating Conditions

Tables A.7.1, A.7.2, and A.7.3 below list the proposed operational parameters and conditions for Injection Well Nos. 1, 2, and 3, respectively, for their respective Upper Frio Sand injection zones ("Green," "Yellow," and/or "Gold" Sands), according to the results of the AoR model runs (see *Module B – Area of Review and Corrective Action Plan*) (40 CFR §146.82(a)(7)(i),(ii)). **Exhibit A.7.1** illustrates the schematic of these calculations.

Table A.7.1. Proposed Operational Procedures: Injection Well No. 1.

Claimed as PBI

Table A.7.2. Proposed Operational Procedures: Injection Well No. 2.

Claimed as PBI

Table A.7.3. Proposed Operational Procedures: Injection Well No. 3.

Exhibit A.7.1. Schematic of Pressure Calculation.

Method for Calculating Maximum Injection Pressure:

Maximum Surface Injection Pressure (MASIP) is calculated using the following equation (Hovorka et al., 2003).

$$MASIP = P_{frac} - P_{hydro} - 100 \text{ psi}$$

Where:

P_{frac} = Fracture Pressure (psi)
P_{hydro} = Hydrostatic Column Pressure (psi)
P_{hydro} = (0.433 x $SG_{injectate}$) x Depth
Depth = Bottom of the well screen interval for each Upper Frio Sand layer

$SG_{injectate}$ = Specific gravity of injectate and ranges between 0.661 – 0.740 for supercritical CO_2 based on the model. $SG_{injectate}$ is a function of temperature and pressure as shown in **Exhibit A.7.2**. The Frio Gold has lower $SG_{injectate}$ despite the layer having higher temperature than the other Upper Frio sand layers. This is because the pressure increase from CO_2 is smaller than the other Upper Frio sand layers due to its higher permeability.

The maximum bottomhole injection pressure was estimated at 80% maximum allowable pressure based on the fracture gradient (CARB, 2018, p. 74). Further details on the fracture gradient calculations are provided in *Module B - Area or Review and Corrective Action Plan*.

Exhibit A.7.2. Relationship between Temperature, Pressure, and Density of CO_2.

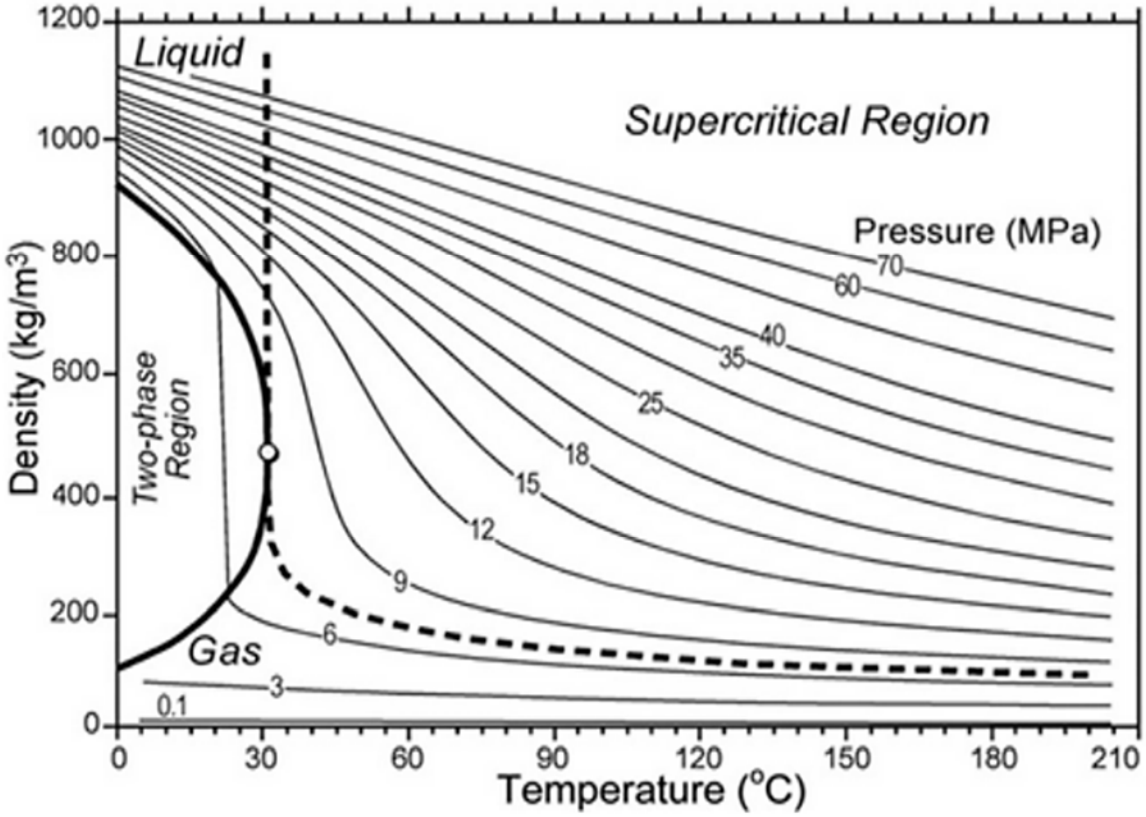

Method for Calculating Average Injection Pressure:

The TOUGH model was used to simulate formation pressures ($P_{bottomhole\ at\ Well\ X}$), which were used to calculate the operational pressures (surface and bottomhole injection pressures).

The bottomhole pressure (P_{bottom}) was calculated using the following equation:

$$P_{bottomhole\ at\ Well\ X} = \frac{\Delta P_{formation\ due\ to\ Well\ X}}{(1 - aquifer\ loss)} + initial\ P_{formation} + \Delta P_{formation\ due\ to\ other\ wells}$$

Where:

$P_{formation}$ = Formation pressure (psi).
$\Delta P_{formation}$ = Induced formation pressure (psi).

$\Delta P_{formation}$ accounts for the cumulative induced pressure from three CO_2 injection wells; therefore, it needs to be separated into two components; (1) induced pressure from just injection well and (2) induced pressure from other two wells. To determine induced pressure from each injection well, three separate models were developed. Each model simulated the pressures with two injection wells active and the third one inactive. With one well inactive, the pressure difference (dP) between three wells operating (P_{3w}) and two wells active with one inactive (P_{2w}) can be interpreted as the pressure induced by the inactive well (well X). The contributions from the other two wells can be estimated by subtracting the induced pressure due to Well X from the total induced pressure.

$$dP_{at\ Well\ X} = P_{3w} - (P_{2w})_{well\ X\ turned\ off} = \Delta P_{formation\ due\ to\ Well\ X}$$

$$\Delta P_{formation\ due\ to\ other\ wells} = total\ \Delta P_{formation\ at\ Well\ X} - \Delta P_{formation\ due\ to\ Well\ X}$$

The estimated induced pressures for each Upper Frio sand layer at Injection Well Nos. 1, 2, and 3 are provided below in **Tables A.7.4, A.7.5, and A.7.6**, respectively.

Table A.7.4. Induced Pressure at Injection Well No. 1.

Claimed as PBI

Table A.7.5. Induced Pressure at Injection Well No. 2.

Claimed as PBI

Table A.7.6. Induced Pressure at Injection Well No. 3.

Claimed as PBI

The $aquifer\ loss$ coefficient is then calculated using:

$$aquifer\ loss\ coefficient = \frac{measured\ P_{formation}}{measured\ P_{formation} + formation\ loss\ estimated\ from\ Thiem\ equation}$$

where, $aquifer\ loss$ is estimated using the Thiem equation (1906).

$$aquifer\ loss = \frac{pgQ}{2\pi T}\ln\left(\frac{R_o}{R_w}\right)$$

Where:

Q = Modeled injection volumetric rate
T = Modeled transmissivity of the Upper Frio Sand layer (using thickness and permeability used in the model)
R_o = Effective radius of the model cell
$R_w = 4.8$" = well casing radius.

Effective radius (R_o) is defined by Chen and Zhang (2009) as:

$$R_o = \sqrt{\frac{A}{8\pi}}$$

where A is the area of the cell perpendicular to the depth.

The estimated $aquifer\ loss$ for each Upper Frio sand layer at Injection Well Nos. 1, 2, and 3 are provided below in **Tables A.7.7, A.7.8, and A.7.9**, respectively.

Table A.7.7. Aquifer Loss: Injection Well No. 1.

Claimed as PBI

Table A.7.8. Aquifer Loss: Injection Well No. 2.

Claimed as PBI

Table A.7.9. Aquifer Loss: Injection Well No. 3.

Claimed as PBI

The surface injection pressure ($P_{Surface}$) is calculated using:

$$P_{surface} = P_{bottom} - hydrostatic\ pressure\ in\ borehole\ (\rho gZ)$$

Where hydrostatic pressure is calculated from the density (ρ) of CO_2 which is 740 kg/m, the highest value obtained from the model. g is acceleration of gravity, and Z is the depth of the individual injection well.

These calculations assume that well efficiency is constant over the injection period. Also, these calculations do not take into account the skin losses. These losses will be included based on the data collected during the operational testing. A falloff test will be conducted to determine the well loss pressure loss due to skin effects, which will then be used to update the total well efficiency, comprising both aquifer loss and well loss.

Method for Calculating Maximum and Average Injection Rates and Volumes:

The values indicated here are the CO_2 injection rates and volumes used in the model (see *Module B – Area of Review and Corrective Action Plan*). The maximum and average injection rates are the same because a constant injection rate of CO_2 was applied to individual wells in the model. For the same reason, the maximum and average injection volumes are the same.

Annulus Pressure and Annulus Pressure/Tubing Differential Calculation:

Annulus pressure is estimated based on the minimum annulus pressure/tubing differential of 100 psi (USEPA, 2017). The required annulus pressure will be supplemented by the hydrostatic pressure of the annulus column and surface applied annulus pressure. The surface annular pressure will be based on pressure/tubing differential, the Mechanical Integrity Test document (USEPA, 2017).

Exhibits A.7.3 through A.7.9 below present the pressure variations for the three injection wells in their respective Upper Frio Sand injection intervals. The exhibits present Formation Pressure, Bottomhole Pressure, Surface (Wellhead) Pressure, 80 Percent Fracture Gradient Pressure (based on CARB LCFS) and the 90 Percent Fracture Gradient Pressure (based on USEPA Class VI Permit Guidance). The formation pressures represent the simulated formation pressures at each of the three injection wells.

Exhibit A.7.3. Pressure Variation vs. Time at Injection Well No. 1: Frio Green Sand.

Exhibit A.7.4. Pressure Variation vs. Time at Injection Well No. 1: Frio Yellow Sand.

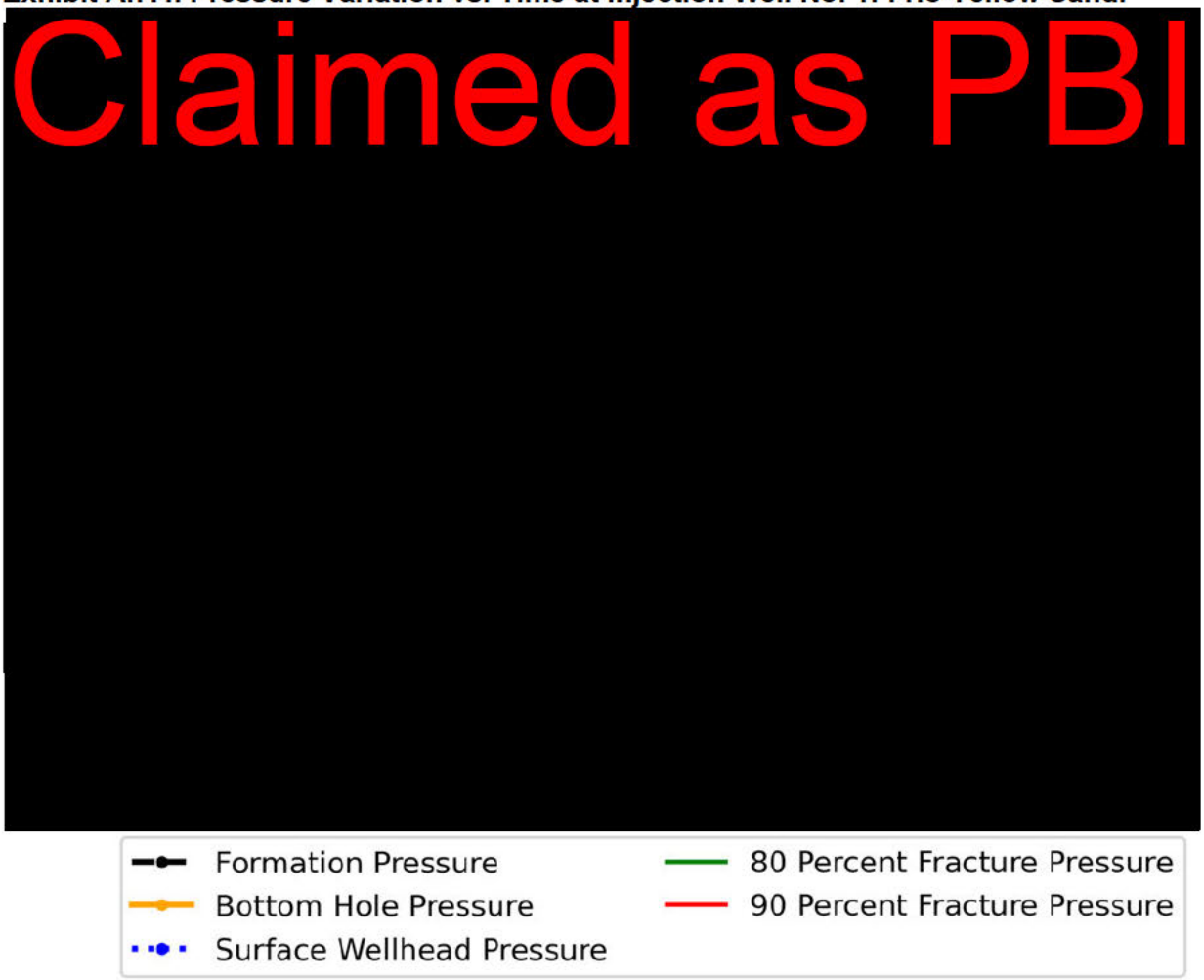

Exhibit A.7.5. Pressure Variation vs. Time at Injection Well No. 2: Frio Green Sand.

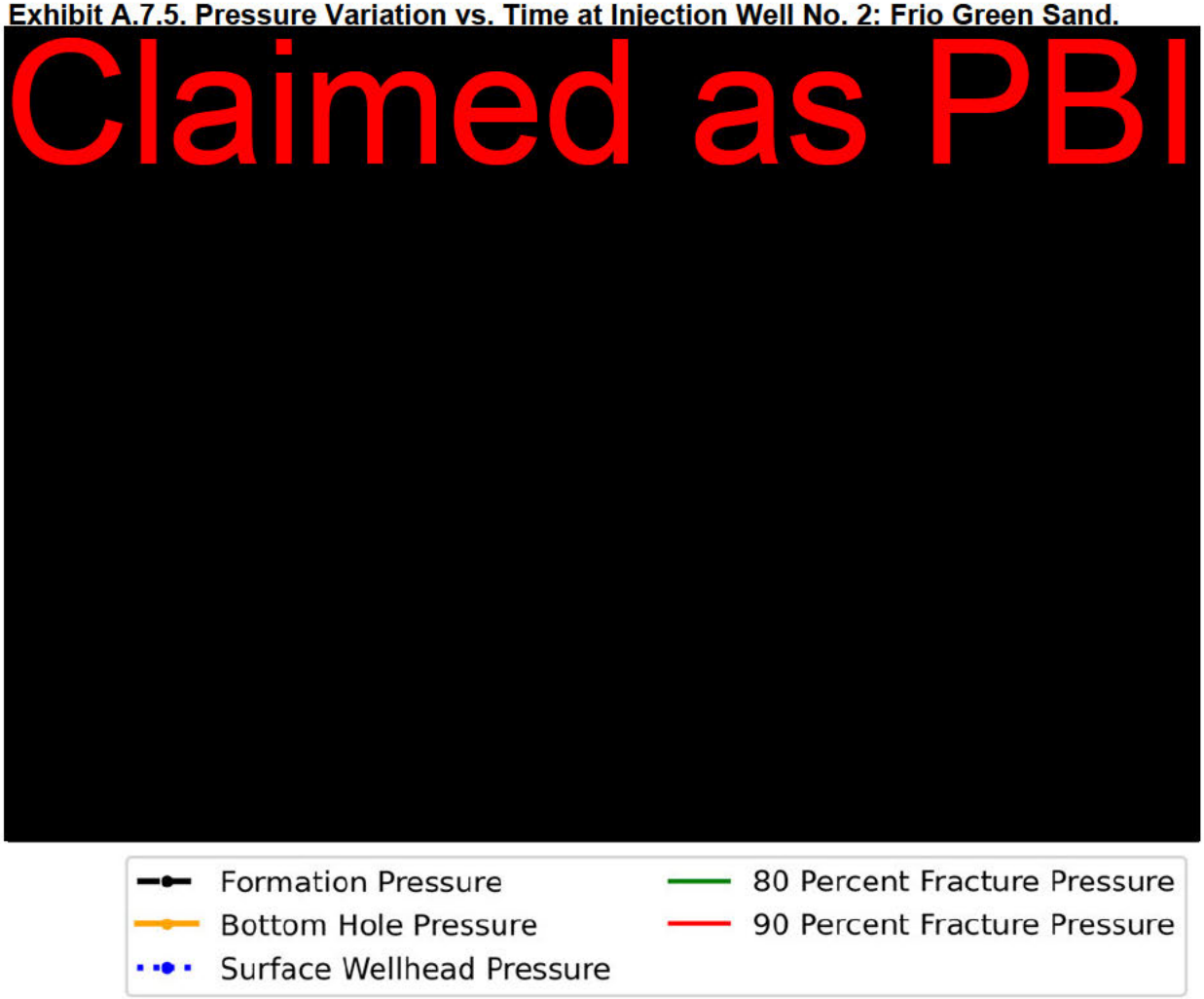

Exhibit A.7.6. Pressure Variation vs. Time at Injection Well No. 2: Frio Yellow Sand.

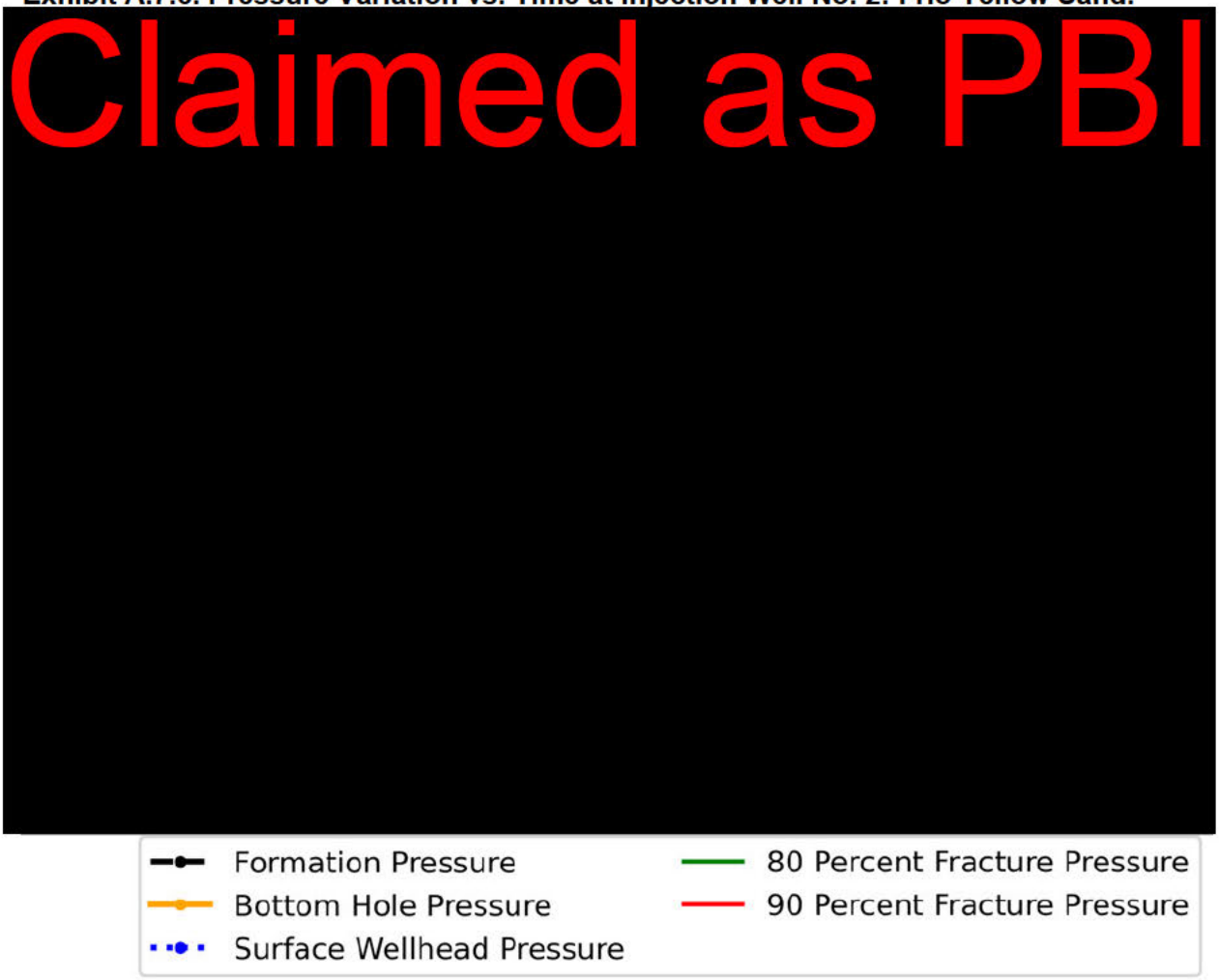

Exhibit A.7.7. Pressure Variation vs. Time at Injection Well No. 2: Frio Gold Sand.

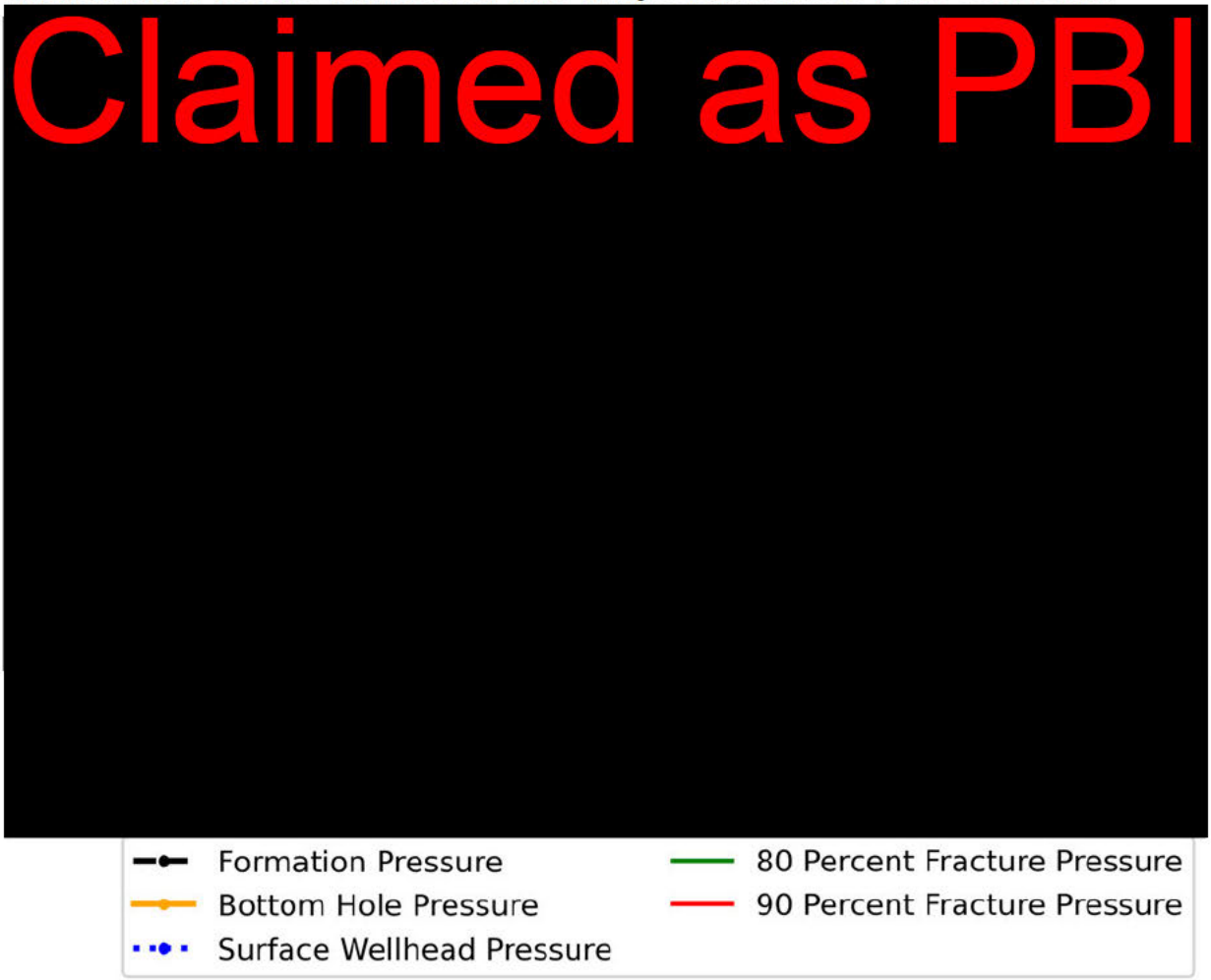

Exhibit A.7.8. Pressure Variation vs. Time at Injection Well No. 3: Frio Green Sand.

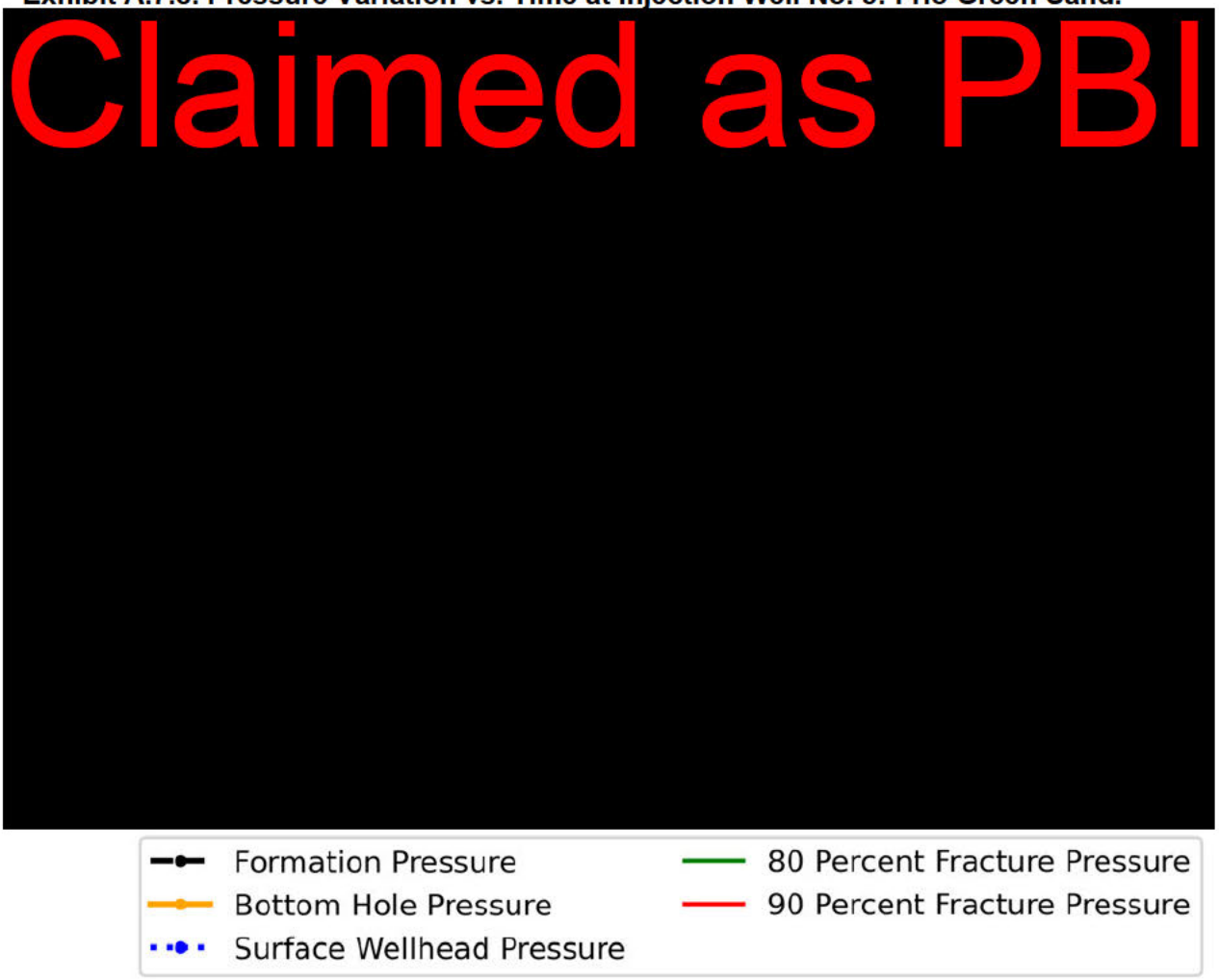

Exhibit A.7.9. Pressure Variation vs. Time at Injection Well No. 3: Frio Yellow Sand.

Claimed as PBI

As shown in **Exhibits A.7.3 through A.7.9**, no injection well indicates that formation pressures will surpass the 80% fracture gradient requirement. This indicates that the Upper Frio Formation will remain within a safe operating range; and therefore, the injection of CO_2 will not present a significant risk to the integrity of the storage reservoir.

Claimed as PBI

The proposed operational procedures are subject to change based on more accurate model runs, final composition of the subsurface, and other well testing results. A final version of model values and operational procedures will be submitted to the UIC Program Director for approval prior to operation if data indicate that any of the operational procedures will materially differ from those specified in this application.

The operational parameters are likely to stay constant for the lifetime of the injection project. However, if the source or composition of the CO_2 stream changes at any point during operation, Caliche may reevaluate and adjust the operating pressures.

8.0 TESTING AND MONITORING PLAN

Caliche has uploaded the *"Testing and Monitoring Plan"* (T&M Plan) to *Module E.1* of the USEPA GSDT Portal, which abides by all requirements of 40 CFR §146.82(a)(15) and §146.90. Caliche designed the T&M Plan to monitor the Caliche Beaumont Sequestration Project Site for the life of the project under USEPA (40 CFR §146.90). The T&M Plan also meets the requirements of the Monitoring, Measurement, and Verification Plan required under CARB LCFS Subsection C.4.3.2.

The purpose of the T&M Plan is to demonstrate that the injection wells are operating as planned, that the CO_2 plume and pressure front are moving as predicted, and that there is no endangerment to the overlying USDW. The T&M data may be used to validate and adjust the computational model used to predict the distribution of CO_2(sc) and pressure front within the target storage reservoir to support AoR reevaluations and a non-endangerment demonstration. Additionally, the T&M Plan can be utilized to detect and quantify CO_2 leakage from the target storage reservoir to the USDW and atmosphere, if necessary.

The spatial distribution of the monitoring network for the Caliche Beaumont Sequestration Project includes various surface and subsurface media, spread, at a minimum, over the extent of the modeled AOR. To demonstrate compliance with the USEPA Class VI and CARB LCFS requirements, the monitoring components for the Caliche Beaumont Sequestration Project may be installed at various depths within the Caliche Beaumont Sequestration Project Site including the: Injection Zone, First Transmissive Zone Above the Confining Zone, Lowermost USDW, Near-Surface, and Surface. The data obtained from these zones will be used to inform and improve operational decisions on the quantity, quality, and rate of CO_2 injected while ensuring containment within the storage complex. The T&M Plan is designed to confirm compatibility between the CO_2 stream and injection infrastructures (e.g., pipelines, pumps, and injection wells) and ensure the integrity of the injection infrastructures during the life of the project.

The T&M plan is also designed to monitor and coordinate response actions identified in the *Module E.4 – ERRP* associated with risks related to the injection and sequestration of CO_2 in the Upper Frio Sands. All T&M activities will be conducted per the Quality Assurance and Surveillance Plan (QASP; see **Appendix E.1.A** to *Module E.1*), according to 40 CFR §146.90(k) and CARB LCFS (Subsection C.4.1(a)(13)(D)). Caliche will report the results of all T&M activities to the USEPA and CARB in compliance with the requirements under 40 CFR §146.91 and CARB LCFS requirements. **Table E.1.1** provides an overview of the T&M Plan objectives, and monitoring and reporting frequencies.

Testing and Monitoring GSDT Submissions
GSDT Module: Project Plan Submissions ***Tab(s):*** Testing and Monitoring tab Please use the checkbox(es) to verify the following information was submitted to the GSDT: ☒ Testing and Monitoring Plan ***[40 CFR §146.82(a)(15) and §146.90]***

9.0 INJECTION WELL PLUGGING PLAN

Caliche has uploaded the *"Injection Well Plugging Plan"* to *Module E.2* of the USEPA GSDT Portal, which abides by all requirements of 40 CFR §146.82(a)(16) and §146.92(b). Caliche also has designed the Injection Well Plugging Plan to abide by the requirements of CARB LCFS (CARB, 2018, Subsection C.5.1). The Injection Well Plugging Plan ensures that the plugging and abandonment activities do not allow for formation fluid or CO_2 leakage out of the target reservoir that may endanger the overlying USDW. Per CARB LCFS, Caliche plans to plug and abandon all three injection wells within 2 years of cessation of injection operations.

Plugging plans and schematics are provided for each injection well as part of *Module E.2*. Before plugging is commenced, a bottomhole falloff test will be performed to ensure the appropriate density of plugging fluids, per 40 CFR §146.92(b)(1). Mechanical integrity tests (MITs) will also be performed on each well before plugging to demonstrate that the long-string casing and cement left behind will maintain integrity over time, per 40 CFR §146.92(b)(2) and CARB LCFS Subsection C.4.2. All injection wells will be plugged across the completion zones and the across the bottom of the surface casing using Halliburton CO_2 Resistant CORROSACEM™ (or equivalent) cement, which will be squeezed through the retainer.

In compliance with 40 CFR §146.92(c), Caliche will notify the UIC Program Director in writing of intent to plug at least 60 days prior to plugging the injection wells (at least 30 days for CARB LCFS (CARB, 2018, Subsection C.5.1(h)), during which time the final well plugging procedures will be finalized, as needed, and confirmed with the UIC Program Director (and CARB LCFS Executive Officer). A final plugging report will be filed with the UIC Program Director within 60 days after the completion of plugging operations, as required by 40 CFR §146.92(d) and CARB LCFS Subsection C.5.1(k).

The elements of the Injection Well Plugging Plan may be modified at a later date based on information generated during the operational phase of the project (USEPA, 2016, p. 5; CARB, 2018, p. 38). Any modifications to this Injection Well Plugging Plan will be submitted to the USEPA UIC Program Director and CARB LCFS Executive Director for their approval.

Injection Well Plugging GSDT Submissions

GSDT Module: Project Plan Submissions
Tab(s): Injection Well Plugging tab

Please use the checkbox(es) to verify the following information was submitted to the GSDT:
☒ Injection Well Plugging Plan ***[40 CFR §146.82(a)(16) and §146.92(b)]***

10.0 POST-INJECTION SITE CARE (PISC) AND SITE CLOSURE PLAN

Caliche has uploaded the *"Post-Injection Site Care and Site Closure Plan"* to *Module E.3* of the USEPA GSDT Portal, which abides by all requirements of 40 CFR §146.82(a)(17) and §146.93(a). Caliche also designed the Post-Injection Site Care (PISC) and Site Closure Plan to meet the requirements of the CCS Protocol under the CARB LCFS (Subsection C.5.2).

Caliche will not cease PISC monitoring until a demonstration of non-endangerment of the overlying USDW has been approved by the UIC Program Director under 40 CFR §146.93(b)(3) or until a demonstration that no CO_2 leak is occurring has been approved by the CARB Executive Officer under CARB LCFS (Subsection 5.2(b)(1)). Caliche will implement an adaptive PISC for 100 years in accordance with CARB LCFS (Subsection C.5.2(b)(2)), which is more than the 50 years PISC period minimum per 40 CFR §146.93(b)(1) to demonstrate conformance and containment. This will be demonstrated using part or all the monitoring components proposed in the *Module E.1 - Testing and Monitoring Plan*.

Note that components of the above confining zone monitoring program may be modified during post-injection phase, as needed, and with approval of the UIC Program Director and CARB Executive Officer, as more data and information are evaluated for the Caliche Beaumont Sequestration Project.

Following approval for site closure, Caliche will plug all monitoring wells, decommission other monitoring components, restore the site to the extent practicable to its original condition, and submit a site closure report and associated documentation.

PISC and Site Closure GSDT Submissions
GSDT Module: Project Plan Submissions ***Tab(s):*** PISC and Site Closure tab Please use the checkbox(es) to verify the following information was submitted to the GSDT: ☒ PISC and Site Closure Plan ***[40 CFR §146.82(a)(17) and §146.93(a)]***
GSDT Module: Alternative PISC Timeframe Demonstration ***Tab(s):*** All tabs (only if an alternative PISC timeframe is requested) Please use the checkbox(es) to verify the following information was submitted to the GSDT: ☐ Alternative PISC timeframe demonstration ***[40 CFR §146.82(a)(18) and 1§46.93(c)]***

11.0 EMERGENCY AND REMEDIAL RESPONSE PLAN

Caliche has uploaded the *"Emergency and Remedial Response Plan"* (ERRP) to *Module E.4* of the USEPA GSDT Portal, which abides by all requirements of 40 CFR §146.82(a)(19) and §146.94(a)). The ERRP describes actions that Caliche shall take in the event of an emergency that has the potential to endanger public health or the environment during the construction, operation, or post-injection site care periods per 40 CFR §146.94(a) and CARB LCFS (CARB, 2018, Section 6.0). The ERRP also describes actions that Caliche shall take to address the movement of the injected CO_2 or other formation fluids in a manner that may endanger the USDW.

Emergency and Remedial Response GSDT Submissions
GSDT Module: Project Plan Submissions ***Tab(s):*** Emergency and Remedial Response tab Please use the checkbox(es) to verify the following information was submitted to the GSDT: ☒ Emergency and Remedial Response Plan ***[40 CFR §146.82(a)(19) and §146.94(a)]***

12.0 INJECTION DEPTH WAIVER AND AQUIFER EXEMPTION EXPANSION

For this Class VI permit application, an injection depth waiver and aquifer expansion are not required and therefore are not being requested for the Caliche Beaumont Sequestration Project.

Injection Depth Waiver and Aquifer Exemption Expansion GSDT Submissions

GSDT Module: Injection Depth Waivers and Aquifer Exemption Expansions
Tab(s): All applicable tabs

Please use the checkbox(es) to verify the following information was submitted to the GSDT:
☐ Injection Depth Waiver supplemental report ***[40 CFR §146.82(d) and §146.95(a)]***
☐ Aquifer exemption expansion request and data ***[40 CFR §146.4(d) and §144.7(d)]***

13.0 OPTIONAL ADDITIONAL PROJECT INFORMATION

Caliche is applying for the UIC Class VI injection well permit under the USEPA and will subsequently apply to the Texas Railroad Commission. Caliche plans to qualify and receive authorization to inject under both Federal and State agencies. In addition, Caliche plans to apply to the CARB LCFS.

Caliche has performed an additional environmental justice (EJ) assessment of the communities within a 1-mile buffer of the AoR (EJ Area). Caliche utilized the USEPA EJScreen tool to develop an understanding of the current environmental burdens within the EJ Area and to determine if Caliche Beaumont Sequestration Project activities may exacerbate existing disproportionate impacts.

A summary of Caliche's EJ review is provided below.

13.1 Environmental Justice Review

On behalf of Caliche, GSI has completed an environmental justice (EJ) review of the community that surrounds the leased property proposed for the geologic sequestration (GS) of CO_2. This report provides the results, rationale, and potential community impacts in this area, as well as the potential benefits of the Caliche Beaumont Sequestration Project. The purpose of this report is to determine if the surrounding community is already economically, environmentally, or socially disadvantaged and whether activities of a Class VI carbon capture and sequestration (CCS) project may exacerbate existing disproportionate impacts.

The United States Environmental Protection Agency (USEPA) defines EJ in part as the *"just treatment and meaningful involvement of all people, regardless of income, race, color, national origin, Tribal affiliation, or disability, in agency decision-making and other Federal activities that affect human health and the environment"* (USEPA, 2023a, Executive Order 14096). It is well known that CO_2 is a major contributor to global climate change and increased global average temperatures. The sequestration of CO_2 is a vital step towards mitigating the effects of climate change (UNFCCC, 2024). As such, Caliche aims to make this CCS project a positive and beneficial undertaking for both the immediate community and society as a whole.

13.1.1 Site Location

As shown in **Exhibit A.13.1** below, the proposed Class VI injection wells are located within the Caliche leased property (City of Beaumont Acreage) located in Southeast Texas just south of the City of Beaumont within Jefferson County. To the east lies the Louisiana - Texas border, and to the south, the Gulf of Mexico. The proximity to the coast creates an abundance of saline reservoirs below the surface, which is suitable for the injection and containment of CO_2 while maintaining protection of the USDW. The City of Beaumont Acreage is an approximately Claimed as PBI extent which resides in mostly undeveloped and agricultural land. The maximum extent of the modeled AoR is approximately Claimed as PBI which includes most of the City of Beaumont Acreage. A 1-mile buffer has been applied around the Caliche EJ AoR, encompassing a Claimed as PBI ("Caliche EJ Area"; see **Exhibit A.13.1** above). Locations of USEPA-regulated facilities, including Superfund, hazardous waste, water discharges, air pollution, and Brownfields sites, are presented on **Exhibit A.13.2** below.

Exhibit A.13.1. Caliche AoR and EJ Area.

Exhibit A.13.2. USEPA-Regulated Facilities within Caliche EJ Area.

SOURCE: Data obtained from EJScreen Tool.

13.1.2 Data Review

According to the guidance developed by the Council on Environmental Quality's (CEQ) *Environmental Justice Guidance Under the National Environmental Policy Act* (NEPA) (CEQ, 1997), the USEPA's *Additional Tools for UIC Program Directors Incorporating Environmental Justice Considerations into the Class VI Injection Well Permitting Process* (USEPA, 2011), and the USEPA's *Promising Practices for EJ Methodologies in NEPA Reviews* (USEPA, 2016), the determination of EJ impacts entails an evaluation of *demographic* and *socioeconomic* (race, income, unemployment rate, limited English speaking household, education, and age), and *environmental* (air and diesel particulate matter, ozone, air toxics, traffic, lead paint, superfund proximity, industrial facility proximity, hazardous waste proximity, underground storage tanks, and wastewater discharge) indicators for a defined geographic area (USEPA, 2023b). Once potentially affected communities with EJ concerns have been identified, UIC Class VI well owners or operators can assess whether the Caliche Beaumont Sequestration Project also will produce impacts that are high and adverse that would disproportionately affect minority and low-income populations (USEPA, 2011; 2023c).

GSI compiled data on demographic, socioeconomic, and environmental indicators within a Claimed as PBI the Caliche EJ AoR, encompassing a Claimed as PBI ("Caliche EJ Area"; see **Exhibit A.13.1** above) using the USEPA Environmental Justice Screening Tool ("EJScreen") and the US Census Bureau American Community Survey ("ACS") program. A summary of the data and information obtained from EJScreen and the ACS program is provided in the sections below.

13.1.3 EJScreen

EJScreen is a screening and mapping tool that *"utilizes standard and nationally-consistent data to highlight places that may have higher environmental burdens and vulnerable populations"* (USEPA, 2023b). The EJScreen Tool considers a *combination* of demographic, socioeconomic, and environmental indicators (i.e., EJ Indices and Supplemental Indices) for defined Census block groups within a user-defined geographic area. As mentioned above, the Caliche EJ Area encompasses the Caliche EJ AoR plus a Claimed as PBI

The results of the EJScreen analysis indicate the presence of potentially economically, environmentally, or socially disadvantaged populations within the Caliche EJ Area; however, Caliche Beaumont Sequestration Project activities are not expected to exacerbate existing potentially disproportionate impacts. Installation and operation of the Class VI injection wells are *not* expected to generate air emissions that will have significant effects beyond the localized footprint of the injection site or have significant environmental impacts – mitigating the need for a larger EJScreen area extent. Further, the extensive direct and indirect Testing and Monitoring Plan is designed to proactively *"prevent any adverse impacts to USDWs from all activities throughout the lifetime of the project"* (USEPA, 2023c).

The results of the EJScreen Tool, as accessed on 21 March 2024, are summarized below and included in **Appendix A.H** to this submittal.

13.1.3.1 Community Information

The population of the Caliche EJ Area is approximately 2,053 people. As shown on **Exhibit A.13.3** below, most of the population resides in the northern extent of the Caliche EJ Area; leaving the remainder of the Caliche EJ Area which overlies the majority of the CO_2(sc) plume unpopulated.

The per capita income of these residents is $31,340 with around 30% of the population considered low-income. Approximately 76% of residents are male, and 24% are female. 77% of residents are persons of color; a breakdown by race provides that approximately 52% of the population is Black, 23% Hispanic, 23% White, 1% Asian and ~1% of two or more races. Approximately 8% of residents are people with disabilities. The unemployment rate for the area is 25%, and the population with less than a high school education is 19%. The average life expectancy in this area is 75 years.

Exhibit A.13.3. Population Density (per square mile) in Caliche EJ Area.

SOURCE: Data obtained from EJScreen Tool.

13.1.3.2 EJ Indexes

The results of the EJScreen Tool show that all EJ Indices for single environmental indicators (pollution and sources; e.g., Particulate Matter, Ozone, Air Toxics Cancer Risk, Risk Management Program (RMP) Facility Proximity, etc.) for the Caliche EJ Area exceed the 50th percentile compared to both the State and Nation; except for Particulate Matter (43rd percentile), Traffic Proximity (29th percentile) and Underground Storage Tanks (44th percentile) for the state percentile and Traffic Proximity at the 46th percentile for the nation. The same results apply to all EJ Supplemental Indices for the same environmental indicators exceed the 50th percentile compared to both the State and Nation except for Particulate Matter (40th percentile), Traffic Proximity (27th percentile) and Underground Storage Tanks (43rd percentile) for the state percentile and Traffic Proximity at the 36th percentile for the nation. The indices indicate that air quality, particularly toxic releases to air and air toxics cancer risks and Wastewater Discharge are among the highest environmental risks for the Caliche EJ Area.

Socioeconomic factors are also presented in **Appendix A.H**. All socioeconomic indicators listed for the Caliche EJ Area are above the national averages, except for Limited English-speaking households (1% vs. 5% for the nation). The most notable socioeconomic indicator is People of

Color (77% vs. 39% for the nation) (hence a 60% demographic index compared to 35% for the Nation).

13.1.4 US Census Bureau Socioeconomic and Demographic Evaluation

Detailed information regarding race and ethnicity, English language proficiency, poverty status, age, sex, income, education attainment, and disability status were obtained from ACS program and are summarized in attached **Tables A.13.1 to A.13.6**. All statistics are based on 2022 ACS 1-Year Estimates, except for race and ethnicity which are based on the 2020 Census.

13.1.4.1 Race and Ethnicity

Within Jefferson County and the City of Beaumont, approximately 75% to 80% of residents, respectively, identify as one race alone. This does not include 23% of Jefferson County residence and 18% of Beaumont residence who identify as Hispanic or Latino. Of the residents who identify as one race alone:

- **Jefferson County:** 37% identify as white alone, and 33% identify as Black or African American alone.
- **City of Beaumont:** 28% of residents identify as white alone, and 47% identify as Black or African American alone.

In comparison, in Texas as a whole, 58% of the residence identify as one race alone, while 39% of residents identify as Hispanic or Latino. Of the 58% of residence who identify as one race alone: 38% identify as white alone, and 12% identify as Black or African American alone.

13.1.4.2 Language Proficiency

Language proficiency across the US, the State of Texas, and Jefferson County does not differ significantly. While 8.4% of American's speak English *less than* "very well," 12.8% of Texans fall within this category, and 8.8% of Jefferson County residents. Jefferson County residents (91%) fall similarly in line with the national averages (92%) for the ability to speak English Only or speak English "very well." Additionally, approximately 95% of Americans that are 18 years and older speak only English or speak English "very well" while 96% of Jefferson County residents do. Insufficient data was available to compile these statistics for the City of Beaumont residents; however, based on the Jefferson County information available, and the EJScreen statistics for the Caliche EJ Area, a language barrier is not a concern within or around the Caliche Beaumont Sequestration Project Site.

13.1.4.3 Age and Sex

Populations of people who are either very young or very old are considered to be more sensitive and susceptible groups to environmental harm. Information from the ACS allows us to look at the percentage of people below the age and 5 and above the age of 75 across multiple regions. Between the US, the State of Texas, Jefferson County, and the City of Beaumont, there is only a very slight difference in the percentage of these groups. The percentage of people under the age of 5 are 5.5%, 6.3%, 6.4%, and 6.8% respectively, for the groups listed above. The same goes for people 75 years and older; 7.2%, 5.2%, 6.3%, and 7.2%, with the difference between the national average and the City of Beaumont being zero.

13.1.4.4 Educational Attainment and Poverty Status

Of the total population of the City of Beaumont, 18% of income in the last 12 months was below the poverty level versus the national average of 11%.

In the US, 24% and 28% of males and females, respectively, of residence living on an income below the poverty level received some college or an associate's degree; while 16% of males and 15% of females received a bachelor's degree or higher. Comparatively, City of Beaumont residence males (14%) and females (26%) received some college or an associate's degree, and males (5%) and females (16%) received a bachelor's degree or higher.

For US residence living on income above the poverty level, approximately (27%) male and (15%) female received some college or an associate's degree while (37%) male and (20%) female received a bachelor's degree or higher. For City of Beaumont residents who are male (34%) and female (35%) and male (28%) and female (34%) fall under these categories respectively.

13.1.4.5 Low Income - Poverty Status

The poverty status for City of Beaumont residents is 20% while poverty status of US citizens is 12.6%. The City of Beaumont residents exceed the national and state percentages of people living below the poverty line for all categories which includes age, sex, race, education attainment, employment status, and work experience.

13.1.4.6 Disability

Those living with a disability in the City of Beaumont are 14.2% of the population while nationally 13.4% of people live with a disability. Overall, the percentage of City of Beaumont residents living with a disability do not differ significantly from the national population disability categories which include; sex, race, and age. More females live with a disability in City of Beaumont than nationally or in the State of Texas while more people who are Black or African American alone live with a disability in the City of Beaumont.

13.1.4.7 Tribal Lands and Indigenous Peoples

According to the Bureau of Indian Affairs, there are three federally recognized tribes in the State of Texas (BIA, 2023); none of which fall within or near the Caliche Beaumont Sequestration Project Site.

13.1.5 Environmental Health Impacts and Benefits

The environmental and health impacts that occur during well installation may minorly decrease air quality in proximity to the drill rig. Increased vehicle traffic to and from the Caliche Beaumont Sequestration Project Site is also an air quality risk factor; however, the effects are expected to be minimal and short-term. Once well construction is complete, operational impacts (air emissions, noise) are expected to be minimal and contained to a local extent around the injection site.

As discussed in *Module E.1 - Testing and Monitoring Plan*, the primary objective of Caliche Beaumont Sequestration Project testing and monitoring approach is to proactively *"prevent any adverse impacts to USDWs from all activities throughout the lifetime of the project"* (USEPA, 2023c). Caliche plans to conduct direct and indirect testing and monitoring utilizing the best available technologies during the injection and post-injection phases of the Caliche Beaumont

Sequestration Project to confirm the extent of the CO_2(sc) plume and to demonstrate that no CO_2 leakage is occurring and that the USDW is protected, as required by the Class VI Rule 40 CFR §146.93(b)(1) and CARB LCFS Subsection C.5.2(a)(2). The *Module E.1 - Testing and Monitoring Plan* has been designed to aid in the early detection of potential CO_2 leaks from the target injection reservoir, if any, which will mitigate potential environmental effects to the USDW or community.

13.1.6 Cumulative Impacts and Mitigation

The environmental, health, and social impacts of the construction, use, and long-term maintenance of injection wells for the sequestration of CO_2, while not nonexistent, are minimal. For example, construction activities might temporarily affect local air quality, transportation, and noise levels, and facility operations might have aesthetic, transportation, and/or noise level effects.

However, the benefits of the Caliche Beaumont Sequestration Project compared to the impact on localized communities far outweigh the costs. The ability to sequester carbon and remove it from the atmosphere will help to reduce greenhouse gas emissions and reverse the effects of climate change. The Caliche Beaumont Sequestration Project may create new employment opportunities and higher wages in the Caliche EJ Area and promote local businesses and contractors. The Caliche Beaumont Sequestration Project may improve communications (cell and internet) in the area as well, as the site will require sufficient communications to transmit remote testing and monitoring data. Already disadvantaged communities who might experience disproportional impacts from climate change may see great long-term advantages from CO_2 sequestration efforts.

The Testing and Monitoring Plan, among other sections of this permit application, helps to mitigate any risks to the long-term safety and health of local residents and the environment that may be caused by the Caliche Beaumont Sequestration Project. If an accidental release of CO_2 were to occur, the ERRP details the actions that Caliche shall take to address movement of the injection fluid or formation fluid in a manner that may endanger the USDW during the construction, operation, or post-injection site care periods.

13.1.7 Public Engagement

GSI, on behalf of Caliche, has completed this EJ review to identify *"communities potentially adversely and disproportionately affected by human health, environmental, climate-related, and/or other cumulative harms or risks"* (i.e., communities with potential EJ concerns; USEPA, 2023c) to help ensure proactive engagement and just treatment of the public.

Caliche is committed to an open and honest discussion regarding the risks and benefits of carbon sequestration. On 31 August 2023, Caliche posted a public announcement on their Newsroom of their agreement with the City of Beaumont to lease pore space for the long-term sequestration of CO_2 (Caliche, 2023). In addition, Caliche representatives presented their upcoming Caliche Beaumont Sequestration Project to business leaders and community members at the Port Arthur Chamber of Commerce's 3rd Annual Carbon Summit on 1 November 2023 (Houston CCS Alliance, 2023).

Overall climate change awareness is a significant predictor of risk and benefit perceptions by the public (Wallquist et al., 2010; Seigo et al., 2014). Caliche is planning to meet with community leaders and representatives in the area and discuss the general public's perceptions of CCS and its risks and benefits, including discussions of key CCS concepts such as pressurization, leakage, socioeconomics, storage mechanisms, CO_2 knowledge, impacts to subsurface microbial communities, and climate change awareness (Wallquist et al., 2010). Caliche will consider key

community challenges, such as language and cultural barriers and lack of technical resources or transportation means, as it develops and implements its community engagement plans. Caliche is exploring a variety of community engagement tools, such as open houses, neighborhood association and town hall meetings, and press releases, that will employ effective visual tools and communication materials. Caliche is dedicated to enhanced community engagement and a path forward that includes meaningful involvement of all persons in the community regardless of age, sex, race and ethnicity, or disability.

13.1.8 Conclusions

The objective of this EJ review is to ensure that undue burden is not placed members of the community surrounding the Caliche Beaumont Sequestration Project. The results of the EJScreen analysis indicate the presence of potentially economically, environmentally, or socially disadvantaged populations within the Caliche EJ Area; however, Caliche Beaumont Sequestration Project activities are not expected to exacerbate existing conditions or create potentially disproportionate impacts. The majority of the Caliche EJ Area has a low population density and effects from drilling and maintenance are expected to be brief, localized, and minimal. Further, the Testing and Monitoring Plan is designed to proactively *"prevent any adverse impacts to USDWs from all activities throughout the lifetime of the project"* (USEPA, 2023c).

In conclusion, based on a review of demographic, socioeconomic, and environmental indicators for the local community within the Caliche EJ Area, disproportionately high adverse impacts on minority or low-income populations are not expected as a result of the Caliche Beaumont Sequestration Project.

14.0 CITED REFERENCES

SECTION 1.0

USEPA, 2022. Facility Level Information on Greenhouse Gases Tool. 2021 Greenhouse Gas Emissions from Large Facilities. United States Environmental Protection Agency. Data as of 12 August 2022. Available at https://ghgdata.epa.gov/ghgp/main.do.

Swanson S.M., A.W. Karlsen, and B.J. Valentine, 2013. Geologic assessment of undiscovered oil and gas resources: Oligocene Frio and Anahuac Formations, United States Gulf of Mexico coastal plain and State waters. United States Geological Survey. Open-File Report 2013–1257. https://doi.org/10.3133/ofr20131257.

Chowdhury, A.H. and M.J. Turco, 2006. Geology of the Gulf Coast Aquifer, Texas. Texas Water Development Board. Chapter 2.

SECTION 2.0

Section 2.1

Baker, 1979. Stratigraphic and Hydrogeologic Framework of Part of the Coastal Plain of Texas. Texas Department of Water Resources Report 236, July 1979.

Bebout et al., 1978. Frio Sandstone Reservoirs in the Deep Subsurface along the Texas Gulf Coast: Their Potential for Production of Geopressured Geothermal Energy. Bureau of Economic Geology, University of Texas at Austin, Report of Investigations No. 91.

Coleman, 1990. Depositional Systems and Tectonic/Eustatic History of the Oligocene Vicksburg Episode of the Northern Gulf Coast. Dissertation of Janet Marie Combes Coleman presented to the faculty of the Graduate School of the University of Texas at Austin, December 1990.

Dodge and Posey, 1981. Structural Cros Sections, Tertiary Formations, Texas Gulf Coast. Bureau of Economic Geology, University of Texas at Austin.

Ewing and Reed, 1984. Depositional Systems and Structural Controls of Hackberry Sandstone Reservoirs in Southeast Texas. Bureau of Economic Geology, Geological Circular 84-7.

Ewing, 1986. Structural Styles of the Wilcox and Frio Grown-Fault Trends in Texas: Constraints on Geopressured Reservoirs. Bureau of Economic Geology, Report of Investigations No. 154.

Galloway, et al., 1982. Frio Formation of the Texas Gulf Coast Basin – Depositional Systems, Structural Framework, and Hydrocarbon Origin, Migration, Distribution, and Exploration Potential. Bureau of Economic Geology, Report of Investigations No. 122.

Galloway, 2008. Depositional Evolution of the Gulf of Mexico Sedimentary Basins, in Hsu, editor, Sedimentary Basins of the World, Volume 5, The Sedimentary Basins of the United States and Canada. Elsevier, pp. 505-549.

George, et al., 2011. Aquifers of Texas. Texas Water Development Board Report 380, July 2011.

Halbouty, 1979. Salt Domes: Gulf Region, United States and Mexico. Gulf Publishing, Second Edition.

Hosman, 1996. Regional Stratigraphy and Subsurface Geology of Cenozoic Deposits, Gulf Coastal Plain, South-Central United States. U.S. Geological Survey Professional Paper 1416-G.

Jackson and Galloway, 1984. Structural and Depositional Styles of Gulf Coast Tertiary Continental Margins: Applications to Hydrocarbon Exploration: American Association of Petroleum Geologists, Continuing Education Note Series No. 25, p. 226.

Swanson et al., 2013. Geologic Assessment of Undiscovered Oil and Gas Resources – Oligocene Frio and Anahuac Formations, United States Gulf of Mexico Coastal Plain and State Waters. U.S. Geological Survey, Open-File Report 2013-1257.

Thorkildsen and Quincy, 1990. Evaluation of Water Resources of Orange and Eastern Jefferson Counties, Texas. Texas Water Development Board, Report 320, January 1990.

UT-BEG, 1992a. Geology of Texas. Published by Bureau of Economic Geology, University of Texas at Austin.

UT-BEG, 1992b. Geologic Atlas of Texas – Beaumont Sheet. Published by Bureau of Economic Geology, University of Texas at Austin.

UT-BEG, 1997. Tectonic Map of Texas. Published by Bureau of Economic Geology, University of Texas at Austin.

Williamson et al., 1990. Ground-Water Flow in the Gulf Coast Aquifer Systems, South Central United States – a Preliminary Analysis. U.S. Geological Survey, Water-Resources Investigations Report 89-4071.

Young et al., 2012. Updating the Hydrogeologic Framework for the Northern Portion of the Gulf Coast Aquifer. Prepared for Texas Water Development Board, June 2012.

Young et al., 2016. Identification of Potential Brackish Groundwater Production Areas – Gulf Coast Aquifer System. Prepared for Texas Water Development Board, August 2016.

Young and Draper, 2020. The Delineation of the Burkeville Confining Unit and the Base of the Chicot Aquifer to Support the Development of the Gulf 2023 Groundwater Model. Prepared for the Harris-Galveston Subsidence District and the Fort Bend Subsidence District, October 2020

Section 2.2

Alexander, L. L., and Handschy, J. W., 1998. Fluid flow in a faulted reservoir system: Fault trap analysis for the Block 330 Field in Eugene Island, South Addition, Offshore Louisiana: Am. Assoc. Petroleum Geologists Bull., v. 82 n. 3, p. 387-411.

Allen, U. S., 1989. Model for hydrocarbon migration and entrapment within faulted structures: Am. Assoc. Petroleum Geologists Bull., v. 8, p. 803-811.

Antonellini, M., and Aydin, A., 1994. Effect of faulting on fluid flow in porous sandstones: petrophysical properties: Am. Assoc. Petroleum Geologists Bull., v. 78, n. 3, p. 355-377.

Aronow, S., and Wesselman, J. B., 1971. Groundwater Resources of Chambers and Jefferson Counties, Texas: Texas Water Development Board Report No. 133.

Baker, E. T., 1979. Stratigraphic and hydrogeologic framework of part of the coastal plain of Texas: Texas Department of Water Resources, Report 236, Austin, Texas, p. 43.

Bebout, D. G., Loucks, R. G., and Gregory, A. R., 1978. Frio sandstone reservoirs in the deep subsurface along the Texas Gulf Coast, their potential for production of geopressured geothermal energy: Bureau of Economic Geology, Report of Investigations No. 91, The University of Texas at Austin, Austin, Texas, p. 92.

Berg, R. R., 1975. Capillary pressures in stratigraphic traps: Am. Assoc. Petroleum Geologists Bull., v. 59, p. 939-956.

Berg, R. R., and Avery, A. H. 1995. Sealing properties of Tertiary growth faults, Texas Gulf Coast: Am. Assoc. Petroleum Geologists Bull., v. 79, n. 3, p. 375-393.

Bouvier, J. D., Kaars-Sijpesteijn, C. H., Kluesner, D. F., and Onyejekwe, C. C, 1989. ThreeDimensional seismic interpretation and fault sealing investigations, Nigeria: Am. Assoc. Petroleum Geologists Bull., v. 72, p. 1397-1414.

Clark, J. A., and Halbouty, M. T., 1952. Spindletop: Random House, New York, 306 p.

Clark, J. E., Howard, M. R., and Sparks, D. K., 1987. Factors that can Cause Abandoned Wells to Leak as Verified by Case Histories from Class II injection, Texas Railroad Commission files: International

Symposium on Subsurface Injection of Oilfield Brines, Underground Injection Practices Council, New Orleans, LA., p. 166-223.

Clark, J. E., Papadeas, P. W., Sparks, D. K., and R. R. McGowen, 1991. Gulf Coast Borehole Closure Test Well, Orangefield, Texas; UIPC 1991 Summer Symposium, Reno, Nevada, talk presented July 30, 1991.

Davis, K. E., 1986. Factors Effecting the Area of Review for Hazardous Waste Disposal Wells: Proceedings of the International Symposium on Subsurface Injection of Liquid Wastes, New Orleans, National Water Well Association, Dublin, OH, p. 148-194.

Dodge, M. M., and Posey, J. S., 1981. Structural Cross Sections, Tertiary Formations, Texas Gulf Coast; Bureau of Economic Geology, Austin, Texas.

Doughty, C., Freifeld, B.M., and Trautz, R.C., 2008. Site characterization for CO2 geologic storage and vice versa: The Frio Brine Pilot, Texas, USA as a case study. Environmental Geology. 54. 1635-1656. Doi: 10.1007/s00254-007-0942-0.

Dow, 2018. Dow Beaumont Aniline Frio EPA Reissuance: Unpublished UIC Petition, Houston, Texas.

Downey, M. W., 1984. Evaluating Seals for Hydrocarbon Accumulations: Am. Assoc. Petroleum Geologists Bull., v. 68, n. 11.

Eaton, B. A., 1969. Fracture gradient prediction and its application in oil field operations: Journal of Petroleum Technology, pp. 1353-1360.

Eby and Halbouty, 1937. Spindletop Oil Field, Jefferson County, Texas. Bulletin of the American Association of Petroleum Geologists. Vol. 21. No. 4., pp. 475-490. April 1937.

Engelder, 1974. Cataclasis and the generation of fault gouge: Geological Society of America Bulletin, Volume 85, p. 1515-1522.

Ewing, 1986. Structural Styles of the Wilcox and Frio Growth-Fault Trends in Texas: Constraints on Geopressured Reservoirs. Bureau of Economic Geology, The University of Texas at Austin. Report of Investigations No. 154.

Fisher, WL, LF Brown, Jr., JH McGowen, and CG Groat, 1973. Environmental Geologic Atlas of the Texas Coastal Zone: Beaumont – Port Arthor Area. Bureau of Economic Geology. The University of Texas at Austin. Note that Geologic Atlas of Texas, Beaumont Sheet was revised in 1992.

Galloway, W. E., Murphy, T. D., Belcher, B. C., Johnson, B. D., and Sutton, S., 1977. Catahoula Formation of the Texas Coastal Plain: Depositional systems, composition, structural development, groundwater flow history, and uranium distribution: Bureau of Economic Geology, Reports of Investigations No. 87, The University of Texas at Austin, Austin, Texas, p. 56.

Galloway, W. E., Hobday, D. K., and Magara, K., 1982a. Frio Formation of the Texas Gulf of Mexico Basin-depositional systems, structural framework, and hydrocarbon origin, migration, distribution, and exploration potential: Bureau of Economic Geology, Report of Investigations No. 122, The University of Texas at Austin, Austin, Texas, p. 78.

Galloway, W. E., Henry, C. G., and Smith, G. E., 1982b. Depositional framework, hydrostratigraphy, and uranium mineralization of the Oakville sandstone (Miocene) Texas Coastal Plain: Bureau of Economic Geology, Report of Investigations No. 113, The University of Texas at Austin, Austin, Texas, 59 p.

Galloway, W. E., 1985. Depositional framework of the lower Miocene (Fleming) episode Northwest Gulf Coast Basin: Gulf Coast Association of Geologists Society Transactions, v. 35, pp. 67-73.

Galloway, W. E., Jirik, L. A., Morton, R. A., and DuBar, J. R., 1986. Lower Miocene (Fleming) depositional episode of the Texas Coastal Plain and continental shelf: Structural framework, facies, and hydrocarbon resources: Bureau of Economic Geology, Report of Investigations No. 150, The University of Texas at Austin, Austin, Texas, 50 p.

Gray, G. R., Darley, H. C. H., and Rodgers, W. F., 1980. Composition and Properties of Oil Well Drilling Fluids: Gulf Publishing Company, Houston Texas.

Halbouty, MT, 1967. Salt Domes – Gulf Region, U.S. and Mexico. Pp. xiv-xv. June 1967.

Halbouty, MT, 1990. Geological Evaluation DuPont Beaumont Works Jefferson County, Texas. Appendix 3-10.

Harding, T. P., and Tuminas, A. C., 1989. Structure of hydrocarbon traps sealed by basement normal block faults at stable flank of foredeep basins and at rift basins: Am. Assoc. Petroleum Geologists Bull., Volume 73, p. 812-840.

Hovorka, S.D., Holtz, M.H., Sakurai, S., Knox, P.R., Collins, D., Papadeas, P., and Stehli, D., 2003. Frio pilot in CO2 sequestration in brine-bearing sandstones: The University of Texas at Austin, Bureau of Economic Geology, report to the Texas Commission on Environmental Quality to accompany a class V application for an experimental technology pilot injection well. GCCC Digital Publication Series #03-04.

Hovorka, S., Y. Kharaka, H. Nance, C. Doughty, S. Benson, B. Freifeld, R. Trautz, T. Phelps, and T. Daley, 2006. Monitoring CO2 storage in brine formations: lessons learned from the Frio field test one year post injection.

Jackson, M. P. A., and Galloway, W. E., 1984. Structural and depositional styles of Gulf Coast Tertiary continental margins: Application to hydrocarbon exploration: Am. Assoc. Petroleum Geologists, Continuing Education Course Note Series No. 25, p. 226.

Jev, B. I., Kaars-Sijpesteijn, C. H., Peters, M. P. A. M., Watts, N. L., and Wilkie, J. T., 1993. Akaso Field, Nigeria: Use of integrated 3-D seismic, fault slicing, clay smearing, and RFT pressure data on fault trapping and dynamic leakage: Am. Assoc. Petroleum Geologists Bull., Volume 77, p. 1389-1404.

Johnston, O. C., and Greene, C. J., 1979. Investigation of Artificial Penetrations in the Vicinity of Subsurface Disposal Wells: Texas Department of Water Resources.

Jones, T. A., and Haimson, J. S., 1986. Demonstration of Confinement: An Assessment of Class 1 Wells in the Great Lakes and Gulf Coast Regions: Journal of the Underground Injection Practices Council, Number 1, pp. 279-317.

Knipe, R. J., 1992. Faulting processes and fault seal: in R. M. Larsen, H. Brekke, B. T. Larsen, and E. Talleras, eds., Structural and tectonic modeling and its application to petroleum geology: Elsevier, Amsterdam, p. 325-342.

Knipe, R. J., 1997. Juxtaposition and seal diagrams to help analyze fault seals in hydrocarbon reservoirs: Am. Assoc. Petroleum Geologists Bull., v. 81, n. 2, pp. 187-195.

Lehner, F. K., and Pilaar, W. F., 1991. On a mechanism of clay smear emplacement in synsedimentary normal faults: Am. Assoc. Petroleum Geologists Bull., v. 75, p. 619.

Lindsey, N. G., Murphy, F. C., Walsh, J. J., and Watterson, J., 1993. Outcrop studies of shale smear on fault surfaces; International Association of Sedimentologists Special Publication 15, p. 113-123.

PB-KBB, Inc., 1990. Technical Report Supporting Application for Development of Underground Hydrocarbon Storage Facility at Spindletop Salt Dome, Jefferson County, Texas.

Petra Nova, 2021. West Ranch Oil Field CO2 Monitoring, Reporting and Verification (MRV) Plan: Petra Nova monitoring submittal to EPA.

Pitmann, E. D., 1981. Effect of fault-related granulation on porosity and permeability of quartz sandstones, Simpson Group (Ordovician), Oklahoma: Am. Assoc. Petroleum Geologists Bull., v. 65, n. 11, p. 2381-2387.

Secor, D. T., 1965. Role of fluid pressure in jointing: American Journal of Science, v. 263, p. 633-646.

Smith, D. A., 1966. Theoretical Considerations of Sealing and Non-Sealing Faults: Am. Assoc. Petroleum Geologists Bull., v. 50, n. 12, p. 363-374.

Smith, D. A., 1980. Sealing and Non-Sealing Faults in Louisiana Gulf Coast Salt Basin: Am. Assoc. Petroleum Geologists Bull., v. 64, n. 2, p. 145-172.

Spencer, E. W., 1977. Introduction to the Structure of the Earth: McGraw-Hill, Inc., New York, 640 pp.

Swanson, S.M., Karlsen, A.W., and Valentine B.J., 2013. Geologic assessment of undiscovered oil and gas resources—Oligocene Frio and Anahuac Formations, United States Gulf of Mexico coastal plain and State waters: U.S. Geological Survey Open-File Report 2013–1257, 66 p., http://dx.doi.org/10.3133/ofr20131257.

Vialle, S., Druhan, J.L., and Maher, K., 2016. Multi-phase flow simulation of CO2 leakage through a fractured caprock in response to mitigation strategies: International Journal of Greenhouse Gas Control, v. 44, p. 11–25, doi:10.1016/j.ijggc.2015.10.007.

Vrolijk, PJ, JL Urai, and M Kettermann, 2016. Clay smear: Review of mechanisms and applications. Journal of Structural Geology. Vol 86. Pp. 95-152.

Warner, D. L., and Syed, T., 1986. Confining layer study-supplemental report: prepared for U.S. EPA Region V, Chicago, Illinois.

Warner, D. L., 1988. Abandoned oil and gas industry wells and their environmental implications: prepared for the American Petroleum Institute.

Weber, K. J., 1978. The role of faults in hydrocarbon migration and tapping in Nigerian growth fault structures: Annual Offshore Technology Conference Proceedings, Volume 4, p. 2643-2653.

Yielding, G., Freeman, B., and Needham, D. T., 1997. Quantitative fault seal prediction: Am. Assoc. Petroleum Geologists Bull., v. 81, n. 6, p. 897-917

Section 2.3

Baker, 1979. Stratigraphic and Hydrogeologic Framework of Part of the Coastal Plain of Texas. Texas Department of Water Resources Report 236, July 1979.

Ellis, J.H., Knight, J.E., White, J.T., Sneed, M., Hughes, J.D., Ramage, J.K., Braun, C.L., Teeple, A., Foster, L., Rendon, S.H., and Brandt, J., 2023, Hydrogeology, land-surface subsidence, and documentation of the Gulf Coast Land Subsidence and Groundwater-Flow (GULF) model, southeast Texas, 1897–2018: U.S. Geological Survey Professional Paper 1877, 407 p., https://doi.org/ 10.3133/ pp1877.

GeoHydroLogicPro LLC, 2018. EPA No-Migration Petition Dow Beaumont Aniline Frio Sand Reissuance II 2020. Section 3 – Geology. December 2018.

George, Peter G., R.E. Mace, and R. Petrossian, 2011. Aquifers of Texas. Texas Water Development Board, Report 380. July 2011.USEPA, 2013. Geologic Sequestration of Carbon Dioxide: Underground Injection Control (UIC) Program Class VI Well Site Characterization Guidance. United States Environmental Protection Agency. EPA Guidance Document 816-R-13-004. May 2013.

Geostock Sandia (Geostock), 2022. BASF Corporation Beaumont Site UIC Class I Permit Application Section V-Geology Report. TCEQ Permit Renewal Application. November 2022.

Ryder and Ardis, 1991. Hydrology of the Texas Gulf Coast Aquifer Systems. United States Geological Survey, Regional Aquifer-System Analysis. Open-File Report 91-64.

Texas Water Development Board, 2022a. 2022 State Water Plan. Accessed 6 December 2023. https://texasstatewaterplan.org/county/Jefferson

Texas Water Development Board, 2022b. Water Service Boundary Viewer. Accessed 8 December, 2023. https://www3.twdb.texas.gov/apps/WaterServiceBoundaries/

Texas Water Development Board, 2023. Groundwater Conservation Districts. Accessed 8 December 2023. https://www.twdb.texas.gov/groundwater/conservation_districts/index.asp

Thorkildsen and Quincy, 1990. Evaluation of Water Resources of Orange and Eastern Jefferson Counties, Texas. Texas Water Development Board. Report 320. January 1990.

Wade, S.C., 2022. GAM Run 21-019 MAG: Modeled Available Groundwater for the Gulf Coast Aquifer System in Groundwater Management Area 14. Texas Water Development Board. 8 September 2022.

Wesselman, J.B. and S. Aronow, 1971. Ground-water Resources of Chambers and Jefferson Counties, Texas. United States Geological Survey in cooperation with the Texas Water Development Board (TWDB). TWDB Report 133. August 1971.

Young, S. C., Ewing, T., Hamlin, S., Baker E., and Lupton, D., 2012. Updating the Hydrogeologic Framework for the Northern Portion of the Gulf Coast Aquifer. Prepared for Texas Water Development Board, June 2012.

Young, S. C., Jigmond, M., Deeds, N., Blainey J., Ewing, T., Banerj, D., 2016. Final Report: Identification of Potential Brackish Groundwater Production Areas – Gulf Coast Aquifer System. TWDB Contract Number 1600011947. August 2016.

Young and Draper, 2020. The Delineation of the Burkeville Confining Unit and the Base of the Chicot Aquifer to Support the Development of the Gulf 2023 Groundwater Model. Prepared for the Harris-Galveston Subsidence District and the Fort Bend Subsidence District, October 2020.

Section 2.4

Bebout, D.G., Loucks, R.G., Bosch, S.C., Dorfman, M.H., 1976. Geothermal Resources: Frio Formation, Upper Texas Gulf Coast, Geological Circular 76-3.

Davis, S.N., Whittemoreh, D., Fabryka-martinc, J., 1998. Uses of Chloride / Bromide Ratios in Studies of Potable Water.

Fatah, A., Mahmud, H. B., Bennour, Z., Gholami, R., & Hossain, M. (2022). Geochemical modelling of CO2 interactions with shale: Kinetics of mineral dissolution and precipitation on geological time scales. Chemical Geology, 592, 120742. https://doi.org/10.1016/j.chemgeo.2022.120742

Harvey, O. R., Qafoku, N. P., Cantrell, K. J., Lee, G., Amonette, J. E., & Brown, C. F. (2013). Geochemical Implications of Gas Leakage associated with Geologic CO 2 Storage—A Qualitative Review. Environmental Science & Technology, 47(1), 23–36. https://doi.org/10.1021/es3029457

Hovorka, S.D., Sakurai, S., Kharaka, Y.K., Nance, H.S., Benson, S.M., Freifeld, B.M., Trautz, R.C., Phelps, T., 2006. Monitoring CO2 storage in brine formations: lessons learned from the Frio field test one year post injection.

Jessen, F.W., Rolhausen, F.W., 1944. Waters from the Frio Formation, Texas Gulf Coast. Trans. Am. Inst. Min. Metall. Eng. 155, 23–38.

Kharaka, Y.K., Callender, E., Wallace, R.H., 1977. Geochemistry of geopressured geothermal waters from the Frio Clay in the Gulf Coast region of Texas. Geology 5, 241–244. https://doi.org/10.1130/0091-7613(1977)5<241:GOGGWF>2.0.CO;2

Kharaka, Y.K., Cole, D.R., Gunter, W.D., Thordsen, J.J., Kakouros, E., 2005. Gas-Water-Rock Interactions in Saline Aquifers Following CO2 Injection: Results from Frio Formation, Texas, USA. Paper GC12A-08. GCCC Digit. Publ. Ser. #05-03e.

Kharaka, Y.K., Cole, D.R., Thordsen, J.J., Kakouros, E., Nance, H.S., 2006. Gas-water-rock interactions in sedimentary basins: CO2 sequestration in the Frio Formation, Texas, USA. J. Geochemical Explor. 89, 183–186. https://doi.org/10.1016/j.gexplo.2005.11.077

Kharaka, Y. K., Thordsen, J. J., Hovorka, S. D., Seay Nance, H., Cole, D. R., Phelps, T. J., & Knauss, K. G. (2009). Potential environmental issues of CO2 storage in deep saline aquifers: Geochemical results

from the Frio-I Brine Pilot test, Texas, USA. Applied Geochemistry, 24(6), 1106–1112. https://doi.org/10.1016/j.apgeochem.2009.02.010

Morton, R.A., Garrett, J.C.M., Posey, J.S., Han, J.H., Jirik, L.A., 1981. Salinity Variations and Chemical Compositions of Waters in the Frio Formation, Texas Gulf Coast.

Reed, M.J., Mariner, R.H., 1991. Quality control of chemical and isotopic analyses of geothermal water samples, in: Proceedings Sixteenth Workshop Geothermal Reservoir Engineering, January 23-25, 1991. Sixteenth Workshop on Geothermal Reservoir Engineering, Stanford University, pp. 9–13.

Schlumberger, 1987. Log Interpretation Principles/Applications. Schlumberger Educational Services, Houston, Texas.

Søvik, J. (2012). Interactions between CO2 and rock in heterogeneous reservoirs during CO2 storage [Master's thesis in Petroleum engineering, University of Stavanger]. https://uis.brage.unit.no/uis-xmlui/handle/11250/183468

Xu, T., Kharaka, Y. K., Doughty, C., Freifeld, B. M., & Daley, T. M. (2010). Reactive transport modeling to study changes in water chemistry induced by CO2 injection at the Frio-I Brine Pilot. Chemical Geology, 271(3–4), 153–164. https://doi.org/10.1016/j.chemgeo.2010.01.006

Young, S.C., Jigmond, M., Deeds, N., Blainey, J., Ewing, T., Banerj, D., 2016. Final Report: Identification of Potetnial Brackish Groundwater Production Areas - Gulf Coast Aquifer System. TWDB Contract Number 1600011947.

Section 2.5

Byerlee, J., 1978. Friction of rocks: Pure and Applied Geophysics, v. 116, pp. 615-626.

Jaeger, J. C. and N. C. W. Cook, 1969. Fundamentals of rock mechanics (third edition): London, Chapman & Hall.

Jung, J., Singh, D., Espinoza, D. N., Wheeler, M. F., 2018. Quantification of a maximum injection volume of CO2 to avert geomechanical perturbations using a compositional fluid flow reservoir simulator. Advances in Water Resources, Volume 112, 2018 pp. 160-169

Hovorka, S. D., Benson, S. M., Doughty, C., Freifeld, B. M., Sakurai, S., Daley, T. M., ... & Knauss, K. G., 2006. Measuring permanence of CO2 storage in saline formations: the Frio experiment. Environmental Geosciences, 13(2), 105-121.

Moore, P.L., 1986. Drilling practices manual. Second edition. Petroleum Pub.Co.

Nicholson, A.J., Meckel, T.A., Liu, J., and Trevino, R., 2014. Gulf of Mexico Miocene CO2 Site Characterization Mega Transect Final Scientific/Technical Report, CHAPTER 4: Fault Seal Properties for CO2 Sequestration, Offshore Texas Miocene. US Department of Energy National Energy Technology Laboratory.

Streit, J. E. and R. R. Hillis, 2004. Estimating fault stability and sustainable fluid pressures for underground storage of CO2 in porous rock: Energy, v. 29,p. 1445-1456.

Section 2.6

BEG, 2023. Earthquake Catalog. University of Texas, Bureau of Economic Geology, TexNet. 2023. https://www.beg.utexas.edu/texnet-cisr/texnet/earthquake-catalog. Last accessed 7 November 2023.

Ewing, T. E., 1986, Structural styles of the Wilcox and Erio growthfault trends in Texas: Constraints on geopressured reservoirs: Bureau of Economic Geology, University of Texas at Austin,

Report of Investigations 154, 86 pHiQuake, 2023. The Human-Induced Earthquake Database (HiQuake). March 2023. https://inducedearthquakes.org/. Last accessed 7 November 2023.

Jackson M.P.A., and Wilson B.D., 1982. Fault Tectonics of the East Texas Basin. Geological Circular 82-4, The University of Texas at Austin, 1982.

Looff, K.M. and Looff, K.M., 2000. Subsidence, Sinkholes, and Piping Associated with Gulf Coast Salt Domes. SMRI Fall 2000 Meeting, San Antonio, Texas, October 15-18, 2000, pp.275-301.

NOAA publication 'Earthquake History of the Gulf Coast Region

Texas Almanac, 2021. Earthquakes in Texas. Updated in 2021 https://www.texasalmanac.com/articles/earthquakes-in-texas. Last accessed 7 November 2023.

Sage, 2023. Seismological Facility for the Advancement of Geoscience (SAGE). 2023. https://ds.iris.edu/wilber3/find_event. Last accessed 7 November 2023.

USGS, 2016. USGS Map of 21 Areas Impacted by Induced Earthquakes. United States Geological Survey, Earthquake Hazards Program, 29 March 2016. https://www.usgs.gov/media/files/usgs-map-21-areas-impacted-induced-earthquakes. Last accessed 7 November 2023.

USGS, 2019a. 2018 Long-term National Seismic Hazard Map. United States Geological Survey, Earthquake Hazards Program, 24 October 2019. https://www.usgs.gov/media/images/2018-long-term-national-seismic-hazard-map. Last accessed 7 November 2023.

USGS, 2019b. 2014 United States (Lower 48) Seismic Hazard Long-term Model. United States Geological Survey, Earthquake Hazards Program, 23 December 2019. https://www.usgs.gov/programs/earthquake-hazards/science/2014-united-states-lower-48-seismic-hazard-long-term-model. Last accessed 7 November 2023.

USGS, 2023a. Increasing Rate of Earthquakes Beginning in 2009. United States Geological Survey, Earthquake Hazards Program, January 2023. https://www.usgs.gov/media/images/increasing-rate-earthquakes-beginning-2009. Last accessed 7 November 2023

USGS 2023b. Search Earthquake Catalog. United States Geological Survey, Earthquake Hazards Program, 2023. https://earthquake.usgs.gov/earthquakes/search/. Last accessed 7 November 2023.

Section 2.7

Hinton D.D., and R.M. Olien, 2002. Oil in Texas: The Gusher Age, 1895–1945. University of Texas Press. Published 15 March 2002. https://books.google.com/books?id=SbhaBAAAQBAJ&pg=PT13&source=gbs_toc_r&cad=3#v=onepage&q&f=false.

US EIA, 2023a. Oil and petroleum products explained Where our oil comes from. United States Energy Information Administration. https://www.eia.gov/energyexplained/oil-and-petroleum-products/where-our-oil-comes-from.php. Last accessed 29 September 2023.

US EIA, 2023b. Annual Energy Outlook 2023, Table 1: Total Energy Supply, Disposition and Price Summary. Released March 2023.

Hammer, E.J., 1939. Amelia Oil Field, Jefferson County, Texas. AAPG Bulletin (1939) 23 (11): 1635–1665. https://doi.org/10.1306/3D933132-16B1-11D7-8645000102C1865D.

Kraye, R.F., 1962. Lovells Lake Field, Jefferson County, Texas. Houston Geological Survey. Typical Oil and Gas Fields of Southeast Texas. 1962.

US DOE, 2020. Produce Water: From a Waste to a Resource, September 2, 2020. United States Department of Energy, Office of Fossil Energy and Carbon Management. https://www.energy.gov/fecm/articles/produced-water-waste-resource#:~:text=Produced%20water%20that%20has%20been,even%20non%2Dedible%20crop%20irrigation.

Kyle J.R. and B.A. Elliott, 2019. Past, Present, and Future of Texas Industrial Minerals. Mining, Metallurgy & Exploration (2019) 36:475–486. 28 February 2019. https://doi.org/10.1007/s42461-019-0050-1.

Callaghan R.M., 2019. The Mineral Industry of Texas. US Geological Survey. 2014 Minerals Yearbook. Texas [Advance Release]. September 2019.

BGE, 2023. Texas Mineral Resources Map. Bureau of Economic Geology. The University of Texas at Austin. https://coastal.beg.utexas.edu/txmineralresources/#!/. Accessed on 2 October 2023.

RRC, 2022. Texas Gas Storage Operation. Texas Railroad Commission. 31 December 2022.

RRC, 2023. Public GIS Viewer (Map). Texas Railroad Commission. https://www.rrc.texas.gov/resource-center/research/gis-viewer/. Last accessed on 2 October 2023.

Wendler, A.P., 1946. Geophysical history of the Lovell Lake oil field, Jefferson County, Texas. Geophysics (1946) 11 (3): 302–311. 1 July 1946. https://doi.org/10.1190/1.1437250.

Section 7.0

Hovorka, S. D., Holtz, M. H., Sakurai, S., Knox, P. R., Collins, D., Papadeas, P., and Stehli, D., 2003. Frio Pilot in CO2 Sequestration in Brine-Bearing Sandstones. Texas Commission on Environmental Quality.

CARB, 2018. Carbon Capture and Sequestration Protocol under the Low Carbon Fuel Standard.

Chen, Z. and Y. Zhang, 2009. Well flow models for various numerical methods. International Journal of Numerical Analysis & Modeling, 6(3).

Djebbas, Faycal & Aziez, Zeddouri and Cherif, Khelifa, 2015. Impact of the Fractures on the Capacity and Security CO 2 Geological Storage. Conference Proceeding from Advances in Environmental and Geological Science and Engineering.

Thiem, G., 1906. Hydrologische Methoden: Leipzig, Germany, J.M. Gebhardt, 56 p.

USEPA, 2017. Conducting Part I Mechanical Integrity Tests (MITs) Without an EPA Representative Present – Unwitnessed MITs. Retrieved from https://www.epa.gov/sites/default/files/2017-06/documents/unwitnesed_mit_compliance_assistance_05-31-17.pdf on March 28, 2024.

Section 13.0

BIA, 2023. Search Federally Recognized Tribes. U.S. Department of the Interior. Indian Affairs. Accessed January 2023. https://www.bia.gov/service/tribal-leaders-directory/federally-recognized-tribes.

Caliche, 2023. Caliche Development Partners II Reaches Agreement with City of Beaumont to Lease Space for the Long-Term Sequestration of CO2 and Hires Director of Energy Transition. Caliche Development Partners II Newsroom. https://calichestorage.com/caliche-development-partners-ii-reaches-agreement-with-city-of-beaumont-to-lease-space-for-the-long-term-sequestration-of-c02.html. 31 August 2023.

CEQ, 1997. Environmental Justice, Guidance Under the National Environmental Policy Act. Council on Environmental Quality. 10 December 1997.

Houston CCS Alliance, 2023. Southeast Texas leaders learn about carbon capture at Port Arthur Chamber of Commerce's annual summit. Houston CCS Alliance Newsroom. https://houstonccs.com/newsroom/southeast-texas-leaders-learn-about-carbon-capture-at-port-arthur-chamber-of-commerces-annual-summit/. 2 November 2023.

Seigo, S.L., J. Arvai, S. Dohle, and M. Siegrest, 2014. Predictors of risk and benefit perception of carbon capture and storage (CCS) in regions with different staged of deployment. International Journal of Greenhouse Gas Control. Vol 25, June 2014. pp. 23-32.

UNFCCC, 2024. Carbon capture, use and storage. United Nations Framework Convention on Climate Change. https://unfccc.int/resource/climateaction2020/tep/thematic-areas/carbon-capture/index.html. Accessed on21 April 2024.

USEPA, 2011. Geologic Sequestration of Carbon Dioxide – UIC Quick Reference Guide. Additional Tools for UIC Program Directors Incorporating Environmental Justice Considerations into the Class VI Injection Well Permitting Process. United States Environmental Protection Agency. Office of Water. EP 816-R-11-002. June 2011.

USEPA, 2016. Promising Practices for EJ Methodologies in NEPA Reviews. Report of the Federal Interagency Working Group on Environmental Justice and & NEPA Committee. United States Environmental Protection Agency. March 2016.

USEPA, 2023a. Learn About Environmental Justice. USEPA. Accessed January 2023. https://www.epa.gov/environmentaljustice/learn-about-environmental-justice.

USEPA, 2023b. EJScreen Environmental Justice Mapping and Screening Tool EJScreen Technical Documentation for Version 2.2. United States Environmental Protection Agency. Office of Environmental Justice and External Civil Rights. July 2023.

USEPA, 2023c. Memorandum: Environmental Justice Guidance for UIC Class VI Permitting and Primacy. United States Environmental Protection Agency. Office of Water. 17 August 2023.

Wallquist, L., V.H.M. Visschers, and M. Siegrest, 2010. Impact of Knowledge and Misconceptions on Benefit and Risk Perception of CCS. Environmental Science and Technology. Vol 44 (17), September 2010. pp. 6557-62.

CLASS VI PERMIT
PROJECT NARRATIVE
Caliche Beaumont Sequestration Project
Beaumont, Jefferson County, Texas

TABLES *(attached)*

CLASS VI PERMIT
PROJECT NARRATIVE
Caliche Beaumont Sequestration Project
Beaumont, Jefferson County, Texas

FIGURES

CLASS VI PERMIT
PROJECT NARRATIVE
Caliche Beaumont Sequestration Project
Beaumont, Jefferson County, Texas

APPENDICES

Appendix A.A	Local Well Logs (RRC Database)
Appendix A.B	TGS Well Logs
Appendix A.C	2D Seismic Data for Caliche Beaumont Sequestration Project
Appendix A.D	Temperature Logs for Golden Triangle Storage No. 5 and Stanolind Gladys City No. B-4
Appendix A.E	Resistivity Profiles for Golden Triangle Storage Disposal Well Nos. 1A, 2A, 4A, and 5A
Appendix A.F	Tubular Stress Calculations
Appendix A.G	Cementing Cost Estimate
Appendix A.H	EJScreen Report